Swansea University
Prifysgol Abertawe

FEASIBILITY TESTING OF A NEW NANOTHERAPY FOR OVARIAN CANCER

by
DENISE DE MEIJER

Supervisors: Dr A.R. Godfrey &
Dr L.W. Francis

Academic Year: 2020-2021

DECLARATION

This work has not previously been accepted in substance for any degree and is not being concurrently submitted in candidature for any degree.

Signed

Date 30-09-2021

STATEMENT 1

This thesis is the result of my own investigations, except where otherwise stated. Where correction services have been used, the extent and nature of the correction is clearly marked in a footnote(s).

Other sources are acknowledged by footnotes giving explicit references. A bibliography is appended.

Signed

Date 30-09-2021

STATEMENT 2

I hereby give consent for my thesis, if accepted, to be available for photocopying and for inter-library loan, and for the title and summary to be made available to outside organisations.

Signed

Date 30-09-2021

Contents

List of Abbreviations

ACN	Acetonitrile
DAD	Diode Array Detector
dSPE	Dispersive Solid-Phase Extraction
ED	Encapsulated Drug
EE	Encapsulation Efficiency
ESI	Electrospray Ionisation
FD	Free Drug
FSH	Follicle Stimulating Hormone
GnRH	Gonadotropin-Releasing Hormone
IEX	Ion Exchange
LC	Liquid Chromatography
LH	Luteinizing Hormone
LOD	Limit of Detection
LLOQ	Lower Limit of Quantification
ME	Matrix Effect
MeOH	Methanol
NP	Normal Phase
OC	Ovarian Cancer
QuEChERS	Quick Easy Cheap Effective Rugged Safe
RP	Reversed Phase
RSD	Relative Standard Deviation
SD	Standard Deviation
UV	Ultraviolet

Abstract

Currently the primary treatment of ovarian cancer (OC) is surgery with chemotherapy. Chemotherapy is effective but platinum-based drugs commonly employed for OC, function with a specific mode of action, and are prone to adverse side effects and drug resistance, limiting the efficacy of the therapy.[1] BAY-784 is a GnRH-R antagonist which offers significant potential as an alternative therapy by functioning through alternative biochemical pathway, limiting cell replication by inhibiting growth hormones. However, this mechanism of action for OC is less well-defined in comparison to platinum therapies, with antagonist and agonist effects observed when non-specific drug administration routes are used. Because of the toxicity levels of BAY-784, liposomes were used to encapsulate this drug and induce the activity of BAY-784 on cancer cells.

To monitor the drug, we have developed an LC-DAD quantitative method and evaluated the tripartite sample preparation approach to provide absolute values of encapsulation. This latter method has shown a need for further method development due to incompatibilities with the liposome design, following formation via Thin-Film Hydration. As such, the encapsulation efficiency was determined using an NMR approach and calculated to be 40%. The successful liposomal BAY-784 drug was tested on OVCAR-3 and SKOV-3 ovarian cancer cell lines and showed improved efficacy as an encapsulated therapy. However, the MoA of liposomal BAY-784 has not been monitored yet, free BAY-784 has shown a different mode of action, when using cell painting, on SKOV-3 cells affecting mostly the nucleus.

1. Chapter 1: Introduction

1.1. Introduction to oncology therapies

Cancer is a metabolic disease whereby cells divide uncontrollably resulting in an aggregated mass known as a tumour. The causes of cancer can differ, with tumours triggered by a genetic disease, errors in cell division or by DNA damage caused by exposure to environmental pollutants. There are three main ´drivers´ for cancer: proto-oncogenes, tumour suppressor genes, and DNA repair genes.[2] These genes cause normal cells to became cancerous when they are mutated. Conventional oncology treatments involve a combination of chemotherapy, surgery and radiotherapy, however, this is dependent on which type of cancer, the stage of the cancer and the phase of the cancer.[3] Surgery and radiotherapy are localised therapies as they treat the tumour in a specific area in the body, while chemotherapy is a systemic treatment because of the impact on the whole body. However, chemotherapy is a more developed treatment and has a broader range of use. Chemotherapy is used for depleting small amounts of cancer cells after surgery or shrinking large tumours before surgery in OC.

1.1.1. Challenges of current oncology therapies

Although, cancer is one of the most common causes of death in the world, cancer treatments still have less than 100% efficacy in treatments. In addition, the breadth of cancers observed often shows a range of efficacies for different cancers. [3] There are number of factors that contribute to this, for example, current cancer treatments assume that all cancer cells have similar malignant characteristics however, this is not necessarily the case with studies showing differing physiologies of tumours and causes of cancer.[4] Furthermore, cancer stem cells can also exhibit cellular changes that make them resistant to anticancer drugs after prolonged exposure. Additionally, the lack of biomarkers makes it difficult to diagnose patients at an early stage of ovarian cancer. This makes treatments more difficult given this reduces the options to a clinician. Thereby the diagnosis of cancer is a challenge which makes the treatment difficult. And in addition, the most challenging problem to overcome during oncology therapy is metastasis. Metastasis is the spread of cancer to different parts in the body. This type of cancer is unpredictable and hard to control as it is difficult to treat due to the spread to surrounding parts in the body. In general, different challenges need to be overcome for oncology therapy treatments.

1.1.2. Therapies for Ovarian Cancer

Ovarian cancer (OC) is the fifth most common cause of cancer death in women and the leading cause of death among gynaecological cancers.[5] The survival rates differ over the stages in which the cancer is detected and decreases rapidly as the cancer progresses. For example, in stage 1, where cancer is found in one or both ovaries, the survival rate over five years is around 90% while, in stage 2, where the cancer has spread into other areas of the pelvis, the survival rate decreases to 70%. Sadly, when the cancer has spread to the abdomen at stage 3, the five year survival rate is about 39%, and decreases to 17% when the spread exceeds the abdomen during stage 4.[6] The main contributors of the high mortality rates are the late detection of tumours (at stage III or IV [7]) due to non-specific symptoms associated with OC, and the development of resistance to conventional platinum-based chemotherapy agents.[8]

1.1.2.1. Current state of play of nanotherapeutics for Ovarian Cancer (OC)

The need of new therapies for ovarian cancer is increasing. Due to resistance of platinum-based drugs, current treatments are not effective in every situation. New and alternative/complimentary therapies are developed which uses drugs with another mode of action. An upcoming solution treatment for this problem is nanotherapy. Nanotherapy has different mode of actions which improves the efficacy of OC treatments. Problems that are found in the conventional therapies is discussed in section 1.1.2. which stated that platinum-based therapies are not effective in a later stage of cancer, due to resistance of the cancer cells to the therapy. Nanotherapy makes it possible to treat cancer without affecting healthy cells which causes side effects. This type of therapy uses small nanoparticles, with a size ranging from 5 to 500 nm, to deliver a drug in a specific area of the body. Nanoparticles that are frequently used in nanotherapy (both approved an in clinical trial) are, among others, liposomes, dendrimers, micelles, gold-particles, polymer and peptides whereby liposomes are most used. Liposomes are small spherical vesicles that consist of a double layer membrane made from cholesterol and phospholipids, capable of trapping both hydrophilic and hydrophobic compounds.[9]. Due to their low toxicity levels, good biodegradability, biocompatibility and the ability to encapsulate both hydrophilic and hydrophobic compounds, there use is wider applicable. Furthermore, different options are available to synthesize liposomes which makes them easy to adjust to the choice of drug. Adjusting the liposomes synthesis can change the surface decoration and mode of action. The mode of action of the drug can be divided in two different target ways: passive and active targeting. Mechanism of passive targeting is based on the enhanced permeability and retention effect (EPR), where molecules with certain sizes has the tendency to accumulate in tumour cells,

thought to be due to tumour specific vasculature [10] Active targeting is more focused on the properties of the particle, for example, the surface decoration. Focusing more on these properties and the target aim, specific particles can be made with less side effects. Nanoencapsulation is a potential method for improving ovarian cancer treatment, due to their ability to be more specific and protect surrounding healthy tissues and cells from the toxicity of drugs.[11][12]

1.1.2.2. GnRH-R antagonists as potential oncology therapies

Gonadotropin releasing hormone (GnRH) is a decapeptide that is formed in the hypothalamus. This hormone is the central regulator of reproduction and causes the synthesis of luteinizing hormone (LH) and follicle-stimulating hormone (FSH) in a pulsatile manner. Both hormones are controlling the testosterone and estrogen levels in respectively, men and women, respectively. GnRH hormones binds especially to GnRH receptors (GnRH-R) and will therefore stimulate or stop the release of the LH and FSH hormones. Stimulating or stopping this process depends on whether an agonist or antagonist the hormone. Two types of hormones can be added, agonist and antagonist, where agonists are stimulating the process of the receptor while antagonist will stop the process.

Chemical characterization and structure-activity analysis of GnRH variants containing systematic amino acid substitutions led to the discovery of GnRH super agonists and antagonists. These peptides are widely used for the treatment of clinical conditions in which modulation of or interference with sex hormone production is beneficial to prevent development or progression of benign conditions (e.g. endometriosis, uterine fibroids) or malignant tumors (e.g. breast, ovarian, endometrial and prostate carcinoma). [13] Indeed, in the recent past, small chemical drugs have been identified as potent antagonists and agonists of the GnRH-R. Some of these non-peptide compounds are sufficiently stable in vivo and possess favourable pharmacological parameters comparable to peptide antagonists.

1.1.2.3. GnRH-R in solid tumour cancer

In several human malignant tumors of the urogenital tract, including cancers of the endometrium, ovary, urinary bladder, and prostate, it has been possible to identify expression of gonadotropin-releasing hormone (GnRH) and its receptor as part of an autocrine system, which regulates cell proliferation. Several examples of dose- and time- dependent growth inhibitory effects of GnRH agonists and antagonists have been explored in cell lines derived from these cancers.[13] The mechanism of action of these drugs is linked to the GnRH receptor activating

a phosphotyrosine phosphatase (PTP) and counteracts with the mitogenic signal transduction of growth factor receptors, which results in a reduction of cancer cell proliferation.[13] GnRH antagonists in contrast to agonists, have been shown to induce apoptosis in cell types linked to reproductive biology and gynaecological oncology.[14] In human endometrial and ovarian cancer cells, this occurs due to a dose-dependent loss of mitochondrial membrane potential and induction of death signals.

1.1.2.4.BAY-784

BAY-784 is one such GnRH-R antagonist, developed as an orally available spiroindoline derivative acting as a potent and selective antagonist of the human gonadotropin-releasing hormone receptor in postmenopausal women [13] BAY-784 is fluorinated structure (see chemical structure in Figure 1.1) of molecular weight 672.11 g/mol containing six aromatic rings with sulfonyl functional groups (see Table 1.1. for further physiochemical information). These aromatic groups are chromophores, offering the potential for detection via UV spectrophotometry, while the log D of the molecule indicates a level of hydrophobicity that could enable solubility in or adsorption to organic media.
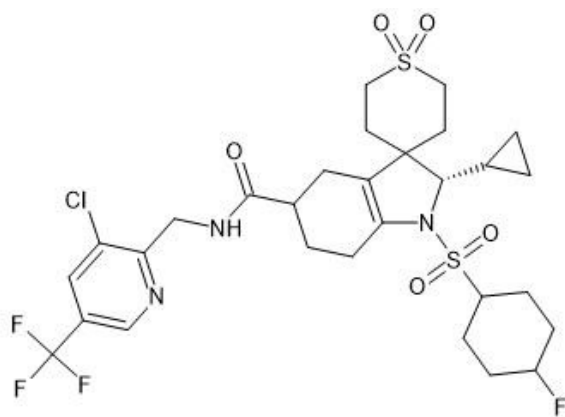
Figure 1.1. Chemical Structure of BAY-784.

BAY-784 is a GnRH-R antagonist, shown to have anti-cancer effects in vitro. This drug however has a poor solubility and is toxic to both GnRH-R expression and non-expressing cells which is evidenced by a low IC_{50} of 21nM in human based on literature.[13][15] When we compare this with the known toxic doxorubicin, with an IC_{50} of 1.9μM [16] which is higher then BAY-784, it can be concluded that BAY-784 is toxic. This study therefore investigates the utility and functionality of encapsulating BAY-784 in nano particle drug delivery vesicles, liposomes.

Table 1.1. Known Physicochemical Properties of BAY-784.

Physicochemical Properties	Values
Molecular weight (M_w)	672.11 g/mol
Monoisotopic weight	671.09 Da
Log D @ pH 7.5	4.1

1.2. Measuring drugs within clinical samples

1.2.1. Sample Separation of Clinical Matrices

Clinical matrices such as blood, plasma or urine are complex samples, with many different biomolecules that can interfere with the detection of target drugs by adversely influencing their measurement when analysed as a mixture. Thus, sample separation to reduce the matrix complexity prior to analysis is essential for reliable measurements from some complex fluids (urine and plasma [17]). There are many different sample preparation methods, however, these can be largely classified as separations based on partition (e.g. liquid-liquid extraction (LLE)), adsorption (e.g. solid-phase extraction (SPE)), porosity (e.g. size exclusion separations) and hybrid protocols that are multi-modal separations (e.g. QuEChERS). Essentially methods are selected with consideration given to the analyte of interest, matrix and detection method. Apart from porosity, the remaining separation modes are dependent on the interaction and affinity of the analyte between two phases, whereby the analyte will move to the phase which has the most compatible environment. This can be dictated by a number of interactions such as, polarity and surface attraction. Molecular polarity is represented by the partition coefficient, log P, is a measure of hydrophobicity or hydrophilicity of an analyte. These mechanisms are underpinned by the type of bonding within the analyte, such as π-π, Van der Waals and hydrogen bonding, and function following a principle of 'like dissolves like' where analytes are most compatible with the matrix environment of similar polarity. However, most analytes contain functional groups that are not only described by molecular polarity, but are ionisable, becoming charged through adjustment of pH. This means that a distribution ratio or dissociation constant (log D) is in fact a more appropriate measure of analyte polarity as this accounts for analyte ionizability and better describes this more complex character.

$$K_D = \frac{[A_2]}{[A_1]}$$

Equation 1.1: Equation describing the distribution ratio or dissociation constant, representing the distribution (D) of an analyte (A) between two phases.

This behaviour is linked to the analyte pKa (see Equation 1.2), which according to Bronsted-Lowry acid theory, represents the likelihood of an acidic analyte becoming charged through loss of a proton. Using this convention, acidic molecules can be therefore, classed as proton donors, with those that are basic, proton acceptors.

$$D = K_D * \frac{[H^+]}{[H^+] + K_a} \qquad\qquad D = K_D * \frac{K_a}{[H^+] + K_a}$$

Equation 1.2: Equations describing the relationship between dissociation constant, K_a (acid dissociation constant) and the concentration of protons in solution for an acidic analyte (left) and a basic analyte (right). See Equation 1.1 for the calculation of K_D.

However, many target analytes in clinical applications have a chemical structure that contains a mixture of chemical functionalities (e.g. non-polar and ionisable groups) and this can lead to an incomplete dissociation of the groups at physiological pH, and less discrete chemical interactions. These weakly ionic or ionisable groups often result in the analyte being present in multiple states (neutral and charged) and can affect its distribution between different environments (e.g. hydrophobic and aqueous conditions) where charged/polar analytes have greater compatibility with more polar (aqueous) conditions, and those that are neutral, a preference for hydrophobic environments. However, this ability to accept or lose a proton enables us to link K_D (and the efficiency of moving the analyte from one phase to another) with pH (e.g. concentration of protons), as represented by the Henderson-Hasselbalch equation (Equation 1.3). Given this, both the pKa of the analyte (and known interferences) and the pH of the sample preparation conditions are important to ensure the analyte is in the correct charge state to undertake or disrupt an ionic interaction (e.g. charged or neutral). Furthermore, this relationship enables the sample preparation (i.e. extraction) conditions to be modified to neutralise the target analyte for the improved recovery into an hydrophobic environment. For example, following the ion exchange concept of 'opposites attract', the transfer of an analyte containing acidic functional groups (high pKa) into a non-polar environment would require a decrease in pH below the

analyte pKa to enable protonation. This selective adjustment enables greater specificity to be applied during method development for improved analyte recovery.

$$pH = pKa + \log\frac{A^-}{HA}$$

Equation 1.3: The Henderson-Hasselbalch equation, representing the relationship between pH, pKa and the charge state of the analyte (A) e.g. as the conjugated base (A-) and the acid (HA).

1.2.1.1. Liquid-Liquid Extraction (LLE)

Liquid-liquid extractions are based on the principle that an analyte can distribute between two immiscible solvents as described by the distribution ratio K_D (Equation 1.1). In LLE, separations are typically based on hydrophobic (Van der Waals), dispersion, dipole and hydrogen bonding interactions and the extractant (organic) phase should be selected based on the polarity of the target analyte (or interference). For example, analytes with a log P (or D) above 1 are relatively hydrophobic and therefore, LLE can provide a good option of clinical applications given the difference in polarity between the analyte (and extractant) and the aqueous sample matrix. The recovery of the analyte during a LLE can be described by Equation 1.4 and shows that K_D, the volume of solvents used in the extraction system and the number of extractions play an important part in the amount of analyte extracted. For example, recovery may be increased by changing the extraction environment that facilitates a higher K_D. This can include an increase in the volume of extractant used (vs. sample matrix), and the addition of buffers (i.e. for adjusting pH) and salt to change the charge state of the analyte and reduce the degree of dissociation of the target analyte. Furthermore, given the sample matrix can be re-extracted, the recovery can be improved by repeating the extraction multiple times and combining the extractant layers.

$$R = \frac{K_D * V_{Organic}}{K_D * V_{Organic} + V_{Aqueous}} * 100\%$$

Equation 1.4: Equation describing the recovery of the analyte during a LLE and the dependence on K_D, the volume of solvents used in the extraction system and the number of extractions.

LLE experiments involve separations based on an immiscible mixture of aqueous and organic solvents. The organic phase should be selected based on the analyte that needs to be extracted. Beside the distribution ratio of a compound, interactions of analytes based on their molecular structure is important. In LLE, separations are typically based on hydrophobic, dispersion, dipole and hydrogen bonding interactions. Hydrophobic interactions are the weakest interaction, involving nonpolar Van der Waals forces. Dispersion interactions are interactions between nonpolar and polar molecules where the polar molecule causes a shift in electrons in the non-polar molecule by making it slightly polar. Dipole interactions are similar to dispersion interactions, however, instead of the interaction between non-polar and polar, it is an interaction between two polar molecules which causes the shift in electrons which makes it slightly nonpolar. Hydrogen bonding are the strongest interactions in which a hydrogen atom that is part of a polar molecule interacts with an electronegative atom that has a lone pair of (or non-bonding) electrons. Knowing these types of interactions and the molecular structure of the analyte can help predicting an organic solvent which is suitable for LLE by predicting interactions that can occur between the organic solvent and the compound of interest.

However, given the dependence of LLE on partition, polarity and appropriate solvent selection, the selectivity of this extraction process is quite limited, particularly where the sample preparation requires the extraction of the target analyte in amongst a mixture of chemically similar analytes. Furthermore, given that typical extraction would consist of x mL of both aqueous and organic solvents per sample, this can become expensive and with the difficulties in automating the process, LLE is undesirable for high-throughput drug analysis. with the high amount of organic phase used and difficulties in automating, this can also prove to be an expensive and labour intensive protocol, undesirable for high-throughput drug analysis.[17]

1.2.1.2. Solid-Phase Extraction

Solid-phase extraction is a sample preparation that is used for the isolation and concentration of analytes, involving the extraction of drug analytes with a solid sorbent. The extraction process can be operated in two ways; firstly by 'catch and release' method, where the target analyte is captured onto the sorbent, isolating it from the sample components, or by capturing target interferences leaving the target analyte in amongst the remaining sample. The approach adopted is dependent on the requirements of the experiment (e.g. complexity of the sample and target analyte sensitivity), and the sorbent characteristics can be strategically selected to achieve this aim. However, given sensitivity is a key aim of trace analysis, the first approach is most commonly adopted, and has been described below:

1) Conditioning of the SPE column

    This is usually carried out with a solvent (usually organic) to activate the sorbent functional groups, followed by a solution that ensures the sorbent environment is optimum for the analyte to interact with the sorbent (e.g. aqueous for retaining a drug via a hydrophobic mechanism from clinical samples).

2) Sample addition

    After the activation of the solid-phase, the analyte is added to the column under appropriate conditions that enable analyte retention (e.g. of compatible solvent polarity, flow rate, pH etc).

3) Wash

    A wash solvent is applied that enables the removal of interferences that are present within the sorbent that are not retained by the same (degree) of interaction as the analyte.

4) Elution

    Here the analyte of interest is eluted using a solvent capable of disrupting the retention mechanism between the analyte and the sorbent. This may involve using a solvent polarity that is more compatible with the analyte than the sorbent or changing the pH so that the ionic interaction with the ion exchange sorbent is neutralised.

To facilitate method development, sorbents are available in a number of different chemistries, enabling highly controlled analyte interaction on the sorbent and good selectivity. Similarly, to LLE, the analyte polarity may be used to separate it from the complex mixture. For example, frequently employed interactions include hydrophobic and polar interactions using reversed-phase and normal-phase sorbents, respectively. However, as discussed in Section 1.2.1, the ionizability of the analyte may also be used as a mode of interaction using an ion-exchange mechanism, or to enhance the interaction through a mixed mode (hydrophobic and ion-

exchange) phase, where more specific retention and elution conditions are required for the extraction. Other cartridge characteristics that can be used to modify the extraction include, the sorbent mass (for analyte loading), flow rate (determines time allowed for retention/elution to occur), particle size (for resolution), pore size (can dictate flow rate but can also block with particulates) etc. Along with automation, these parameters have enabled SPE to become one of the most utilised sample preparation approaches across analytical science. However, difficulties remain with selectivity for analytes of highly similar chemistries and samples with a high amount of large particulate material.

1.2.1.3. QuEChERS

The 'Quick Easy Cheap Effective Rugged and Safe' or QuEChERS sample preparation approach is a multi-modal technique that uses aspects of LLE, SPE, centrifugation and ion-exchange. The method uses a two-step process; an initial extraction, followed by dispersive SPE (dSPE) clean-up. [18] The extraction step involves using a salt counter-ion to neutralise target analytes so that they are more able to transfer into an organic solvent layer, typically acetonitrile or ethyl acetate. In addition to salt, a drying agent is added to help remove any unwanted polar interferences from the organic layer. Following separation via centrifugation, this layer is then transferred to a tube containing dSPE material, which has been specially selected to interact and bind known/anticipated interferences with-in the sample extract. The sample is again centrifuged with the supernatant removed for analysis. Unlike, SPE QuEChERS is unable to operate via 'catch and release' but, this can often have equivalent selectivity and sensitivity due to the additional modes of separation, where it may be viewed as an enhanced LLE. However, the manual approach of QuEChERS remains a challenging aspect of the method for clinical analysis and does require further work to become a high throughput method.

1.2.1.4. Sample separations using Liquid Chromatography

Liquid chromatography (LC) is a widely used technique for the separation of chemical species in a mixture. The main principle of the LC system is to separate the sample analytes under high pressure after their introduction onto the column, through differences in retention between the column's solid stationary phase and a liquid mobile phase. The mobile phase is used as a separation phase but also as a carrier phase to transfer the analyte mixture onto, and off the column following retention. Again, analyte retention is dependent on the degree of interaction with the stationary phase, where species with a great affinity for the stationary phase (analyte 'B' in figure 1.1.) will be more strongly retained and take longer to elute off the column. Therefore,

those species that have a weaker interaction with the stationary phase (analyte 'A' in figure 1.2.) will be recorded first by the detector and presented as an early peak in the chromatogram, illustrating the separation of analytes over time.
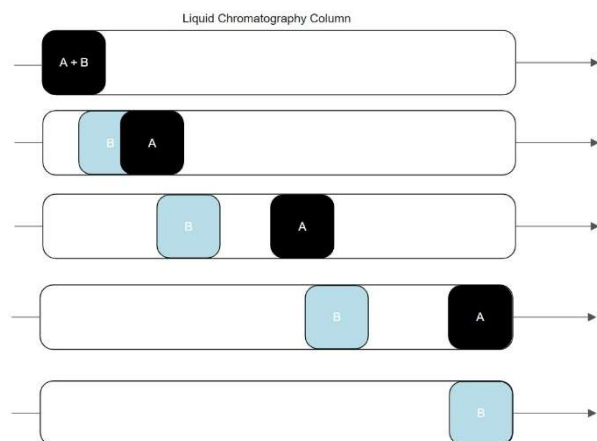
Figure 1.2 Separation process in column using liquid chromatography. Two analytes are extracted based on their interaction with stationary phase in the column where the analyte which has more interaction with the stationary phase is more delayed.

1.2.1.4.1. Optimisation of the separation

Similarly, to the sample preparation techniques described above, the stationary phase of the LC column is chosen based on the degree of interaction anticipated with the target analyte. Again, stationary phases are available based on the separation mechanisms described in Section 1.2.1, with the most common employing the adsorption mechanisms of polarity (normal phase, NP, and reversed phase, RP) and ion exchange (IEX). Of these, RP-LC is the most commonly used approach given this operates with a hydrophobic, non-polar stationary phase, capable of interacting with a wide range of pharmaceuticals and analytes anticipated within biomatrices. [19] Again, similarly to sorbents used in SPE, LC columns can vary according to their dimensions, particle and pore size. However, unlike SPE, there is greater scope for more refined and better resolved separations within LC due to the higher operating pressures and smaller particle sizes available for the stationary phase. Where essentially, higher pressures and smaller particle sizes can result in much improved peak resolution, providing greater scope to separate more chemically similar analytes in a shorter space of time (e.g. using faster mobile phase flow rates). Furthermore, the dimensions of the column (e.g. length) enable much higher peak capacities to separate more complex mixtures than SPE.

However, the stationary phase is only one part of the separation process; the mobile phase composition is also key to facilitating separation and is selected to ensure analyte solubility, retention and elution. The solvent selection is typically dictated according to the target interaction and the degree of separation required. For example, in order for the analytes to interact with the stationary phase, the initial mobile phase conditions during sample loading must not have an elution strength greater than the analyte interaction. Whilst, to facilitate elution, this point should be exceeded to ensure proper removal of the analyte off the column. This often means choosing a combination of solvents of different polarity (aqueous and organic for RP-LC), where the sample is loaded under low elution strength conditions (high aqueous) and eluted by increasing the elution strength (e.g. % organic solvent) over a period of time. This approach is known as a gradient elution profile and are often employed for complex separations. In addition to mobile phase chemistry, its flowrate is also a parameter that can be used to optimise the separation. This is best described by the Van Deemter relationship (see Equation 1.5), which evidences the flow rate to achieve optimum resolution when using specific LC column dimensions.[20]

$$H = A + \frac{B}{u} + C * u$$

Equation 1.5. Equation describing the Van Deemter relationship. Calculating theoretical plate (H), where A stands for Eddy diffusion, B for diffusion coefficient, C for the mass transfer resistance between mobile and stationary phase and u for the velocity.

Therefore, by selecting an appropriate stationary and mobile phase mixture for the analyte chemistry, flow rate and flow profile, the chromatographic parameters should enable the separation of the sample components. Once eluted, these will then be sequentially recorded by the detector and observed as peaks within a chromatogram plot displaying the analyte intensity vs time.

1.2.1.4.2. Evaluating the chromatographic separation

Following data acquisition, a number of metrics are calculated from the resulting chromatogram and used as a measure of separation performance. These include retention time (R_t), peak width (w_b or $w_{0.5h}$), peak resolution (Rs), selectivity factor (α), retention factor (k) and column efficiency (N). Firstly, the retention time is taken from the apex of the peak corresponding to the target analyte; this can be used as an absolute value or a normalised value accounting for the

solvent front and any fluctuations in retention time with the sample injection. The peak width again is taken from the peak corresponding to the target analyte and is measured at the baseline (w_b) or at half the peak height ($w_{0.5h}$), see figure 1.3.[21]
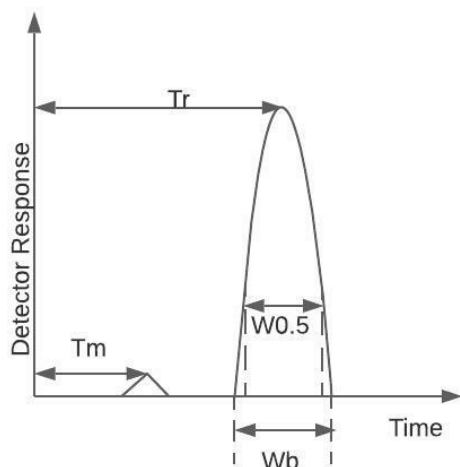
Figure 1.3. Example chromatogram with corresponding factors for following equations.
These values are then used to determine the remaining parameters as described below:

- Resolution (Rs)

The resolution can be described as the meaningful measure of separation between two or more analytes of interest as they are eluted from the column.[22] It is determined by taking into account the position and shape of each peak in the chromatogram in relation to each other (see Equation 1.6). Using this calculation, baseline (and acceptable) separation is deemed to have been reached with a resolution greater than 1.5 and is important in providing numerical evidence that the measurement of the signal in one peak does not influence the other. This latter point is key for substance quantitation where matrix interference from co-eluting sample components can often the skew the amount of target analyte measured by the detector.

$$\text{Resolution (Rs)} = 2 \frac{t_{r2} - t_{r1}}{w_{b1} + w_{b2}}$$

Equation 1.6: Equation describing the chromatographic resolution of a separation where t_{r1}= retention time analyte of interest 1, t_{r2} = retention time analyte of interest 2, w_{b1}= peak width at baseline for analyte of interest 1, w_{b2}= peak width at baseline for analyte of interest 2.

- Retention factor (k)

The retention factor describes the degree of interaction on column for a particular analyte when compared to a unretained analyte. This essentially provides a measure of the amount of analyte

that resides within the stationary phase in comparison to the mobile phase e.g. the analyte distribution constant, see Equation 1.7.

$$\text{Retention factor (k)} = \frac{t_r - t_m}{t_m}$$

Equation 1.7: An equation used to derive the retention factor of a target analyte where, t_r = retention time analyte of interest, and t_m = time on the column of an unretained analyte before it reaches the detector.

- Selectivity factor (α)

The selectivity factor, or separation factor shows the degree of analyte interaction with the column in relation to another sample component. It is represented by the ratio of the relative retention of each sample component as shown in Equation 1.8.

$$\text{Selectivity factor }(\alpha) = \frac{t_{r2} - t_m}{t_{r1} - t_m}$$

Equation 1.8: Equation used to derive the selectivity factor of the separation of two analytes where t_{r1} = retention time analyte of interest 1, t_{r2} = retention time analyte of interest 2, and t_m = time on the column of an unretained analyte before it reaches the detector.

- Column efficiency (N)

Column efficiency represents the column performance and peak dispersion, where a higher column efficiency indicates that there is low peak dispersion as a greater number of sample components can be separated (see Equation 1.9).

$$N = 5.54 \ (t_R / w_{0.5})^2$$

Equation 1.9: Equation used to derive the column efficiency where t_R = retention time analyte of interest and $w_{0.5}$ = peak width at half height

1.2.2. Analyte detection

1.2.2.1. Ultraviolet (UV) Spectrophotometric Detection

UV spectrophotometry functions by measuring the transmission of light from analytes that contain chromophores. Chromophores are chemical functional groups capable of absorbing photons of light with energies that correlate with both visual and UV wavelengths. UV spectrophotometers consist of a deuterium lamp, entrance slit, grating, exit slit, flow cell and a photodiode. The deuterium lamp generates light photons of wavelengths ranging 190-600 nm within ultraviolet and visible light spectrum. When the analyte with chromophore enters the spectrophotometer, it absorbs photons of light where bonding and non-bonding electrons in their ground state are raised to an excited higher energy state. The wavelengths of light that are transmitted to spectrophotometer decreases generating a signal that is converted to absorbance units (AU) using the Beer-Lambert Law (see Equation 1.10).

$$A = \varepsilon * l * c$$

Equation 1.10: Beer-Lambert Law. For calculating the absorbance (A) intensity of a compound where ε is the molar coefficient, l the optical path length in cm and c the concentration of the analyte.

There are three different types of UV detectors available: fixed wavelength, variable wavelength and diode array detectors (DAD), where each of these have a slightly different internal configuration as to whether a selected wavelength, multiple wavelengths or all wavelengths within the range are focussed into the flow cell (see Figure 1.4). Of these systems, the fixed and variable wavelength detectors have the greatest sensitivity however, these are limited to selected wavelengths which can be problematic if the absorbance of the analyte changes during analyte storage or processing. The DAD however, is capable of monitoring the full wavelength range offering more flexibility and capability however, this is with slightly compromised sensitivity due to greater demands in data acquisition.
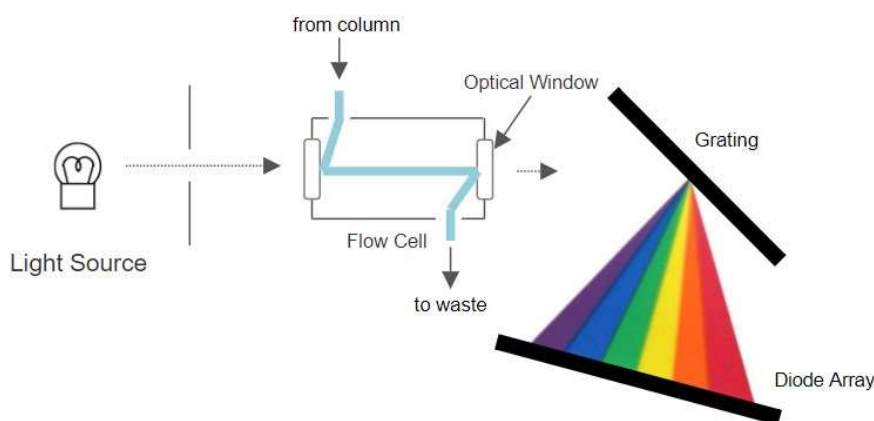
Figure 1.4: Schematic illustrating of the internal configuration of a DAD detector. Light is absorbed by the analyte in the flow cell and portrayed with Diode Array.

1.2.2.2. Mass Spectrometry

Mass spectrometry is a technique that measures gas phase molecule ions under vacuum based on their mass to charge ratio (m/z). A mass spectrometer has the following essential components; an ionization source to create gas phase ions, the mass analyser to separate ions according to their m/z, and the detector to measure the abundance of the ions as an electrical signal which is presented as a plot of relative abundance and m/z, or a mass spectrum. These components are available in different designs and are selected for certain applications dependent on the experimental needs. For example, certain mass analysers are more capable of delivering qualitative information whilst others, are more stable and less prone to signal suppression with increasing amounts of target analyte. This provides a great amount of flexibility for developing methods for the trace measurement of analytes for a range of applications as described in the following sections.

1.2.2.2.1. Ionization sources

In order to measure analytes within the range of matrices encountered within clinical applications, these must first be converted into gas phase ions. Given these matrices are typically liquid based, this requires the desolvation and ionization of the target analyte. Therefore, ionization sources (and sample inlets) are designed to achieve these aims and do this via different ionization mechanisms dependent on the processes employed. For example, ionization sources that impart a high degree of energy into the target analyte often lead to a radical ions, with a high degree of molecular fragmentation and are known as hard ionization techniques. However, maintaining the molecular structure is key for monitoring many target chemistries relevant to

pharmaceutical development to ensure the analyte is accurately characterised and quantified. Therefore, lower energy, soft ionization techniques were required and this led to the development of Electrospray Ionization (ESI), a revolutionary technique for non-volatile, more thermally labile and/or high molecular weight analytes. Given the applicability of this technique for the analytes anticipated in this study, the following discussion will focus on the ESI process.

1.2.2.2.1.1.Electrospray ionization (ESI)

This is an atmospheric pressure ionization (API) technique that is capable of ionising non-volatile, thermally labile, polar analytes, such as biomolecules, within low sample volumes. It involves spraying the sample in a solution through a needle which has an applied potential, creating a mist of fine droplets. These contain a mixture of charged molecules and solvent clusters which are desolvated through application of an inert drying gas, causing the droplets to decrease in size through evaporation (see Figure 1.5).
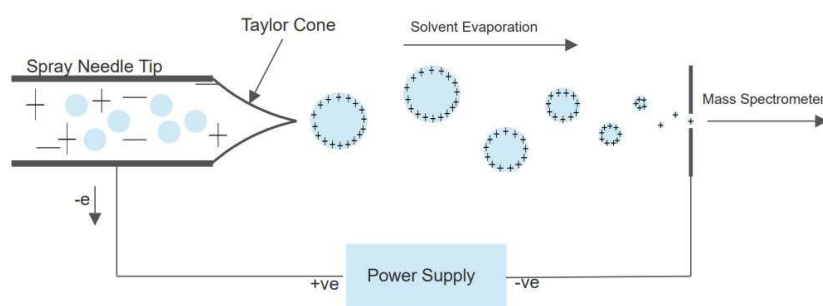
Figure 1.5: Mechanism of Electrospray Ionisation. Solvent is passing through a capillary in an ESI source.

This results in an increase in charge density of the droplet until the surface tension no longer supports the charge (e.g. the Rayleigh limit) as shown in Equation 1.11. When this Rayleigh limit is reached, a Coulombic explosion will follow and the droplets are disperse into smaller droplets. This continues as a sequential process until ~10nm. At this point there are two theories as to how gas phase ions are achieved. The first assumes that this process continues until completion, however, another theory proposes that gas phase ions are directly ejected from the droplet when their Gibbs free energy exceeds the surface tension of the droplet.[23]

$$Qray = 8\pi \sqrt{\gamma \in_0 r_d^3}$$

Equation 1.11: An equation representing the Rayleigh limit of a droplet during ESI, where r is the droplet radius, ε_0 is the vacuum permittivity, γ is the surface tension.

However, regardless which process is followed ESI is capable of generating gas phase ions through largely soft ionization adduct ion formation (e.g. protonation or deprotonation), enabling the measurement of intact molecule ion species (and their relevant isotopes to assist with identification) by the mass analyser. Given this, typical ions formed include $[M+H]^+$ in positive and $[M-H]^-$ in negative mode. However, when other ionisable species are present (e.g. salt, ammonium or formate) adducts are formed of the respective ions such as $[M+Na]^+$, $[M+NH_4]^+$, $[M+CHO_2]^-$ etc. These molecule species are formed for small molecules (≤ 500 Da), however, for higher mass species that have more functional groups, these are able to ionize with multiple charges such as $[M+2H]^{2+}$. This revolutionised the ability to measure large molecular mass species, where their mass exceeded the operating range of the mass analyser, given the relationship of *m/z* enables masses to be observed at a much lower value within the mass spectrum. For example, a molecule ion of mass 10,000 with five charges will be observed at a *m/z* of 2,000, facilitating its measurement across the different analyser designs.[24] However, this dependence on adduct formation does mean that ESI is a competitive ionization process. This can be particularly problematic for measuring a trace level analyte, where sample components of varying degrees of proton affinity are introduced into the ionization simultaneously. This 'matrix effect' can mask the presence of some analytes and therefore, requires separation via techniques such as LC to enable the measurement of these species.
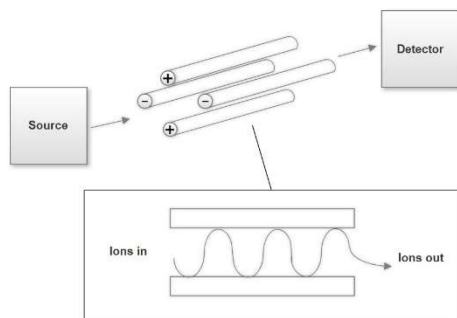
1.2.2.2.2. Mass Analysers

The role the mass analyser is to separate the ions generated by the ionization source according to their *m/z*. There are several types of mass analysers and these can be classified according to their accuracy in measuring mass. Low resolution (unit mass) analysers are generally suited to quantitative experiments, with high resolution instruments geared to qualitative exploratory work. Given the mass spectrometry needs for this project will be largely confirming the presence of molecular BAY-784, with a future view of quantitation, a system operating with a quadrupole mass analyser was selected for use and will be discussed below.

This mass analyser consists of four conducting rods arranged in parallel, where opposing pairs of rods operate with an applied direct current (DC) and radio frequency (RF) voltage of the same polarity (see Figure 1.6) which is switched sequentially. The electric field generated by

rods enables ions of an appropriate *m/z* to have a stable trajectory and oscillate through the quadrupole. By ramping the RF/DC voltage the electric field changes, allowing the sequential transfer of ions to the detector according to their *m/z*. The ions transferred during this RF/DC 'scan' is then used to create a mass scan or mass spectrum, as a plot of the ion abundance vs *m/z*. This design provides the quadrupole with a good degree of robustness, a fast scan speed and a dynamic range of ~4 orders of magnitude, enabling stable and accurate quantitation over a relatively broad concentration range, key for trace level quantitation.


Figure 1.6. Quadrupole Mass Analyser. Analytes are ionised in the source and filtered in the quadrupole.

One of the drawbacks of using the quadrupole with API techniques, is the lack of structural information associated with the measured molecules, given it is largely precursor ion species that are observed. However, given this will only be required for confirmation of BAY-784, additional, more complex instrumentation was not considered for this project.

1.2.2.3. ^{1}H-NMR

^{1}H-NMR is based on the chemical shift of protons under a magnetic field. Protons are shielded with electrons around the nucleus which have a different effect under a magnetic field. When under the influence of a magnetic field the nuclear spin of a hydrogen atom can change, resulting in the atom having two available energy states, a high and low energy spin state. If the atom absorbs energy equivalent to the gap in energy state, this can enable the atom to exist as a higher energy particle. This change in spin state can be measured as a frequency and represented as a ´chemical shift´ in relation to an internal standard compound (e.g. trimethylsilane). This provides a calibrated scale of a change in frequency or chemical shift represented by a ppm unit (see Figure 1.6). The position of protons in terms of their proximity to electronegative atoms or unsaturated bonding within the chemical structure influences their chemical shift, enabling their identification within the structure. However, peaks within the NMR spectrum can be

observed as clusters – these split peaks (and the distance between them) represent the number of neighbouring hydrogen atoms within the structure. In figure 1.7 these have been highlighted with the relevant colours within the chemical structure and the spectrum. Finally, the peak area within the NMR spectrum can also be helpful in providing structural information, where the integral of this peak area is directly proportional to the number of hydrogen atoms associated with that chemical shift.
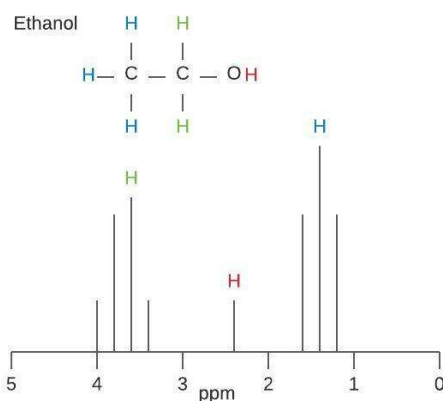
Figure 1.7. Example ^{1}H-NMR Spectrum for ethanol.

1.3.   Analytical method quantitation

To quantify a target analyte, a number of metrics must first be established to provide confidence in the measurement. First, and foremost, the analytical method must evidence selectivity; this is the ability to distinguish the target analyte from the remaining components of the sample. This is often established by comparing what is believed to be the target analyte signal (derived from a high purity standard solution) versus the background signal of the method (e.g. what is observed from the solvents etc., when the analyte is absent from the sample). Therefore, analyte selectivity is described by the measurement parameters of the analytical approach (e.g. retention time, wavelength etc). Once established, the analytical method should be able to evidence this selectivity with a high degree of precision (repeatability and reproducibility) by evaluating the replicate data acquired over continuous operation on day 1 versus that acquired on another day, respectively. The repeatability is represented by a %relative standard deviation (%RSD), and the variance from each data set is compared using a statistical Fisher´s exact test or F-test to determine if there was a significance difference, establishing the reproducibility of the process. With these calculations, a %RSD below 15% is desirable (good precision) and a calculated F-

value that is lower than the statistical measure is considered an insignificant difference between the two datasets (see Methods and Materials as to how this is applied).

Following selectivity, it is then important to characterise the relationship between analyte response and concentration of the method and its sensitivity. This former metric is key to quantifying an unknown analyte within a sample and is achieved using regression statistics by establishing the instrument response in samples where a known amount of the analyte is present. This calibration of analyte response and concentration is represented by an equation that may be derived using the regression process along with a measure of linearity (e.g. the coefficient of determination, R^2). This equation provides key information about the data set, including the gradient and level of background observed in the data (e.g. at the y-intercept) represented by the level of response observed when no analyte is present. Once established, this relationship may be used to calculate the amount of analyte within an 'unknown' sample by inputting the measured response of this sample into the equation (see Equation 1.12).

$$y = bx + a$$

Equation 1.12. Linearity Regression Equation, where b stands for the slope, a for the level of the fitted line, x the independent variable and y the dependent variable.

However, this relationship does not provide a measure of the quantitative accuracy or precision to understand the validity of the determined concentration. This is established by using the calibration relationship to determine the concentration of samples where the amount of analyte is known (e.g. through use of quality control samples or QCs). These are prepared and measured as replicate samples to establish the accuracy and precision using the equations below (see Equation 1.13 and 1.14)

$$\bar{x} = \frac{x_1 + x_2}{n}$$

Equation 1.13. Calculation of Average ($\bar{x}$). The equation of calculating the average where x_1, x_2 (etc) stands for the value of the different datasets and n for the amount of different datasets are used.

$$SD = \sqrt{\frac{(x_1 - \bar{x})^2 + (x_2 - \bar{x})^2}{n - 1}}$$

Equation 1.14. Calculation of Standard Deviation (SD). The equation for calculating the standard deviation where x_1, x_2 is the value of the different datasets, $\bar{x}$ the average of the total dataset and n the value of the amount of different datasets.

Unfortunately, instrumentation often has greater variability in determining analyte responses at extreme ends of the measurement scale (e.g. at high and low abundance). This can often skew the regression model, resulting in a relationship that doesn't fully reflect the accuracy of the dataset. This heteroscedasticity of the data is important to establish and characterise; this may be achieved by determining the weighting factor applied to the regression data that provides the lowest relative error across the calibration relationship.[25]

1.3.1. Method sensitivity: Limit of Detection (LOD) and Lower Limit of Quantitation (LLOQ)

Method sensitivity can be described as the ability of the approach to detect changes in analyte signal with concentration.[21] However, more commonly, this metric is described using the limit of detection (LOD) and lower limit of quantitation (LLOQ as this provides a more practical assessment of the ability of the method to measure the analyte. The LOD is the lowest concentration the system is able to detect using the optimised method, in addition, the LLOQ is the lowest concentration where the performance of a method is acceptable to use.[26] There are a number of approaches that may be used to describe the LOD, these can include using the analyte signal-to-noise (S/N), or a statical evaluation of a blank sample (e.g. using the standard deviation). Regulations controlling the measurement of drugs within clinical samples require both metrics to be determined, along with a lower limit of quantitation (LLOQ), which is described as the lowest concentration that provides acceptable accuracy and precision.[27] This is calculated using a low concentration QC sample where any measurements that fall below this concentration, cannot be reliably quantified using the analytical method.

1.4. Cell Viability test

Cell viability tests are necessary to figure out if the developed therapy is safe to use and what the survival chances of the cells are. Most important is to find out if the therapy is not toxic for the body.

Cell viability tests are used for dual functions in drug development.[28] During pre clinical development cell viability is tested to assess drug efficacy, in their ability to kill cells and induce

death. Furthermore, viability is also used as an important metric for wider compatibility and toxicity/safety testing.[29]

For example, cell proliferation test (XTT Kit) is a colorimetric assay whereby the viability, cellular proliferation and cytotoxicity will be determined. This test is a colorimetric assay which analyse the number of viable cells by cleavage where tetrazolium salts are added to the culture medium. The salt is cleaved to formazan by the succinate-tetrazolium reductase system, this bio-reduction occurs in viable cells only. This is related to NAD(P)H production through glycolysis. Therefore, the amount of formazan dye formed a direct correlation to the number of metabolically active cells in the culture.[30]

Another cell viability test is Real-Time Glo (RT-Glo) bioassay. RT-Glo is a bioassay generally used to determine the half-maximal inhibitory concentration (IC_{50}) of drugs. This measure represents the concentration of drug required to inhibit the relevant biological response by 50% and is used as a descriptor of drug efficacy. The RT-Glo bioassay is used to quantify the biological impact of a drug on a cell, were both potential cytotoxicity or proliferative effects of the treatments are covered. With RT-Glo, 'NanoLuc® luciferase' and a prosubstrate, 'MT Cell Viability Substrate' are introduced to cells causing the viable or alive cells to reduce the prosubstrate into NanoLuc® substrate. This generates a luminescent signal only observed with viable cells given lysed (dead) cells do not contain an intact plasma membrane and the substitution to NanoLuc® substrate is unable to form.[31]

1.5.   Research hypothesis, aims and objectives

1.5.1. Hypothesis

Currently the primary treatment of ovarian cancer (OC) is surgery with chemotherapy using platinum-based drugs. However, these chemotherapies are prone to adverse side effects and drug resistance, limiting the efficacy of the therapy.[1] GnRH receptor antagonists offers significant potential as an alternative therapy given these function via an alternative biochemical pathway that limit the proliferative and metastatic potential of cancer cells (section 1.1.2.2.) Furthermore, these drugs are known to exhibit adverse side effects such as toxicity, and appropriate mitigation measures are required for these to become a viable therapy. Encapsulation using liposomes can be an effective approach in reducing the toxic effects of a broad range drugs on healthy tissue. Liposomes can encapsulate a range of drug chemistries and are of suitable size to be taken up, in contrast to healthy cells, by cancer cells through enhanced

permeability and retention effect (EPR). This provides a therapy targeting OC cells that operates on a different biochemical pathway to platinum-based drugs which will avoid resistance against the treatment.

In this research, we investigated the biological efficacy and stability of a liposome-based nano-encapsulated GnRH-R antagonist, BAY-784, as a possible treatment for OC. By using biodegradable and highly biocompatible liposome nanovectors, we aim to circumvent any systemic toxicity ot non cancer cell effects as a result of free drug administration, however this is not tested in this pre-clinical analysis, only the cancer cell cytotoxicity of BAY-784 in both free drug and liposome encapsulated form. By characterising this drug encapsulation and release from the particle, biological efficacy and stability within the tumour environment, an analytical method was set up to quantify BAY-784. An additional analytical approach to determine the encapsulation efficiency was set up but is still in development.

1.5.2. Aims and objectives

To test this research hypothesis, we will seek to deliver the following research objectives and work programs:

Work program 1: Develop a detection method for measuring 'free' and nano-encapsulated forms of BAY-784 within neat aqueous and complex matrix (ascites and plasma) conditions.

Work program 2: Confirm the biological efficacy of ´free´ and encapsulated BAY-784.

Work program 3: Assess the efficiency and kinetics of drug encapsulation and release vs. an established drug (e.g. Doxil) under aqueous and in vitro conditions; this will include testing the drug in neat aqueous solutions, following pH adjustment to represent the tumour environment and in a complex matrix (e.g. plasma and ascites).

In work program 3, Doxil was utilised as a positive control, as it is used in clinic for treatment of recurrent and resistant Ovarian Cancer. At this late disease stage, chemotherapy resistance occurs, for reasons as yet unknown Carboplatin with paclitaxel represents the standard first-line chemotherapy regimen for ovarian cancer patients however, only 40%–60% of patients will achieve complete remission, with a high risk of neurotoxicity, which can persist more than a year after the treatment Consequently, other more efficacious or tolerable options were

evaluated, i.e. pegylated liposomal doxorubicin (PLD). It is an anthracycline encapsulated within a sterically stabilized liposome which increase the agent's circulating half-life in the body and limit its toxicity profile, significantly lowering cardiac toxicity and myelosuppression than conventional doxorubicin It is now a widely used agent for the treatment of patients with recurrent or refractory ovarian cancer, but there are not many indications as monotherapy regimen. In this study, dox was purchased from Sigma and utilised as a free drug version.

2. Chapter 2: Materials and Methods

2.1. General Laboratory Equipment

- Mettler Toledo EL204 analytical balance (4 decimal places)
- 64 Boston Road Beaumont Leys Leicester LE4 1AWFisher brand FB15012 vortex mixer
    - Bishop Meadow Rd, Loughborough LE11 5RG
- SPE Vacuum Box
- Eppendorf centrifuge 5810R
- 10 µL, 100 µL, 1 mL, 10 mL Transferpette air displacement pipettes
- Techne Sample Concentrator
- Fisher Scientific Freeze Dryer
    - Bishop Meadow Rd, Loughborough LE11 5RG
- Büchi Rotavapor
    - Unit 6, Goodwin Business Park, Willie Snaith Road Newmarket Suffolk, CB8 7SQ
- MF-Millipore® Membrane Filter, 0.45 µm & 0.2 µM pore size
- Invitrogen™ Exosome Spin Columns (MW 3000)
- Cole-Parmer Sonicator
    - 9, Orion Court, Colmworth Business Park, Ambuscade Rd, Eaton Socon, Saint Neots PE19 8YX
- NanoDrop™ One/OneC Microvolume UV-Vis Spectrophotometer
    - Bishop Meadow Rd, Loughborough LE11 5RG
- Dynamic Light Scattering (DLS)

2.2. Chemicals and consumables

2.2.1. Chemicals

Table 2.1. Chemical and standard solutions.

Chemical	CAS N°	Grade	Supplier
Acetic Acid	64-19-7	98%	Fisher Scientific
Acetonitrile	75-05-8	HPLC	
Chloroform	67-66-3	99%	
Ethanol	64-17-5	HPLC	
Ethyl Acetate	141-78-6	HPLC	
Formic Acid	64-18-6	99.44%	
4-(2-hydroxyethyl)-1-piperazineethanesulfonic acid (HEPES)	7365-45-9		Sigma Aldrich
Methanol	67-56-1	HPLC	Fisher Scientific
Phosphate buffered saline (PBS)	7647-14-5		Sigma Aldrich
Sodium Hydroxide	1310-73-2	HPLC	Sigma Aldrich
Water	7732-18-5	HPLC	Fisher Scientific
Standards			
BAY-784	1631164-24-3	95%	SGC
Doxorubicin	23214-92-8	98%	Sigma Aldrich
Cholesterol	57-88-5	99%	Sigma Aldrich
Hydrogenated soya phosphatidylcholine (HSPC)	97281-48-6	>98%	Larodan
1,2-distearoyl-sn-glycero-3-[phospho-rac-(glycerol)](sodium salt) (DSPG)	816-94-4	>98%	Larodan
Methoxypolyethelene glycol (Mw 2000)-distearylphosphatidylethanolamine (mPEG2000-DSPE)	9004-74-4		Pegworks
Gases			
Oxygen Free Nitrogen			BOC

2.2.2. Consumables

- 2 mL amber-glass Chromacol Ltd. vials

- 20 mL disposable scintillation vials

- 15 mL and 50 mL Corning Centristar centrifuge tubes

- OASIS HLB cartridge (3 cc, 60 mg)

- QuEChERS Custom Extraction Tube (Q0015-15V)

  - 4 g Magnesiumsulfate ($MgSO_4$)

  - 1.5 g Sodiumacetate (CH_3COONa)

- QuEChERS EN Fruit and Vegetable (F&V) Kit (Q0035-15V)

  - 900 mg $MgSO_4$

  - 150 mg Primary and secondary amine exchange material (PSA)

2.3.   Analytical Instrumentation

An Agilent 1220 Infinity liquid chromatography (LC) system consisting of a dual-channel gradient pump (including degasser), autosampler, column oven and diode array detector, was used throughout this project. Additionally, an Acquity QDa Waters mass spectrometer operating with an electrospray ionization source was used for further molecular confirmation.

2.4. Liquid Chromatography Separation Conditions

To maximise the resolution achievable at sub-UPLC conditions, a CORTECS T3 (3.0 x 75 mm; 2.7µM) column with a coordinating guard column (CORTECS T3: 2.1x5 mm; 2.7µm) was used for the separations. Different mobile phase compositions were tested during the method development to determine optimum separation conditions (e.g. good chromatographic peak shape and reproducible chromatography) and this was obtained using of the following mobile phase solutions:

- **Mobile phase A:** 0.1% Formic Acid (FA) in water (H_2O).
- **Mobile phase B:** 0.1% Formic Acid (FA) in acetonitrile (ACN).

These solutions were prepared by adding 500 µL of formic acid to 500 mL of water or ACN within a Wheaton bottle and mixed thoroughly before use. The column was run using a mobile phase flow rate of 500 µL/minute with the gradient elution programme shown below:

Table 2.2. Gradient LC-DAD method. Gradient method for the detection of BAY-784 and Doxorubicin with LC-DAD.

Time (minutes)	Conditions
0-3	95% A: 5% B
3-15	Linear ramp to 100% B
15-18.5	100% B
18.5-19.5	Linear ramp to 95% A : 5% B
19.5-30	95% A : 5% B
Total run time: 30 minutes	

Following the determination of the optimum injection volume on-column, 20 µL of sample was injected with the needle washed using a separate 100% ACN wash solution to minimise carryover between injections.

2.5. Liquid Chromatography Detection Conditions

2.5.1. Diode Array Detector (DAD) Parameters

To identify an appropriate detection wavelength for the target analytes, the absorbance spectrum and resulting maxima of the target molecule was first recorded over 600 nm wavelength range. The sensitivity of the diode array detector was then optimized by testing the slit and peak widths as recommended by the manufacturer, with final detection parameters shown in Table 2.3.

Table 2.3. DAD settings for detection of BAY-784 and Doxorubicin.

Parameter	Compound	Value
Wavelength	BAY-784	275 nm ± 30 nm
	Doxorubicin	480 nm ± 15 nm
Slit width	BAY-784 + Doxorubicin	4 nm
Peak width	BAY-784 + Doxorubicin	0.1 nm (5 Hz)

2.5.2. Mass Spectrometry Detection Parameters

To provide further molecular confirmation of the species observed within the chromatogram, the flow exiting the DAD was interfaced with a single quadrupole Acquity QDa Waters mass spectrometer operating with an electrospray ionization source in positive ion mode. Data was acquired using a full scan mass spectrum for precursor ion species over the mass range *m/z* 100-1000 and using the conditions highlighted in Table 2.4.

Table 2.4. QDa Mass spectrometer settings. Settings were used to detect BAY-784.

Source conditions	
Spray voltage	0.8 kV
Cone voltage	15 V
Ionization Mode	ES+
Source Temperature	120 °C
Probe Temperature	600°C

2.6. Standard solutions

2.6.1. Stock and sub-stock solutions

The target analytes used in this study are high-value materials with BAY-784 in particular, in short supply. As a result 1 mg/mL stock solutions were made from solid reference materials using the following conditions and vortexed to ensure the material was completely dissolved:

BAY-784: 1 mg of material was weighed into an amber glass Chromacol vial and 1 mL of ethanol added.

Doxorubicin: 1 mg of material was weighed into an amber glass Chromacol vial and 1 mL of water added.

Given no target analyte stability data was available for BAY-784 at the start of this study, the stock solution was aliquoted into smaller volumes of 1000 and 1500 µL and stored at -80 °C to minimise impact of thermal and freeze-thaw degradation. For Doxorubicin, the stock solution was stored at -20 °C in accordance with SDS of this compound.[32]

To achieve the desired dilution factor for the calibration standards and quality control (QC) samples, a 10 µg/mL sub-stock of each solution was prepared by diluting 10 µL of target analyte stock solution.
into an amber glass vial with 1 mL of ethanol:water (50/50%) mixture (BAY-784), or 1 mL of acetonitrile:water (50/50%) mixture (Doxorubicin), and vortexed before use.

2.6.2. Calibration and Quality Control (QC) samples

Calibration standards and quality control samples were prepared by diluting the 10 µg/mL sub-stock solution following the concentration and volumes showed in Tables 2.5 and 2.6. Given the smaller volumes of these samples, these were prepared in amber-glass vials as above but containing 200 µL insert vials to reduce the impact of sample evaporation and mis-injection due to low sample volumes.

Table 2.5. Volumes for preparing calibration of BAY-784 and Doxorubicin.

Stand-ard	Concentration (ng/mL)	Sub-stock solution (µL)	Mobile phase (µL)
S1	500	10	190
S2	1000	20	180
S3	1500	30	170
S4	3000	60	140
S5	4000	80	120
S6	5000	100	100

Table 2.6. Volumes for preparing quality control (QC) samples of BAY-784 and Doxorubicin.

QC	Concentration (ng/mL)	Sub-stock solution (µL)	Mobile phase (µL)
Low	1000	20	180
Medium	2000	40	160
High	4500	90	110

2.7. Preparation of liposomes

The liposomes were prepared using a thin-film hydration method; here the lipids were assembled by following the protocol below, using a total lipid concentration of 50mM with a ratio of constituents of 65/10/10/5. For the encapsulation of BAY-784, 100 µL of 1 mg/mL was added as drug load.

Table 2.7. Lipid contents and mass for preparation of liposomes.

Lipid	Mass (mg)
Hydrogenated soya phosphatidylcholine (HSPC)	127.5
1, 2-distearoyl-sn-glycero-3-[phospho-rac-(glycerol)] (sodium salt) (DSPC)	20
Cholesterol (CHOL)	10
methoxypolyethelene glycol (Mw 2000)-distearylphosphatidylethanolamine (mPEG2000-DSPE)	34.8

1. The lipids and payload were co-dissolved in 5 mL of chloroform as per the amounts in Table 2.7 and evaporated for 3 hours, in total, on a rotary evaporator at 474 mbar, 40°C (2h), then down to 0 bar (1h) for dryness.

2. To ensure the samples are completely dry these were placed in freeze drier for at least a further 3 hours (or during overnight).

3. Samples were then rehydrated with 10 mL 20mM HEPES buffer (pH 7.4 with 1% sucrose) and continuously mixed under nitrogen gas at 60°C for 1 hour and sonicated for 5 minutes in a bath sonicator, delicate mode, at room temperature (20°C).

4. To remove undesirable aggregates the sample was filtered through 0.2 µM filters (e.g. Millex-GP Syringe Filter) and Spin column filters to remove free drug (when using NMR for testing encapsulation efficiency and using liposomes for bioassays).
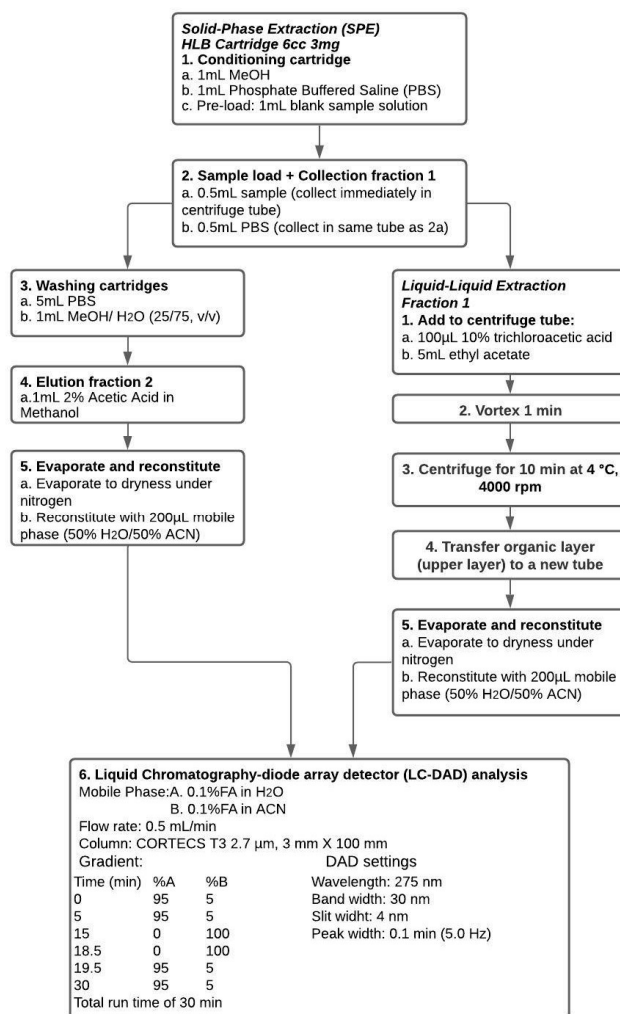
2.8. Analysis of nanoparticles with dispersive light scattering

Dispersive light scattering (DLS) is a technique that can be used to determine the size and size distribution of small particles in solutions by applying laser light onto the solution which causes scattering by different intensities.

1. Add 100µL of 20mM HEPES solution in a cuvette that is appropriate for DLS.
2. Measure this solution as a blank by placing the cuvette in the DLS.
3. Add 100µL of liposome solution in a cuvette that is appropriate for DLS.
4. Measure this solution as sample.

2.9.Analyte extraction for LC-DAD(MS) analysis

The sample preparation approach investigated within this project intended to measure both the amount of drug that had been encapsulated within the liposome and 'free' non-encapsulated drug. This was to mitigate any misinterpretation of encapsulation efficiency where the drug may exhibit improper encapsulation by becoming associated with the exterior of the liposome. This approach was initially tested by Zhong et al.[33] for liposome encapsulated vincristine however, to the best of our knowledge, the use of this approach for BAY-784 remained un-investigated. This method used a combination of solid-phase extraction (SPE) and liquid-liquid extraction (LLE) as a 2-stage protocol to separate the encapsulated and non-encapsulated drug from matrix (and each other - Stage 1, SPE), and then extract the drug from within the liposome (Stage 2, LLE). Each stage was tested and optimized independently to ensure appropriate drug recovery. For example, based on the data derived from the LC conditions, stage 1 was optimized by replacing the methanol solvent in each step with acetonitrile during the SPE process how-ever, superior performance with methanol led to this being used for future work. Furthermore, Stage 2 was optimized for the differing drug chemistries and by replacing the LLE protocol with QuEChERS to test if reduced matrix effects were observed. The general approach is showed in Figure 2.8.

Solid-Phase Extraction (SPE)
HLB Cartridge 6cc 3mg
1. Conditioning cartridge
a. 1mL MeOH
b. 1mL Phosphate Buffered Saline (PBS)
c. Pre-load: 1mL blank sample solution

2. Sample load + Collection fraction 1
a. 0.5mL sample (collect immediately in centrifuge tube)
b. 0.5mL PBS (collect in same tube as 2a)

3. Washing cartridges
a. 5mL PBS
b. 1mL MeOH/ H_2O (25/75, v/v)

4. Elution fraction 2
a.1mL 2% Acetic Acid in Methanol

5. Evaporate and reconstitute
a. Evaporate to dryness under nitrogen
b. Reconstitute with 200µL mobile phase (50% H_2O/50% ACN)

Liquid-Liquid Extraction
Fraction 1
1. Add to centrifuge tube:
a. 100µL 10% trichloroacetic acid
b. 5mL ethyl acetate

2. Vortex 1 min

3. Centrifuge for 10 min at 4 °C, 4000 rpm

4. Transfer organic layer (upper layer) to a new tube

5. Evaporate and reconstitute
a. Evaporate to dryness under nitrogen
b. Reconstitute with 200µL mobile phase (50% H_2O/50% ACN)

6. Liquid Chromatography-diode array detector (LC-DAD) analysis
Mobile Phase: A. 0.1%FA in H_2O
B. 0.1%FA in ACN
Flow rate: 0.5 mL/min
Column: CORTECS T3 2.7 µm, 3 mm X 100 mm

Gradient:			DAD settings
Time (min)	%A	%B	Wavelength: 275 nm
0	95	5	Band width: 30 nm
5	95	5	Slit width: 4 nm
15	0	100	Peak width: 0.1 min (5.0 Hz)
18.5	0	100	
19.5	95	5	
30	95	5	
Total run time of 30 min			

Figure 2.8. Proposed analytical approach of determining the encapsulation efficiency according to Zhong et al.[19]

The sample preparation techniques were evaluated using the method set out by Matuszewski et al.,[34] using spike before extraction (SBE) and spike after extraction QCs to test recovery and matrix effects. These are essentially samples where known amounts of analyte are spiked prior and after the extraction, (SBE and SAE, respectively) as:

- **SBE** - samples prepared in 50 mL centrifuge tubes using 500 µL of HEPES solution with medium and high spike concentrations, respectively 40 µL and 90 µL of drug was added, extracted, evaporated to dryness under a gentle stream of nitrogen and reconstituted in 200 µL of mobile phase.

- **SAE** - samples were prepared in 50 mL centrifuge tubes as a solution of acetonitrile: water (50:50%) was added to a liposome solution which gives a total amount of 500 µL. After extraction and reconstitution, medium and high spike concentrations were added

which are respectively, 40 µL and 90 µL of the drug of interest. These were added to the end solution in a total amount of 200 µL.

2.6. Statistical Analysis

To support the data of the method, some statistical analyses were performed. These tests are briefly described below.

2.6.1. Repeatability and Reproducibility

These calculations were determined for the chromatographic retention time and peak area of the target analyte to establish the repeatability (%RSD, see Equation 2.1.), and the variance (using a Fisher′s exact test or F-test, see Equation 2.2.) from data sets derived from 10 repeat measurements on one day, to a further 6 measurements on another day. With these calculations, a %RSD below 15% is desirable (good precision) and a calculated F-value that is lower than the statistical measure is considered an insignificant difference between the two datasets.

$$\%RSD = \frac{SD}{\bar{x}} * 100\%$$

Equation 2.1. Relative Standard Deviation (RSD) equation. Standard Deviation (SD) is divided by the average ($\bar{x}$) of a dataset.

$$F = \frac{S_1^2}{S_2^2}$$

Equation 2.2. Equation representing the Fisher′s exact test, where the ratio of the variance for each data set (1 and 2) are compared to a statistical value derived from an F-table.

2.6.2. Calibration statistics, quantitative accuracy and precision

The calibration of analyte response and concentration was determined using linear regression and a number of weighting factors evaluated to determine the heteroscedasticity of the data and the relationship that provided the lowest relative error (%) and the best linearity (e.g. the coefficient of determination, R^2, closest to 1). To provide a measure of the quantitative accuracy or precision, the concentration of replicate QC samples (of known concentration was determined and the values used in the equations below (see Equation 2.3 and 2.4).

$$\%Accuracy = \left[\frac{Measured\ concentration - theoretical\ concentration}{Theortetical\ concentration} \right] \times 100$$

Equation 2.3. Equation describing the accuracy of the measured concentrations derived from the calibration graph.

$$\%Precision = \left[\frac{Standard\ deviation\ of\ the\ measured\ concentration}{Mean\ of\ the\ measured\ concentration} \right] \times 100$$

Equation 2.4. Equation describing the precision of the measured concentrations derived from the calibration graph.

2.6.2.1. Limit of Detection (LOD) and Lower Limit of Quantitation (LLOQ)

The LOD was determined using both the S/N and a statistical assessment of the background signal. These were established using the formula shown in equation 2.5.

$$LOD = y_B + 3s_B$$

Equation 2.5. Limit of Detection. Equation of LOD where yB is blank signal and SB the standard deviation of blank sample.

To establish the LLOQ, triplicate QCs were prepared at a concentration near the lowest calibration standard. A valid LLOQ was deemed to be a concentration where both the accuracy and precision were below 20%.

2.6.3. Stability

Stability testing of a method was done by using replicate QCs prepared and stored under the relevant test conditions and measured against those that were prepared fresh on the day of analysis. Storage conditions included post-preparation (e.g. on the autosampler), 24 h at benchtop conditions, and within a -20ºC freezer for short- and medium-term storage (see Chapter 3, Section 3.3.4). As an evaluation of stability, the %RSD of the analyte response of these samples was determined where a %RSD < 15% for medium and high QC samples, and %RSD < 20% for low QC samples was deemed acceptable stability.

2.6.4. Encapsulation NMR methodology

A 500MHz Bruker nuclear magnetic resonance (NMR) instrument was used to collect all ^{1}H spectra. Deuterated HEPES was used to fabricate liposomal formulas to be used in NMR analyses. Output spectra were analysed in MestraNova and the encapsulation efficiency (EE) was calculated using equation 2.6.

$$Encapsulation\ efficiency\ (EE\%) = \frac{drug\ in\ particles}{drug\ used\ in\ NP\ fabrication}\ x\ 100$$

Equation 2.6. Encapsulation efficiency (EE%). Calculation of EE% where the drug that is practically found in nanoparticles is divided by the amount of drug that is added at the beginning of the process.

2.7. Efficacy Testing

Efficacy testing is done by using bioassays for monitoring the cell activity during treatments with the drug. For the efficacy tests, OVCAR-3 and SKOV-3 ovarian cancer cell lines were used as it is known that these cell lines has the GnRH-R.[35]

2.7.1. Real-Time Glo

For determining the IC_{50} of the drug on the cell lines, a well know bioassay is used. The Real-Time Glo bio-assay is based on the activity of the cells by adding NanoLuc® luciferase' and a prosubstrate, 'MT Cell Viability Substrate', to activate a luminescence process.

1. Seed in a luminescence 96-well plate, 24 hours prior to treatment:
    a. OVCAR-3: 3000 cells/100 µL
    b. SKOV-3: 500 cells/100 µL
2. Check after 24 hours if the cells have grown in the well plate.
3. Take off old media and wash with 100 µL.
4. Treat cells with 50 µL RT-Glo reagents whereby the final mixture 1:1000 solution is which is made up in appropriate media.
5. Treat cells with 50 µL of BAY-784 (end concentration of 50µM) solutions in appropriate media.
6. Incubate the cells for at least 1 hour.
7. Incubate the spectrophotometer at 37°C and read on the FLUOstar Omega spectrophotometer.

3. Chapter 3: Analytical Method Development

3.1. Introduction to analytical method development

The aim of analytical method development is to establish a process for the reliable detection of the target analyte, which is then optimised to ensure analyte sensitivity. The selectivity of the method for the target analyte is essential for detection with confidence, as it indicates that the chromatographic system is able to distinguish the analyte in amongst other sample components and is especially important for complex sample matrices. Without reliable selectivity and sensitivity, qualitative and quantitative measurement of the target analytes are not possible. Furthermore, these underpin additional method characteristics or 'figures of merit', with the following typically required for analyte quantitation: linearity, dynamic range, reproducibility, repeatability, LOD and LLOQ. However, other parameters may also be required depending on the degree of sample preparation and the regulatory frameworks within the sector (e.g. analyte recovery, matrix effects, stability etc.). Given this project is concerned with the feasibility testing of a new therapeutic (BAY-784), the aim of this chapter was to develop a quantitative method for a more accurate measurement of both BAY-784 and a gold standard nanotherapeutic (doxil) using LC-DAD during the encapsulation studies. We also aimed to explore the potential of combining these protocols for a dual measurement method of using similar concentrations. The analytical method has been developed and evaluated using FDA guidelines, where key parameters noted above have been evaluated. For this work, a diode array detector (DAD) was used for convenience of operation given BAY-784 was not available with an isotopically labelled internal standard. However, given the analytical method information from past testing of this drug was unavailable prior to evaluation, the chromatographic system and detector were characterised and optimised to ensure the reliable analyte detection, and included optimising the detection wavelength, column, solvent and gradient/isocratic elution conditions.

3.2. Initial selectivity and sensitivity

Following the theory described in Chapter 1, section 1.2.2., the absorption wavelength of the target analyte will be directly related to the chemical structure (chromophoric groups) of the analyte. To provide the best sensitivity for detection, the peak maxima should be selected. However, given BAY-784 has a selection of bonds that can absorb energy from the operating wavelength range of the DAD detector, a spectrum was initially recorded over a broad wavelength range (190-600 nm) using an analyte standard where a signal was clearly observed from the background noise (e.g. 5 µg/mL). Following baseline correction using the automated

reference spectrum function within the software, the resulting analyte spectrum showed two peaks within the wavelength range (at ~210-220 nm and 275 nm). Given signals below and around 200 nm are less specific due to the involvement of (σ and some π) bonding associated with a much greater number of chemical structures (including solvents) these wavelengths are more prone to signal interference, particularly when dealing with complex mixtures where chromatographic resolution cannot be achieved. Therefore, despite having a lower response the second peak for BAY-784 at a wavelength of 275 nm was chosen for further testing, see Figure 3.1.
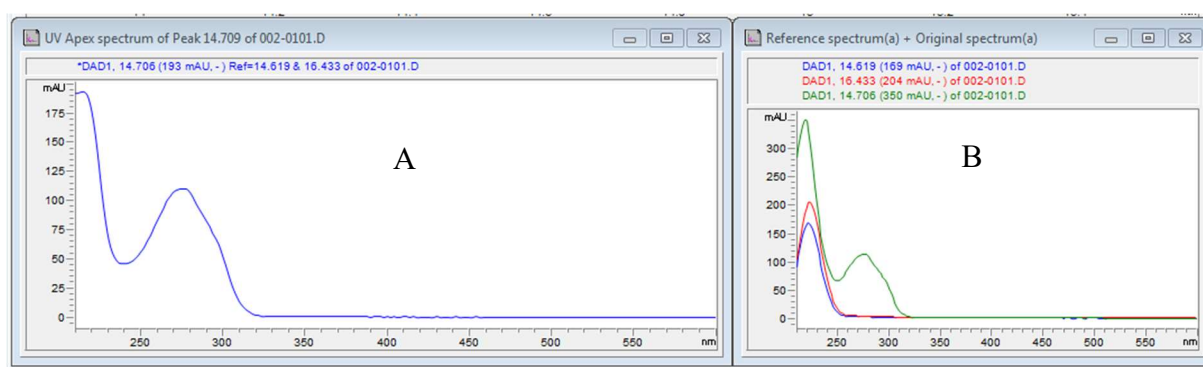
Figure 3.1. A) Spectrum of a 5000 ng/mL BAY-784 sample. Detection is performed using standard settings for Diode Array Detector, which are recommended in the manual: Peak width of 0.1 min; slit width of 4 nm and a band width of 4 nm. B) Reference spectrum that is used for.

3.2.1. Chromatographic separation

Because of the lack of analytical method information on BAY-784, a general chromatographic approach was adopted based on the analyte chemical structure. Given the hydrophobic content of the chemical structure, reversed-phase chromatography was selected, and in particular, a T3 Cortecs column with a particle size of 2.7 μm. The T3 stationary phase is a highly durable packing with improved resistance to dewetting and, has shown good suitability for both polar and non-polar analytes due to the presence of a silanol base group. These characteristics were deemed highly desirable for this project as it offered greater flexibility with method development, and greater coverage of more polar materials (e.g. potential metabolites) for future work. Furthermore, the T3 column was also available in a sub-3 μm particle size without needing UPLC instrumentation; this offered significant potential gains in terms of peak resolution and column efficiency for enhanced separations on the LC system used in this work.

Following column selection, a number of 'reversed-phase' compatible solvents were tested for the elution of BAY-784 using a broad gradient elution method (see Table 3.1) to provide the best possible chance of analyte retention and elution.

Table 3.1. Gradient program LC-DAD method.

Time (min)	A H$_2$O w 0.1%FA (%)	B ACN w 0.1%FA (%)	Flow (mL/min)
0	95	5	0.5
2	95	5	0.5
15	0	100	0.5
20	0	100	0.5
21	95	5	0.5
30	95	5	0.5

Methanol (MeOH) and Acetonitrile (ACN) are commonly used organic mobile phases in reversed-phase LC and were selected for testing. Of these ACN has particular advantages given it is considered a stronger eluent, see eluotropic values in Table 3.2, and more likely to elute more hydrophobic analytes. With a lower UV cut-off, ACN is also known to exhibit less signal interference during the chromatographic separation, offering greater sensitivity at lower detection wavelengths. However, given MeOH is a much cheaper solvent to purchase, this was tested to reduce the costs of the analysis. Furthermore, given BAY-784 contains acidic groups, formic acid was also added to the solvent to reduce the presence of any secondary interactions on column and improve peak shape.

Table 3.2. Eluotropic and UV cut-off values of eluent solvents.

Mobile phase	**Eluotropic values**			UV cut-off
	Alumina	*C18*	*Silica*	**(nm)**
Methanol	0.95	1.0	0.7	210
Acetonitrile	0.65	3.1	0.52	190
Water	-	-	-	-

Pleasingly, both solvent systems showed good Gaussian peak shapes, with a peak width of less than 0.1 minutes, providing a high column efficiency of 3.0×10^5 as expected from the T3 column, potentially enabling the separation of more analytes (and complex samples) during the analysis (see Figure 3.2 and 3.3.).
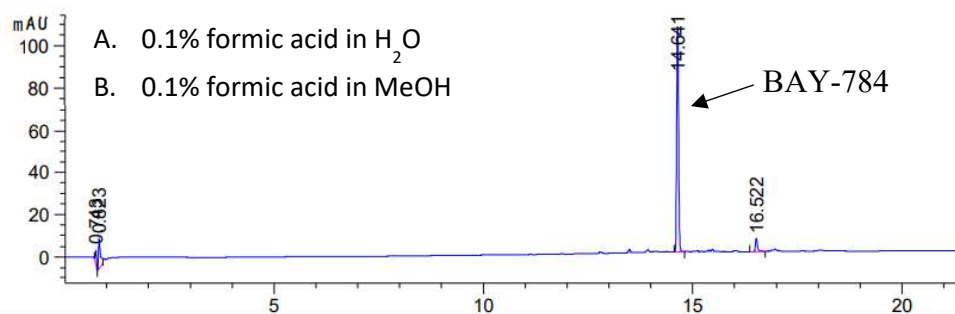
Figure 3.2. Chromatogram of BAY-784. Sample concentration of 5000 ng/mL with a retention time of 14.641 min. Detection is performed with LC-DAD method using H_2O and MeOH as mobile phases.
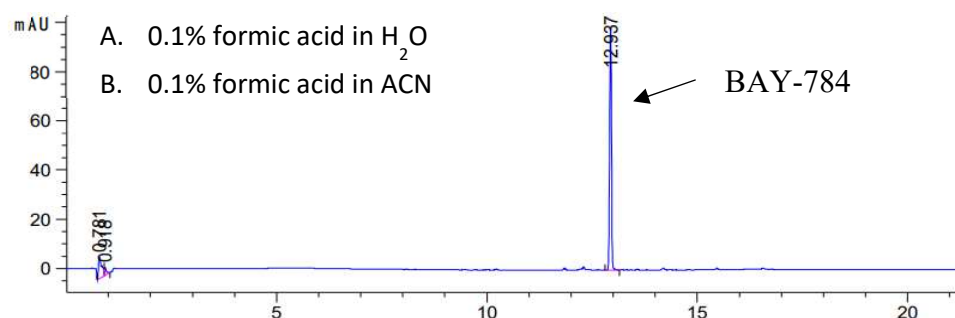
Figure 3.3. Chromatogram of BAY-784. Sample concentration of 5000 ng/mL with a retention time of 12.937 min. Detection is performed with LC-DAD method using H_2O and ACN as mobile phases.

However, the elution strength of MeOH was insufficient for BAY-784, where the analyte was observed to elute near the wash stage of the gradient profile (97% methanol) and was deemed more likely to experience poor selectivity and signal interference with other analytes that may be washed off the column. As expected, ACN showed a greater elution strength (represented by the eluotropic value, see Table 3.2.) on the reversed-phase sorbent with BAY-784 eluting at 85% ACN, providing greater controlled elution and protection against interference from co-eluting species. Sadly, after several repeat injections of the sample, the chromatography appeared irreproducible with inconsistent signal intensity. Due to lack of information about this drug, it is hard to give a direct answer were this irreproducibility comes from, but we suggest that the drug is building up somewhere in the system. To overcome this, the gradient profile was adjusted to stabilise the system during the run. Specifically, the duration of the conditioning period following injection and after the organic solvent wash was increased (see Table 3.3).

Table 3.3. Gradient program which is used in the results of Figure 3.4.

Time (min)	A H$_2$O w 0.1%FA (%)	B ACN w 0.1%FA (%)	Flow (mL/min)
0	95	5	0.5
5	95	5	0.5
15	0	100	0.5
18.5	0	100	0.5
19.5	95	5	0.5
30	95	5	0.5

However, this change caused a shift in the retention time for BAY-784 from 12.8 minutes to 14.2 minutes. This was not an ideal situation as BAY-784 was eluting close to the wash at ~92.4% B, and some inconsistency was still observed. As a result changes were made to the sample solvent composition; from the information available for BAY-784, ethanol was recommended to solubilise the analyte at 1 mg/mL.[15]Given this was different to the selected organic mobile phase, the samples were prepared in H$_2$O: ACN (50/50%) to avoid any issues of chromatographic incompatibility. Additionally, an extra wash step was added, along with a needle wash of 100% acetonitrile to prevent carry over and accumulation of the compound in the system. Pleasingly, these adjustments resulted in a stable chromatographic profile and signal, whilst maintaining sufficient signal intensity at lower concentrations, see appendix 3.

3.2.2. Optimization of detection conditions

Different aspects of the diode array detector (DAD) were optimised for sensitivity, including the optics and data acquisition parameters. For example, the slit width controls the size of the aperture from the lamp to the grating of the DAD. This is important for sensitivity as a wider slit width can provide greater light transmission (and signal intensity, with lower background noise) but, given this can be at the expense of resolution, this can pose greater difficulties in distinguishing between different wavelengths. The second aspect that was optimised was the peak width; this is the response time which describes how fast a detector follows a sudden change of absorbance signal in the flow cell to record the spectrum. This is especially important to increase the S/N ratio were, a smaller peak width should be more sensitive for the detection of the target analyte entering the flow cell. Finally, the band width or the span of the recorded wavelengths was optimised. This is analyte dependent and can be changed to incorporate a higher proportion of the absorbance maxima of the analyte to provide maximum sensitivity. For example, when the wavelength is set on 275 nm and the band width is 4 nm, the detector will register from 273 – 277 nm, providing more of the peak absorbance for detection.

Three different slit widths were tested at 1, 4 and 16 nm as per the manufacturer's recommendations. Of these the highest signal intensity was obtained with a 4 nm slit width with a peak are of 332 mAU and a S/N of ~110 mAU as shown in Table 3.4. As expected, altering the peak width showed no significant difference on the overall peak area, however, a smaller peak width provide greater resolution with the highest abundance of those recorded. This was important given a drop in S/N of ~100:1 to 38:1 was observed by increasing the peak width value from 0.1 to 0.4 minutes (see Figure 3.4.). For the bandwidth, again the manufacturer's recommendations were followed with 4, 12, and 30 nm tested. Sadly, despite 4 and 12 nm showing marginally higher signal intensities, the chromatographic response did vary on the lower concentrations. Therefore, a 30 nm bandwidth was selected as a compromise as this provided decreased variability in signal intensity, essential for reliable analyte quantitation.

Table 3.4. Settings of DAD. Optimization values for DAD.

Optimisation parameter	Parameter setting	Peak area	S/N (mAU)	Peak width at half-height (min)
Slit width	1 nm	332.671	106.6	0.06
	4 nm	332.522	106.1	0.06
	16 nm	326.021	104.2	0.06
Peak width	0.1 min	332.522	106.1	0.06
	0.2 min	332.209	65.6	0.1
	0.4 min	332.399	34.4	0.2
Band width	4 nm	332.522	106.1	0.06
	12 nm	328.624	105.8	0.06
	30 nm	301.380	97.4	0.06
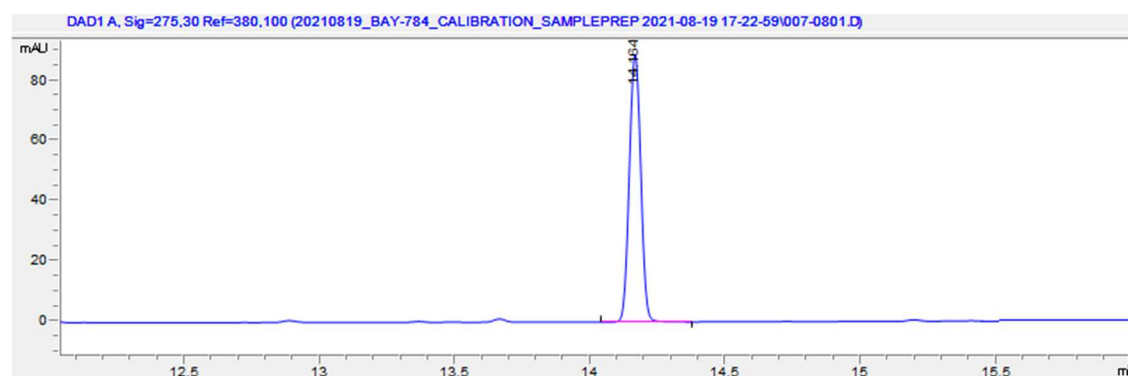
Figure 3.4. Chromatogram of BAY-784. Sample concentration of 5000 ng/mL with a retention time of 14.2 min. Detection is performed with LC-DAD method using H_2O and ACN as mobile phases. Gradient program is as shown in Table 3.4.

3.2.3. Chromatographic Repeatability and Reproducibility

To ensure confident assignment of the target analyte, reliable chromatographic and detection conditions are required. This includes an absence of carryover from the previous sample and retention time stability given the latter metric will be used to discriminate the analyte from other components, along with spectral wavelength. Repeatability (within batch) and reproducibility (between batches) is the variation in data under these conditions and may be represented by a %relative standard deviation (%RSD) and a Fisher´s exact test or F-test (see Methods and Materials section for further information). To assess carryover and the variability in chromatographic retention, To assess carryover and the variability (repeatability and reproducibility) in chromatographic retention, multiple repeat injections of a high concentration standard were recorded (n=10, and n=6) over different days followed by blank samples (see Methods and Materials section for further in-formation). Pleasingly, no evidence of carryover was observed and highly repeatable chromatography with an %RSD 0.021% and 0.013% acquired for day 1 and day 2, respectively. These values were not significantly different between separate days as shown by an F-calculated value that is lower than the critical value (see Table 3.5), indicating that the retention time offers a stable and repeatable measurement to identify BAY-784.

Table 3.5. Overview results of the reproducibility testing of BAY-784. Using a concentration of 5000 ng/mL and injecting the same solution 16 times in total over 2 days. This passed the F-test which means that the variability in retention time is not significant over 2 days.

Retention time Reproducibility		F-calculated value retention time	N = 10 and 6 F (9,5) critical value = 6.681		Pass?
Compound	**BAY-784**	3.33	6.681		Y

3.3. Quantitative performance

3.3.1. Injection repeatability and reproducibility

Repeatability and reproducibility of the analyte peak area is an essential aspect for accurate and reliable quantification as it can represent the reliability of the injection process, the amount of analyte degradation during the batch and the amount of analyte retained on the column. To assess the variability of the peak area multiple repeat injections of a high concentration standard were recorded (n=10, and n=6) and integrated using the automated processing algorithm within ChemStation. This data showed highly repeatable peak areas with an %RSD of 0.21% and 0.1% for day 1 and day 2, respectively. This also continued between separate days as indicated by an

F-calculated value of 4.75 (see Table 3.6.), indicating a stable and repeatable measurement, providing confidence that the amount of analyte injected and retained on the column will be consistent to quantify BAY-784.

Table 3.6. Overview results of the repeatability reproducibility testing of BAY-784. Using a concentration of 5000 ng/mL and injecting the same solution 16 times in total over 2 days. The repeatability data passed with the F-test which means that the repeatability the change in peak area is not significant over 2 days and is reproducible.

Peak Area Reproducibility		F-calculated value peak area	N = 10 and 6 F (9,5) critical value = 6.681		Pass?
Compound	**BAY-784**	4.75	6.681		Yes

3.3.2. Evaluation of Quantitative Calibration

The calibration graph shows the relationship between the analyte response and the concentration. The calibration graph is modelled using regression statistics, however, there are assumptions made with the variation in data in terms of homoscedasticity between the calibration range. Homoscedasticity represents the variance of the regression line; data is homoscedastic when the error or variance between dependent and independent variables is similar throughout the concentrations tested. If this is not the case, it is called heteroscedasticity. However, the true variability of the data may be better represented using a weighting factor given the error observed in the detector response is largely different for the range of concentrations with the calibration graph. Most used factors are x (no weighting), $\frac{1}{x}$ and $\frac{1}{x^2}$ where x is the nominal concentration.

To cover the anticipated concentration range of ng-µg/mL, which is based on the amount of drug that will be found (derived from previous drug information), and the operating sensitivity of the detector, the dynamic range used for BAY-784 spanned 500-5000 ng/mL. The coefficient of determination achieved for these concentrations generally showed a good degree of linearity with an R^2 >0.98. The homoscedasticity of the data was examined along with that for additional weighting factors ($\frac{1}{x}$ and $\frac{1}{x^2}$). From this evaluation, linear weighting was found to provide the lowest relative error for the initial calibration data set, and deemed homoscedastic however, subsequent data sets showed minor heteroscedasticity, with marginal difference between the relative errors observed for each weighting factor. This was unexpected (and unexplained as no

evidence of carryover was observed) and therefore, each calibration data set was individually tested, with the most appropriate weighting factor used for the quantitation.[36]
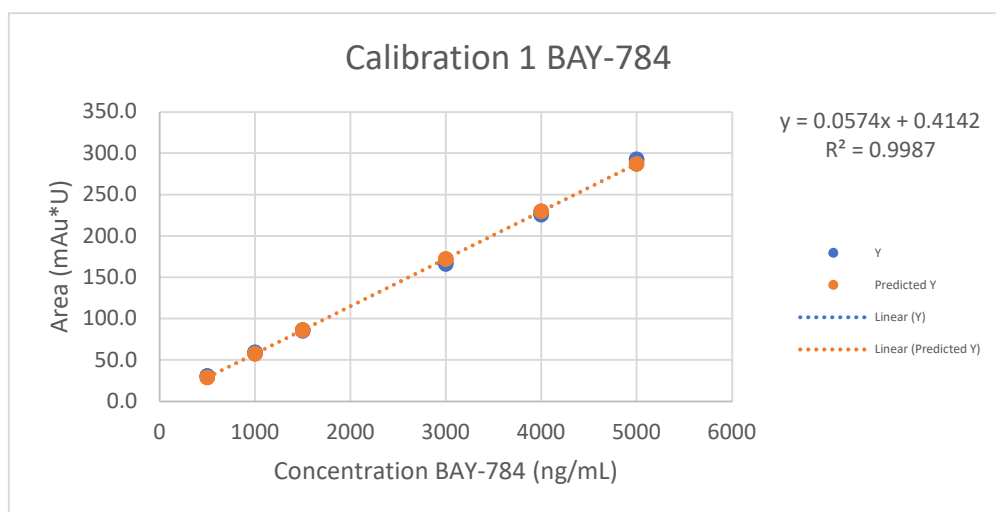
Figure 3.5. Calibration graph of BAY-784. The area is plotted against the concentration in ng/mL. The formula that is formed with this linear line is y= 0.0574x + 0.4142.
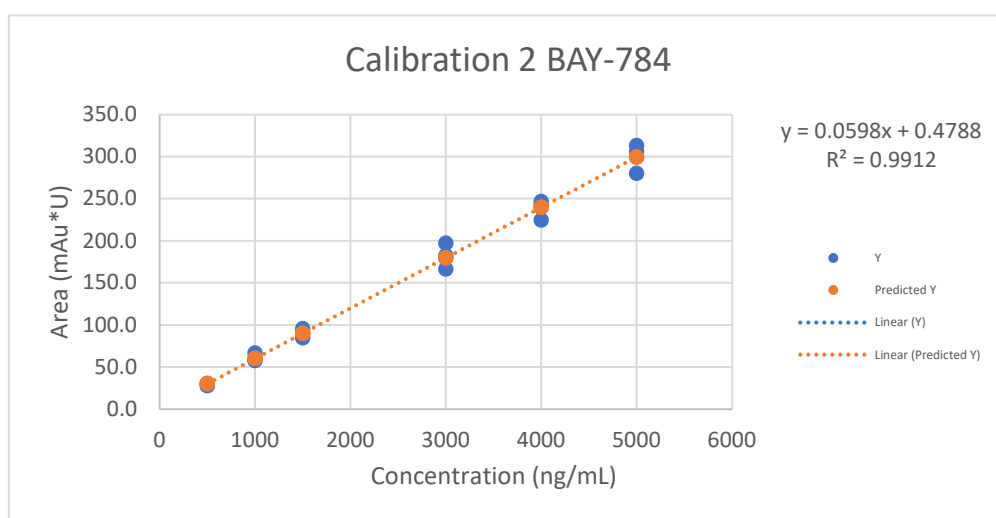
Figure 3.6. Calibration graph of BAY-784. The area is plotted against the concentration in ng/mL. The formula that is formed with this linear line is y= 0.0598x + 0.4788.

For the determination of the sensitivity, the LOD was calculated as per the equations within Chapter 2.6. The calculated LOD is 219-1570 ng/mL indicating the operational limits of the analytical method.

3.3.3. Accuracy and precision (QCs)

To establish the accuracy and precision of the quantitative measurements a set of samples containing a known amount of the analyte of interest (e.g. quality control (QC) samples) are measured as replicates at varying concentrations throughout the dynamic range. In this case, triplicate samples were prepared at a low, medium and high concentration within the calibration range, where the low QC was placed above a S/N of 10 to ensure this is above the LOD. Throughout the method development calibration batches, good accuracy and precision were observed across the concentration range (see Table 3.7) for an example data set and Appendix 1. For example, the accuracy of the QC samples is less than 8% across the concentration range, with an optimum at medium QC levels (of <6%). Furthermore, the precision is at acceptable levels lower than 2.5% RSD. Together it indicates that the method is capable of determining quantitative results within this concentration range with an acceptable degree of accuracy and precision.

Table 3.7. QC samples results of BAY-784. QC samples with accuracy and precision results.

QC Level	Area (mAU)	y	Theo Conc	20%	15%	P/F FDA	Accu-racy	Mean Conc	St Dev	%Acc Mean	% Prec
Low 1	56.3597	945.66	1000	200		P	-5.43				
Low 2	56.9619	955.59	1000	200		P	-4.44	953.67	7.25	-4.63	0.76
Low 3	57.2155	959.77	1000	200		P	-4.02				
Medium 1	112.9609	1879.21	2000		300	P	-6.04				
Medium 2	118.2548	1966.52	2000		300	P	-1.67	1933.42	47.33	-3.33	2.45
Medium 3	117.5279	1954.53	2000		300	P	-2.27				
High 1	251.6792	4167.16	4500		675	P	-7.40				
High 2	252.5246	4181.10	4500		675	P	-7.09	4181.44	14.46	-7.08	0.35
High 3	253.4323	4196.07	4500		675	P	-6.75				

3.3.4. Stability (working solution/sub-stock)

In line with guidance documents for measuring therapeutics [36], analyte stability was determined under selected conditions to ensure the integrity of the standard solutions derived from the reference material. Furthermore, this was particularly important for this project given the limited standard reference material available. The standard reference material was prepared as a stock solution in ethanol (based on initial data) and aliquoted into multiple stock solutions that were stored in -80°C to help mitigate any degradation of the material. Therefore, the stability studies here concerned assessing the analyte following storage of sub-stock and working solutions (QCs) for 24 hours on an autosampler (AS), two freeze-thaw cycles and at -20°C within a freezer for up to 4 weeks. Acceptable stability (within 20% deviation) over these conditions would provide confidence of analyte integrity during the analysis and enable the re-use

of solutions to reduce the wastage of standard solutions. Each stability study was assessed using freshly prepared triplicate QCs covering the concentration range and stored under the relevant conditions and compared against calibration standards and QCs that were prepared fresh on the day of analysis. Pleasingly, the data showed no significant difference in the levels of BAY-784 over a 24-hour period on the AS (see Table 3.8), with accuracies that were within 6% of the theoretical concentration across the concentration range. This data also showed a high degree of reliability with precisions under 2 %RSD, indicating that BAY-784 is stable on the autosampler for at least 24 hours.

Table 3.8. QC samples results of BAY-784. QC samples with accuracy and precision results for autosampler stability test.

QC Level	Area (mAu)	y	Theo Conc	20%	15%	P/F FDA	Accu-racy	Mean Conc	St Dev	%Acc Mean	% Prec
Low 1	58.53	970.45	1000	200		P	-2.96				
Low 2	58.61	971.83	1000	200		P	-2.82	971.52	0.96	-2.85	0.10
Low 3	58.64	972.29	1000	200		P	-2.77				
Medium 1	115.30	1919.52	2000		300	P	-4.02				
Medium 2	116.18	1934.20	2000		300	P	-3.29	1941.18	25.87	-2.94	1.33
Medium 3	118.31	1969.83	2000		300	P	-1.51				
High 1	255.49	4263.13	4500		675	P	-5.26				
High 2	255.44	4262.27	4500		675	P	-5.28	4258.22	7.76	-5.37	0.18
High 3	254.66	4249.27	4500		675	P	-5.57				

To determine the analyte degradation following multiple freeze-thaw cycles (n=2) of the sub-stock solutions in 50:50 ethanol:H_2O, and help estimate the stock solution stability, replicate sub-stocks were stored at -80°C and brought up to room temperature prior to preparing triplicate QCs of relevant concentrations. Testing these sub-stocks, see Table 3.9, showed that BAY-784 exhibited reliable stability in this solvent mixture over two freeze-thaw cycles with data within 6.7 %RSD and accuracies of less than 13% over the concentration range.

Table 3.9. Summary of sub-stock stability results of BAY-784.

Theoretical Conc (ng/mL)	Mean Conc	St Dev	%Acc Mean	% Prec
1000	874.29	60.00	-12.57	6.70
2000	1981.34	119.00	-0.93	5.84
4500	4606.89	241.91	2.38	5.25

Further stability studies concerned the usage of the sub-stock and working solutions following storage of the sub-stock at -20°C over a 2- and 4-week period to facilitate storage under more typical conditions. Again working (QC) solutions were prepared from these sub-stocks and compared to freshly prepared samples. These QCs again showed good stability, with little

difference observed across the concentration range apart from one measurement (see Table 3.10). However, given the good degree of precision across all other QCs, this suggests that the deviation in concentration may be due to alternative sources of error such as those associated with the injection or sample preparation.

Table 3.10. QC samples results of BAY-784. QC samples with accuracy and precision results for 2 weeks and 4 weeks sub-stock stability were sub-stock solutions have been stored in -20°C.

Week	QC Level	Area (mAu)	y	Theo Conc	20%	15%	P/F FDA	Accu-racy	Mean Conc	St Dev	%Acc Mean	% Prec
2	Low 1	63.88	1069.76	1000	200		P	6.98				
	Low 2	55.30	928.25	1000	200		P	-7.17	1016.07	76.68	1.61	7.55
	Low 3	62.70	1050.20	1000	200		P	5.02				
	Medium 1	112.31	1868.42	2000		300	P	-6.58				
	Medium 2	125.21	2081.27	2000		300	P	4.06	1981.37	107.02	-0.93	5.40
	Medium 3	119.95	1994.41	2000		300	P	-0.28				
	High 1	255.61	4231.99	4500		675	P	-5.96				
	High 2	167.10	2772.10	4500		675	F	-38.40	3890.13	992.29	-13.55	25.51
	High 3	281.94	4666.28	4500		675	P	3.70				
4	Low 1	55.0998	872.35	1000	200		P	-12.77				
	Low 2	60.3340	972.25	1000	200		P	-2.77	928.83	51.21	-7.12	5.51
	Low 3	58.7428	941.88	1000	200		P	-5.81				
	Medium 1	112.3420	1964.90	2000		300	P	-1.76				
	Medium 2	110.2461	1924.89	2000		300	P	-3.76	1947.15	20.38	-2.64	1.05
	Medium 3	111.6483	1951.66	2000		300	P	-2.42				
	High 1	247.5247	4545.05	4500		675	P	1.00				
	High 2	257.8817	4742.73	4500		675	P	5.39	4773.65	245.52	6.08	5.14
	High 3											

3.4. Method development Doxorubicin

Doxorubicin was used as a benchmark therapeutic given its liposomal encapsulation both in-house and within the literature was well characterised.[37] Therefore, doxorubicin was added with the analytical method where the absorbance spectrum was checked by running a 5000 ng/mL sample to ensure sensitivity. Unsurprisingly, with the different chemical structure, Doxorubicin had a different spectrum to BAY-784, with a number of wavelengths that could be used (see Figure 3.7). These were tested in terms of sensitivity (signal-to-noise) and an absorbance of 480 nm was shown to provide a more reliable level of sensitivity, presumably due to the lower background noise achievable at this higher wavelength range.
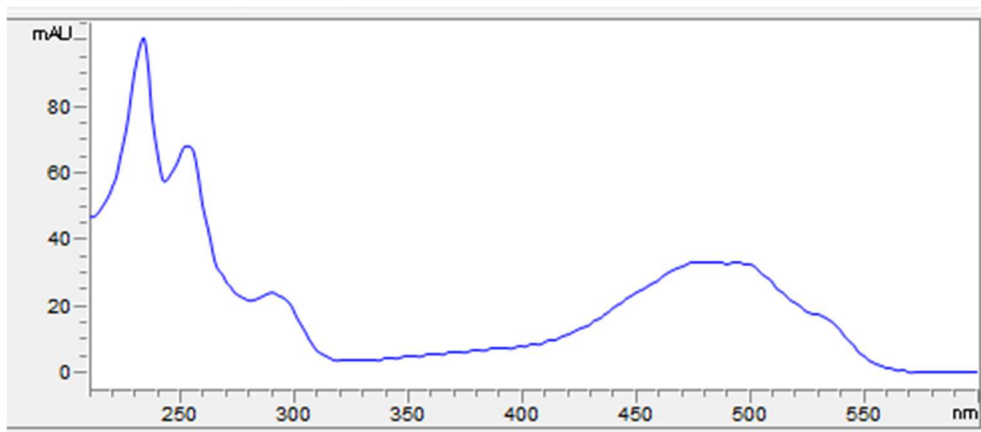
Figure 3.7. Full spectrum Doxorubicin on range 190-600 nm.
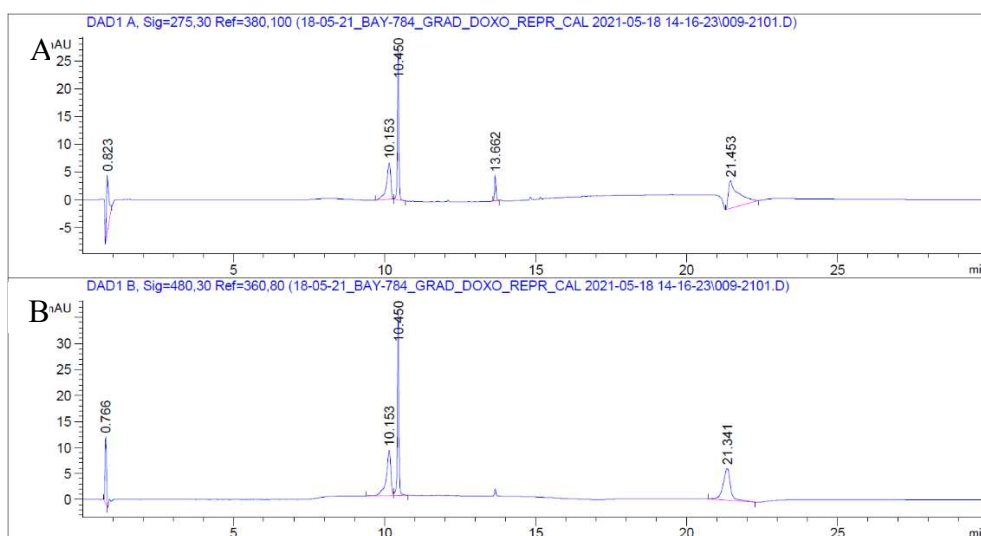
Figure 3.8. Chromatogram of Doxorubicin. Doxorubicin sample at concentration of 5000 ng/mL on wavelength 275 nm A) and 480 nm B)

As can be seen in Figure 3.8, the wavelength which is used for BAY-784 also absorb doxorubicin. However, the retention time of BAY-784 and doxorubicin are far apart from each other and the selectivity, which is 1.4, is acceptable, this is not a problem with this measurement. In addition, a second peak is observed in the chromatogram which belongs to doxorubicin, as it has the same spectrum as doxorubicin at retention time 10.45 min. This second peak is added to the main area with calculating the regression because it is assumed that this is an isomer of doxorubicin. In addition to this, chromatographic retention repeatability and reproducibility was evaluated by performing repeat injections of a high concentration standard (n=10, and n=6) over different days to provide confidence in using the retention time as a selective parameter. This data showed highly repeatable chromatography with an RSD 0.03% and 0.02% for day 1 and day 2, respectively. Pleasingly, these values were not significantly different between

separate days as indicated by an F-calculated value (F_{calc} 3.85) that is lower than the critical value of 6.681 (see Table 3.11). These data indicate that the retention time offers a stable and repeatable measurement, providing confidence that retention time will be a suitable parameter to identify doxorubicin.

Table 3.11. Overview results of the reproducibility testing of Doxorubicin. Using a concentration of 5000 ng/mL and injecting the same solution 16 times in total over 2 days. The repeatability data passed with the F-test which means that the reproducibility is significant over 2 days.

Retention time Reproducibility		**F-calculated value retention time**	N = 10 and 6 F (9,5) critical value = 6.681		Pass?
Compound	**Doxorubicin**	3.85	6.681		Y

Furthermore, the variability of the peak area for quantitation was determined using repeat injections of the high concentration standard (again n=10, and n=6) and integrated using the automated processing algorithm within ChemStation. This data showed highly repeatable peak areas with an RSD of 2.70 % and 3.08% for day 1 and day 2, respectively. This also continued between separate days as indicated by an F-calculated value of 2.58 (see Table 3.12), indicating a stable and repeatable measurement, providing confidence that the amount of analyte injected and retained on the column will be consistent to quantify doxorubicin.

Table 3.12. Overview results of the repeatability testing of Doxorubicin. Using a concentration of 5000 ng/mL and injecting the same solution 16 times in total over 2 days. The repeatability data passed with the F-test which means that the repeatability is significant over 2 days.

Peak Area Reproducibility		**F-calculated value peak area**	N = 10 and 6 F (9,5) critical value = 6.681		Pass?
Compound	**Doxorubicin**	2.58	6.681		Yes

For the determination of the sensitivity, the LOD was calculated. The calculated LOD is 599-1001 ng/mL indicating the operational limits of the analytical method. Similar to BAY-784, the spread of LOD is caused by the dual measurement were both doxorubicin and BAY-784 were made up in the same solution which is discussed further on in this chapter.
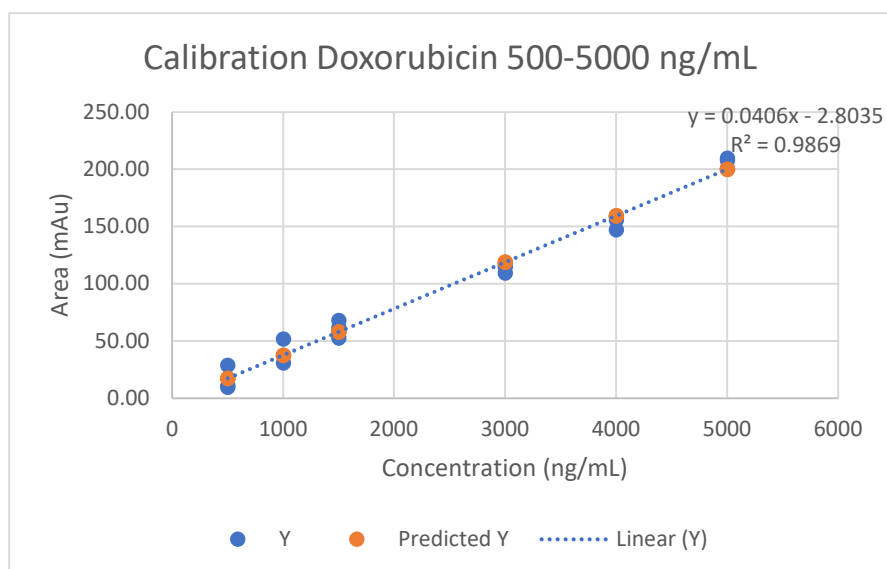
Figure 3.9. Calibration graph for Doxorubicin. On a concentration range from 500-5000 ng/mL

For ease of use as dual quantitative method with BAY-784, the linearity of doxorubicin was tested at similar concentrations. As shown in Figure 3.9, a dynamic range of 500-5000 ng/mL showed acceptable linearity with $R^2 > 0.99$ and no heteroscedasticity was detected for the data set, enabling simple non-weighted linear regression to be used. Similar to the calibration standards, QCs were prepared at concentrations comparative to BAY-784, see Table 3.13. These also showed an acceptable precision and accuracy with values below 7 %RSD and 5% deviation, respectively. These indicate that the method is accurate and precise for quantifying samples containing doxorubicin across the concentration range tested.

Table 3.13. QC samples results of Doxorubicin. QC samples with accuracy and precision results

QC Level	Area (mAu)	y	Theo Conc	20%	15%	P/F FDA	Accu-racy	Mean Conc	St Dev	%Acc Mean	% Prec
Low 1	39.22	1035.57	1000	200		P	3.56	1076.26	36.26	7.63	3.37
Low 2	41.35	1088.06	1000	200		P	8.81				
Low 3	42.04	1105.14	1000	200		P	10.51				
Medium 1	73.34	1876.42	2000		300	P	-6.18	1955.96	115.83	-2.20	5.92
Medium 2	81.96	2088.85	2000		300	P	4.44				
Medium 3	74.41	1902.62	2000		300	P	-4.87				
High 1	169.42	4244.08	4500		675	P	-5.69	4291.05	184.62	-4.64	4.30
High 2	179.59	4494.62	4500		675	P	-0.12				
High 3	164.98	4134.46	4500		675	P	-8.12				

The impact of doxorubicin and BAY-784 as a mixture on quantitative performance were determined for each compound using the concentration ranges quoted previously, to explore the

possibility of using a singular analytical method for evaluating the encapsulation of both compounds, see Figure 3.10. The linearity, dynamic range, quantitative accuracy, precision, LOD and LLOQ were determined. As expected, minor differences in the quantitative performance were observed versus singular standards; from a closer inspection of the data, the S5 calibrant at 4000 ng/mL appears to have an adverse impact on the coefficient of determination (pushing this below 0.98) and regression statistics, with the addition of doxorubicin to BAY-784. Given this is apparent for both analytes and it was not repeated for further batches, it was considered that this was an injection error however, as the standards did not show calculated concentrations beyond 15%, omission of these from the data set could not be justified.
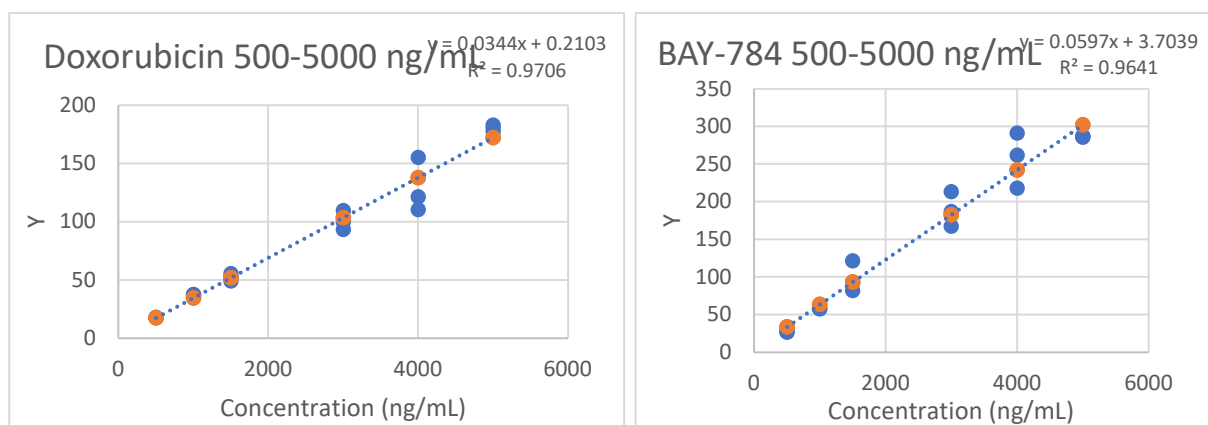
Figure 3.10. Calibration graph Doxorubicin and BAY-784. Calibration graph on a dynamic range of 500-5000 ng/mL with results of doxorubicin in A) and BAY-784 in B). Analytes were added together in the sample solution for measurement.

Interestingly though, even when applying these regression relationships to calculate the concentrations of the QC samples, these remained within an acceptable degree of precision and accuracy (<5 %RSD and 11% accuracy) across the concentration range, suggesting that the method is still appropriate for quantifying both doxorubicin and BAY-784, see Table 3.14.

Table 3.14. QC samples results of Doxorubicin & BAY-784. QC samples with accuracy and precision results. N.B. Low QC = LLOQ if acceptable accuracy and precision.

Week	QC Level	Area (mAu)	y	Theo Conc	20%	15%	P/F FDA	Accuracy	Mean Conc	St Dev	%Acc Mean	% Prec
	Low 1	36.365	1050.56	1000	200		P	5.06				
	Low 2	36.786	1062.80	1000	200		P	6.28	1052.63	9.31	5.26	0.88
	Low 3	36.158	1044.54	1000	200		P	4.45				
Dox-orubi-cin	Medium 1	66.663	1930.95	2000		300	P	-3.45				
	Medium 2	72.461	2099.40	2000		300	P	4.97	2044.28	98.15	2.21	4.80
	Medium 3	72.566	2102.47	2000		300	P	5.12				
	High 1	163.235	4737.08	4500		675	P	5.27				
	High 2	154.875	4494.15	4500		675	P	-0.13	4683.76	169.36	4.08	3.62
	High 3	166.09	4820.04	4500		675	P	7.11				

|											
BAY-784	Low 1	56.282	881.40	1000	200		P	-11.86	897.60	14.69	-10.24	1.64
	Low 2	57.472	901.34	1000	200		P	-9.87				
	Low 3	57.991	910.05	1000	200		P	-8.99				
	Medium 1	113.579	1841.89	2000		300	P	-7.91	1837.26	4.22	-8.14	0.23
	Medium 2	113.086	1833.63	2000		300	P	-8.32				
	Medium 3	113.241	1836.24	2000		300	P	-8.19				
	High 1	262.273	4334.55	4500		675	P	-3.68	4327.13	89.35	-3.84	2.06
	High 2	266.926	4412.55	4500		675	P	-1.94				
	High 3											

3.5. Concluding Remarks Analytical Development

The aim of this chapter was to develop a quantitative method for a more accurate measurement of both BAY-784 and doxorubicin using LC-DAD during the encapsulation studies. We also aimed to explore the potential of combining these protocols for a dual measurement method of using similar concentrations. Pleasingly, a good degree of quantitative precision and accuracy was determined across the calibration range tested for both analytes, indicating the suitability of the method in measuring these therapeutics. As expected, some decrease in performance was observed when analysing both compounds as a mixture however, acceptable precision and accuracy (within 15%) were observed for all QCs tested. Furthermore, we have also examined the stability of diluted solutions of BAY-784 under different operational and storage conditions (for up to 4 weeks). Again, results showed a positive outcome with good stability observed over the conditions tested, enabling storage and reuse of the drug solutions without having to prepare these fresh on the day of each analysis.

3.6. Nano-encapsulation of BAY-784
3.6.1. Uptake of liposomes in OVCAR-3 and SKOV-3

Before using liposomal BAY-784 on cell lines, investigations were undertaken to understand the uptake rates of the liposome in both cell lines. This is important as the drug must be carried by the liposome into the cell and will not influence the cell if it does not internalise. This experiment was done by treating the cells with liposomes that were pre-stained with a fluorescent lipophilic dye Vybrant™ DiD (excitation/emission 644/665 nm). Cells were seeded overnight in an 8-well chamber slide (as replicate samples) and then treated with tagged liposome. After treatment periods, cells were washed with PBS and co-stained with Hoechst, to stain cell nuclei (excitation/emission 358/461 nm) and determine that the tagged liposomes were present within the cell and not freely mobile within the media, see appendix 9 for liposomal uptake in SKOV-3 and OVCAR-3.
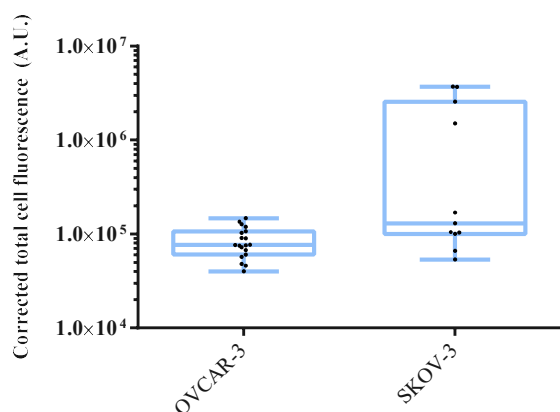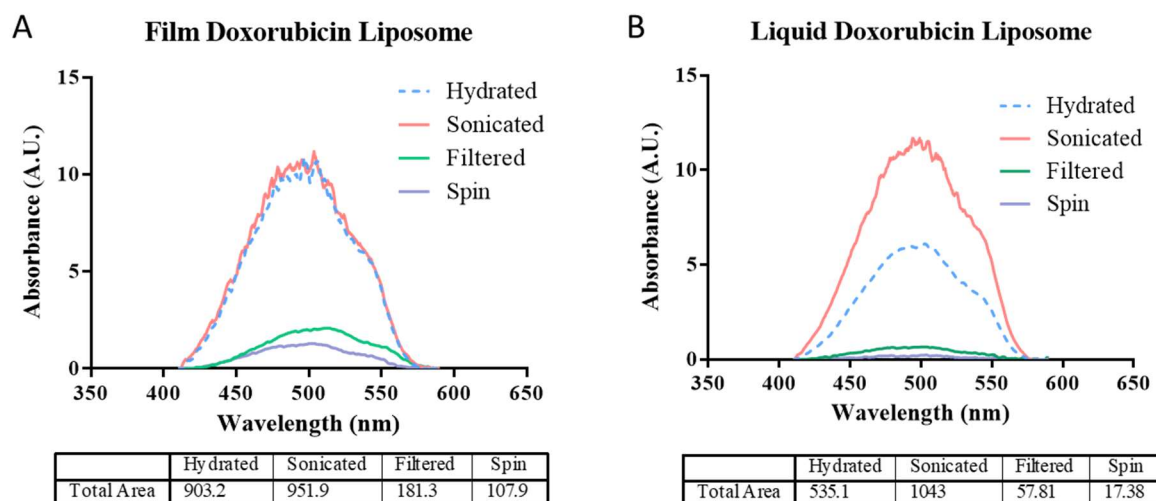
Figure 3.11. Uptake of liposomes in SKOV-3 and OVCAR-3 cell lines. Uptake quantification measured using corrected total cell fluorescence method.

As can be seen in figure 3.11, the uptake in SKOV-3 cells is higher (1.1×10^6 A.U.) in comparison with OVCAR-3 (8.5×10^4 A.U.; ns, p=0.0509). However, a greater spread is seen in SKOV-3, implying that the uptake of liposomes in SKOV-3 was less uniform. This may lead to greater variability in the efficacy of the drug within this cell line and was investigated further in Chapter 4.

3.6.2. Encapsulation vs. incorporation

During nanoparticle loading, the drug can be held inside the liposome via incorporation or encapsulation. During incorporation, the drug of interest is applied during the hydration step, forming of multilamellar vesicles, where the drug will interact with the liposome and intercalate with the outside of the hydrophobic part of the liposome. Whilst, with encapsulation the liposome can either be fabricated as above with the drug embedding within the particle, or it can be actively loaded following assembly. Prior to the application to BAY-784, this process was evaluated for the in-house liposome design, see table 2.7 with a well characterised drug, doxorubicin. Given the intrinsic fluorescence of the molecule (absorbance maximum of 480 nm), this lends itself to easy quantification where UV-spectra were collected across a wavelength range of 400-600 nm using a microvolume spectrophotometer or nanodrop system, over the encapsulation process. In figure 21a, results are shown of the encapsulation (A) vs incorporation (B) test. The area of interest to determine which process is more effective is the "spin" plot, where free doxorubicin has been removed by using spin columns. This data shows a higher signal in this plot with a value of 107.9 compared to 17.38 (figure 3.12b) in the incorporation sample

suggesting that the encapsulation process is more effective in comparison with incorporation given there is a 6.2-fold higher doxorubicin retention rate.


	Hydrated	Sonicated	Filtered	Spin
Total Area	903.2	951.9	181.3	107.9

	Hydrated	Sonicated	Filtered	Spin
Total Area	535.1	1043	57.81	17.38

Figure 3.12. Liposome encapsulation vs incorporation. Drug loading in liposome via Thin-Film Hydration (encapsulation) in A) vs incorporation in B). Area after spin column is 107.9 A.U. with encapsulation and 17.38 A.U. with incorporation.

3.6.3. Encapsulation efficiency (NMR data)

For the calculation of the encapsulation efficiency, NMR was used to have a rough estimate of the encapsulation of BAY-784. To do this, free drug of BAY-784 was measured, figure 3.13, to identify a specific peak shift indicative of BAY-784. This was compared to a solvent only spectrum to confirm the selectivity. There were no published spectra available to compare with, which used the same solvents. The problem with using different solvents is that the shifts in a NMR spectra is also different and therefore cannot be compared with each other. In addition, liposomal BAY-784 was measured and the liposomes erupted with deuterated water or deuterated DMSO to release BAY-784 and the solution was measured again. This was compared to a free BAY-784 sample of the same concentration that the liposomes were treated to calculate the encapsulation efficiency.
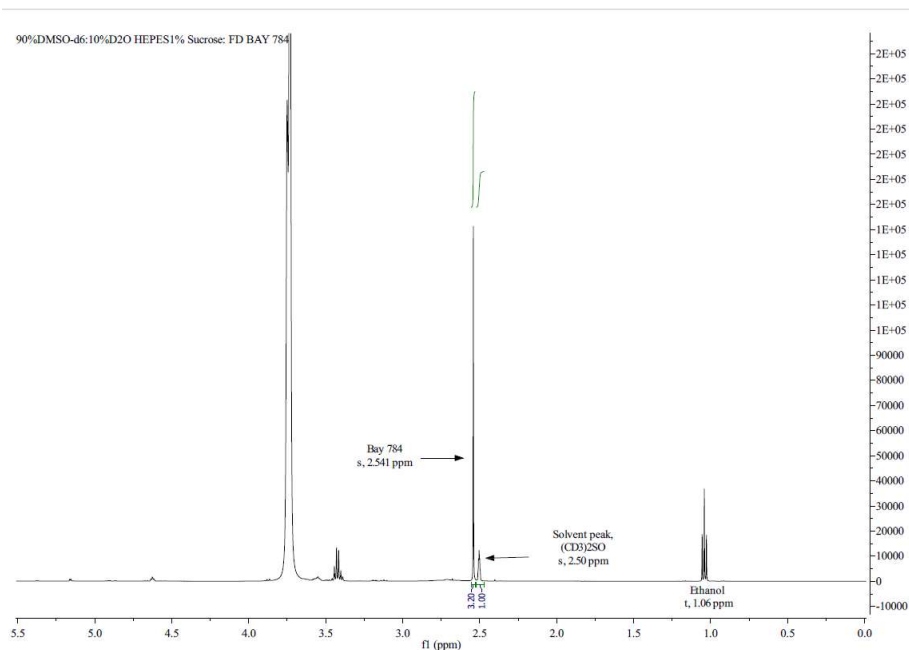
Figure 3.13. ¹H-NMR spectrum of free drug (FD) BAY-784. BAY-784 integration free drug for comparison with liposomal drug.
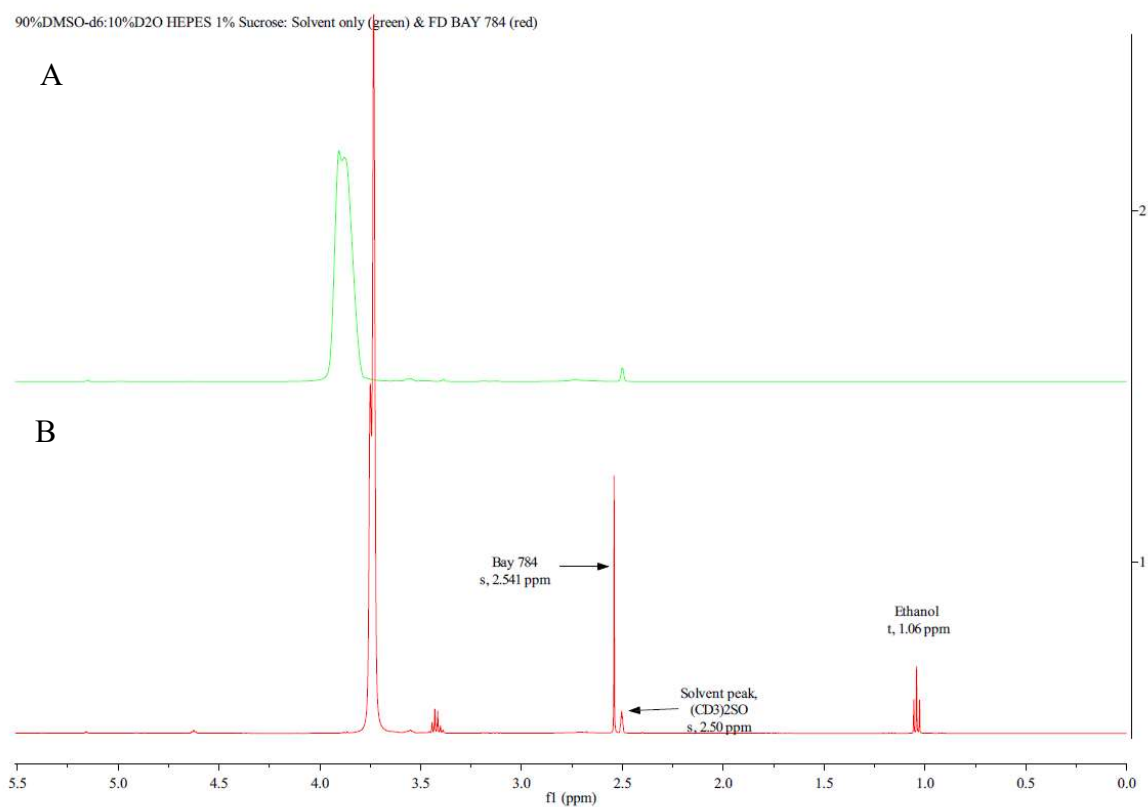
Figure 3.14. ^{1}H-NMR spectrum of BAY-784 and solvent. Solvent solution of HEPES buffer (1% sucrose) in A) and free drug BAY-784 in B).
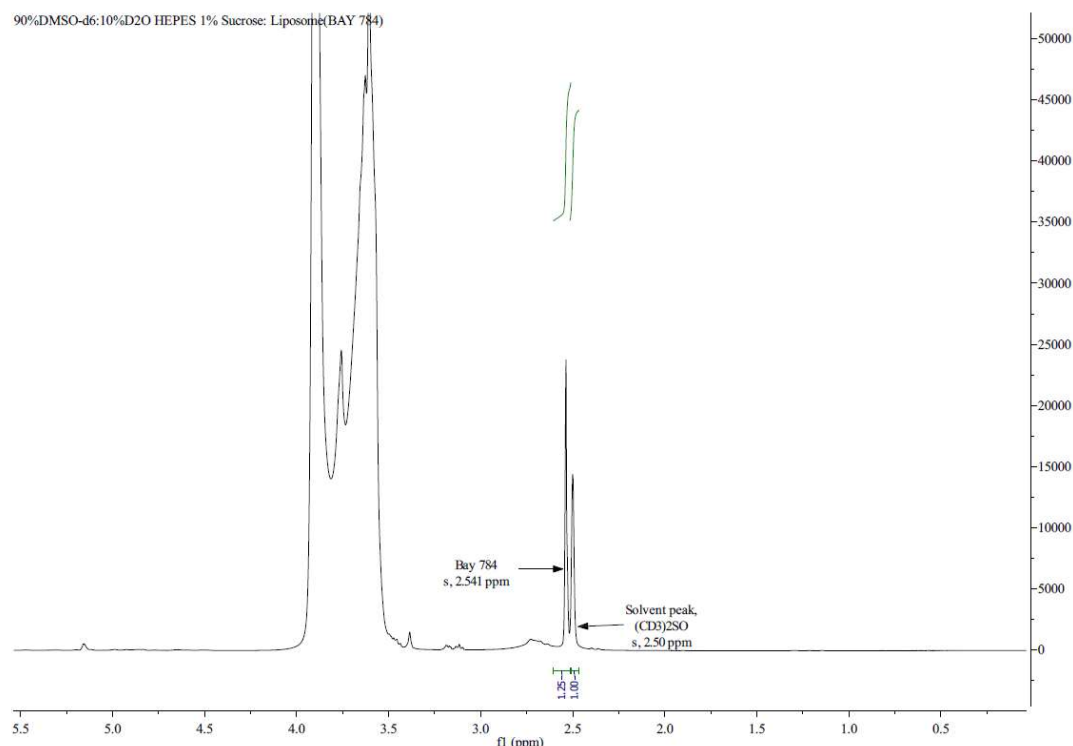
Figure 3.15. ^{1}H-NMR spectrum of free drug (FD) BAY-784. BAY-784 integration free drug after disruption of liposomes

The encapsulation of BAY-784 was calculated using equation 2.6 by comparing the amount of the drug within the particle versus the number of nanoparticles. In figure 3.14, the solvent peak in comparison with free BAY-784 was shown to make sure that the peak that is used for integration is from BAY-784 and not from another peak that is applied during the synthesis. In figure 3.13, the free BAY-784 integral (100% drug retention, s, 2.541 ppm) was determined to be 3.2 A.U., whereas liposomal BAY-784 integral was 1.25 A.U. (figure 3.15, s, 2.541 ppm). Therefore, encapsulation efficiency of BAY-784 was calculated to be 40%.

3.6.4. Drug release and stability

As part of the sample preparation, the liposome encapsulated BAY needs to be released. In order to optimise release, an increasing pH solution was added in order to find the optimal pH at which we get burst release. This experiment was done by measuring the liposomes after sonication and the spin column, in solution with increasing pH, while measuring thire size with DLS. From the DLS profiles, aggregates appear to form following the addition of pH 10 with a much larger set of particles of 1000 nm and above observed. In addition, it is worth noting that all the samples were run on the NIBS DLS setting; this underestimate sizes at micron range

and above, and it is likely that these materials are even larger than what is suggested in the data shown in figure 26. These aggregates can be explained by the formation of globular aggregates/agglomerates from the dispersal of phospholipids and cholesterol in the aqueous media following the lysis of liposomes. These highly hydrophobic structures are not able to exist freely in aqueous solution and, in order to reduce the entropy of the system, create an oil-in-water style assembly, aggregating together. Admittedly, this may pose a difficulty with the resulting drug efficacy in an anticipated acidic tumour environment but highlights the importance of measuring the efficacy of the intact liposomal drug with a relevant OC cell line.
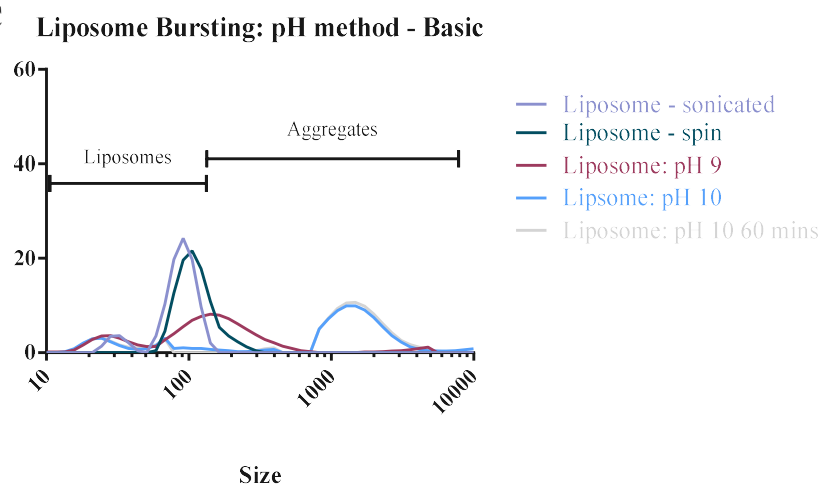
A

Liposome Bursting: pH method

B

Liposome Bursting: pH method - Acidic

C
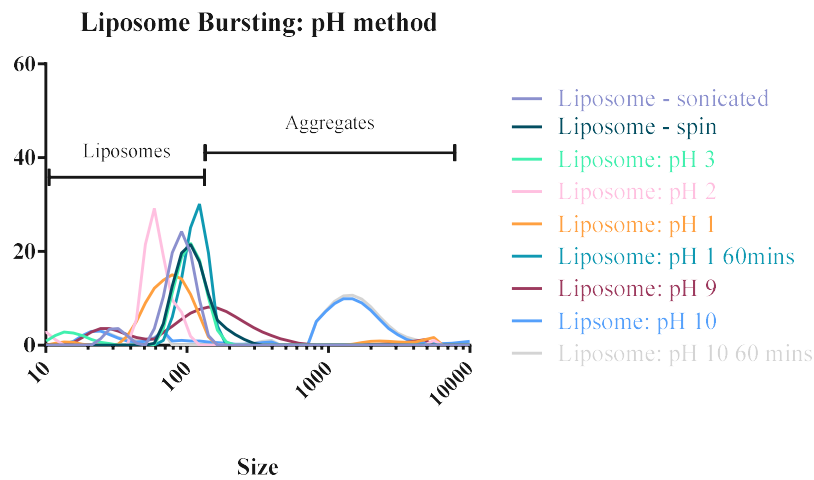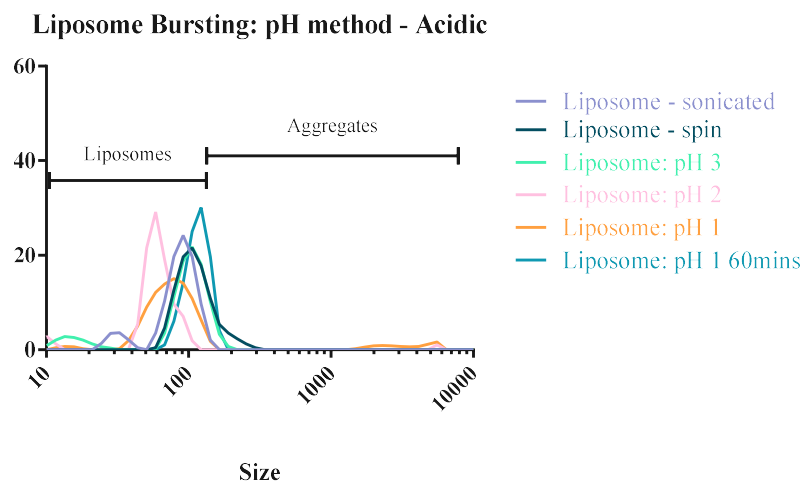
Liposome Bursting: pH method - Basic

Figure 3.16. Liposome disruption graphs using different pH values.

3.6.5. Concluding Remarks Encapsulation Process

To ensure an optimum method was used without wasting BAY-784, the uptake of the liposome tested for each cell line. Both cell lines show the take up of the liposomes, with a higher uptake in SKOV-3 in comparison with OVCAR-3. Once assessed the method of encapsulation or incorporation was investigated using Thin-Film hydration. However, because of different characteristics of drugs (e.g. hydrophobicity), adding the drug in a later stage during hydration was a possible adaptation to this method. The results shows that a 40% encapsulation of BAY was achieved in the liposomes. This efficiency percentage was comparable with in-house data with doxorubicin (at 50%), and all further work conducted was at this level of drug. After forming of liposomal drug, the release process was then tested by adjusting the pH of the solution and testing with DLS. Interestingly, liposomes showed evidence of lysis under basic conditions (pH of 10), with this pH used to burst and check stability and or encapsulation for each preparation.

3.7. Feasibility of a tripartite sample preparation method for determining encapsulated, non-encapsulated and total drug content

3.7.1. Initial testing of the protocol

Many protocols concerning the extraction of liposomal drugs from clinical samples have largely determined the total drug concentration present in the sample. This approach is limited as it fails to establish the true amount of the target pharmaceutical (in this case the encapsulated drug) and its pharmacodynamic integrity and stability following administration; these are critical factors in determining the potential toxicity and efficacy of the nanotherapeutic and are key to its overall viability as a therapy. To overcome these drawbacks, tripartite sample preparation approaches that separate the encapsulated and extraneous free drug have been developed for other liposomal encapsulated therapies of varying chemistry, however, these have not been tested on BAY-784. [38][39] Furthermore, it is also unclear how effective these sample preparation approaches will be for the in-house encapsulation method applied for BAY-784, given previous published work utilized alternative liposome compositions and encapsulation methods whereby none of them are applied to BAY-784..[33][38]. Nevertheless, given the breadth of applicability of this tripartite approach for encapsulating a range of drug chemistries during or post-liposome synthesis, this method was tested for BAY-784.

To establish the extent of drug encapsulation, we must first understand the stages of the sample preparation process and evaluate its performance using appropriate metrics. The process typically involves applying a crude sample containing the encapsulated (ED) and remaining free

drug (FD) to a reversed phase solid-phase extraction cartridge with pore size of 60 μM, where the ED is intended to pass through the cartridge without interaction, whilst the FD will adsorb to the sorbent (see Figure 8). Following cartridge conditioning, this requires the application of the sample, a wash solvent, and an elution solvent to remove the ED and the FD as fractions for collection. To analyse the ED, this will require liposome disassembly to release the drug; this can be achieved through the application of an organic solvent and/or a change in pH.[40][41] Some publications have also combined this latter stage as a liquid-liquid extraction, drawing the drug into the organic solvent, enabling the measurement of the free drug as a cleaner extract, further boosting sensitivity. From previous work completed in-house, the liposome used in this study was believed to be stable under acidic conditions however, it had not been tested under the context of the tripartite method, warranting further investigation on the recovery of the drug using relevant solvents and pH conditions. However, in order to assess these conditions, metrics concerning the reliability and cleanliness of the drug recovery would need to be measured. In the spirit of regulated bioanalytical validation, a method that uses replicate quality control (QC) samples spiked with an appropriate amount of FD was used to determine the precision and average process efficiency, and recovery of the drug.[42] However, to have confidence in the measurements that are taken, it is important to ensure that the method is first reliable, and secondly, effective at recovering the drug. As such, the relative standard deviation (%RSD) was used to determine the repeatability of the extraction, with a value <15% taken as a threshold of acceptability. Once established, the process efficiency (%PE, as a sum of matrix effect (%ME) and drug recovery (%REC) via comparison of a QC spiked before extraction with an unextracted QC), can be used to determine the effectiveness of the extraction, where a higher value provides the best opportunity to detect and quantify the drug. The sample preparation protocol deployed for BAY-784 followed past work with other nanotherapeutics and specifically the papers by Yang et al and Zhong et al, [33][38] for the drug Vincristine given these had similar properties in chemical structure as BAY-784; Oasis HLB cartridges (Waters Corp.) with a pore size of 30 μm were selected given these were thought suitable to enable passage of liposomes anticipated from the thin-film synthesis process (e.g. 100- 200 nm). To control the liposome size the synthesis mixture was placed through a filter of 0.45 μm and this was confirmed via dispersive light scattering (DLS) detection.

Prior to applying the protocol to the ED, each individual stage was tested in terms of %PE (to limit the amount of BAY-784 used in the method development) and optimized using BAY-784 in the presence of the free lipid mixture used to create the liposomes. This was intended to show

the retention of BAY-784 on the SPE cartridge and that it could be removed using the desired elution conditions, followed by the extraction of BAY-784 during the second part of the protocol (e.g. LLE or QuEChERS).

### 3.7.2. Solid-Phase Extraction (SPE)

The SPE protocols that used the HLB cartridges typically involved using a methanol conditioning and elution solvent however, given the stronger elution of BAY-784 during the analytical development for the LC, acetonitrile was also tested in place of methanol (see Table 3.15, Figure 3.17). Therefore, replacing methanol with acetonitrile would in theory be a better eluent in the SPE as it has a similar interaction on the drug.

Table 3.15. SPE Optimization method. Overview of used solvents for SPE optimization

Step	Solvent composition		
	1	**2**	**3**
Conditioning 1	MeOH	MeOH/ACN	ACN
Conditioning 2	PBS	PBS	PBS
Sample Load	Sample	Sample	Sample
Wash 1	PBS	PBS	PBS
Wash 2	PBS	PBS	PBS
Wash 3	MeOH/H_2O (25/75%)	MeOH/ACN/H_2O (12.5/12.5/75%)	ACN/H_2O (25/75%)
Elution	2% AA in MeOH	2% AA in MeOH/ACN	2% AA in ACN

Samples were determined in duplicate with precision results RSD of 9.33% and 1.04% for respectively, method 1 and method 2. For method 3, no RSD was calculated as the duplicate sample was not detected by the detector.

Interestingly, extractions using methanol exhibited a higher %PE, indicating the subtle differences in retention according to the sorbent chemistry versus the reversed phase stationary phase used in the LC method. The smallest changes can already have impact on the activity of the drug. Especially with BAY-784 which is a new drug and has a great variety in binding due to the different functional groups.
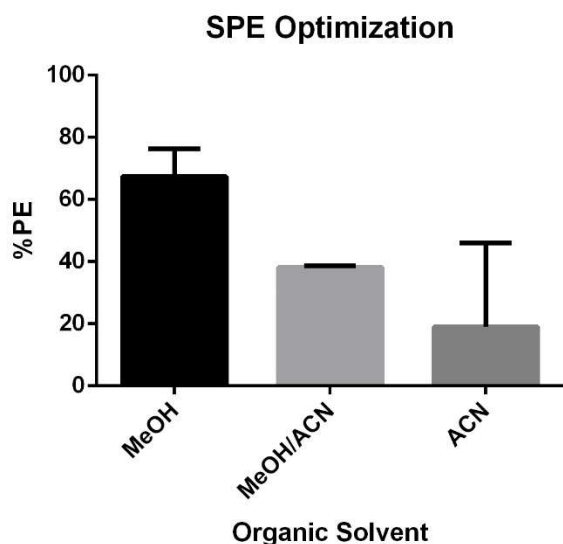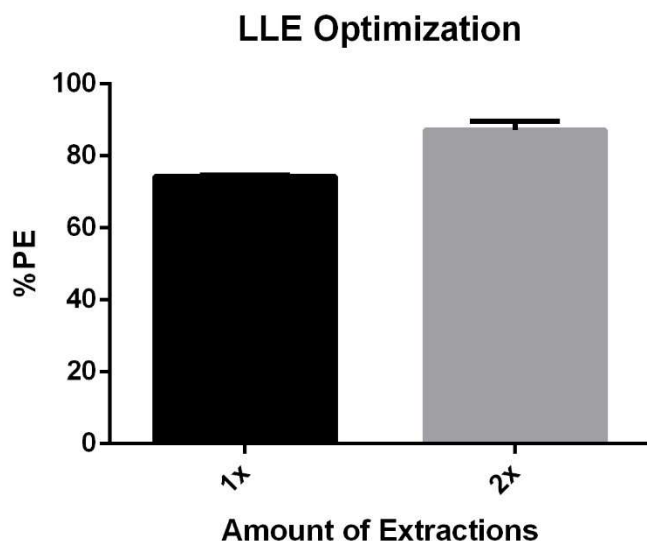
Figure 3.17. SPE Optimization Process. Testing of different organic solvents during the SPE process using duplicate samples with calculated process efficiency.

3.7.3. Liquid-Liquid Extraction (LLE)

For the detection of the encapsulated drug, a simple LLE is used to enable release of the drug from the liposome whilst acting as a clean-up step. Similar to the SPE, an initial test with FD in the presence of lipids was performed to test the efficiency of the protocol on BAY-784. For the LLE, a number of variables known to be related to analyte recovery and release from the particle were changed; these included the number of extractions, the type of extraction solvent and the pH of the extraction (see Section 1.2.1.1.).

The LLE process showed excellent precision between the two samples with a %RSD of 0.37% for 1x extraction and 1.99% of 2x extractions. This shows that the method is precise as the %RSD is method is very reliable lower than the overall used 15% (QC samples).
The %PE that is shown in figure 3.18, the extraction is suitable for BAY-784 as the PE is more than 50%. Including an extra extraction step has improved the PE from ~74% to ~85%. However, this is just an improvement of 10%, whereby extra solvent and gas is used. Including these factors, the choice of staying with one time extraction was made due to extra costs for a low improvement.
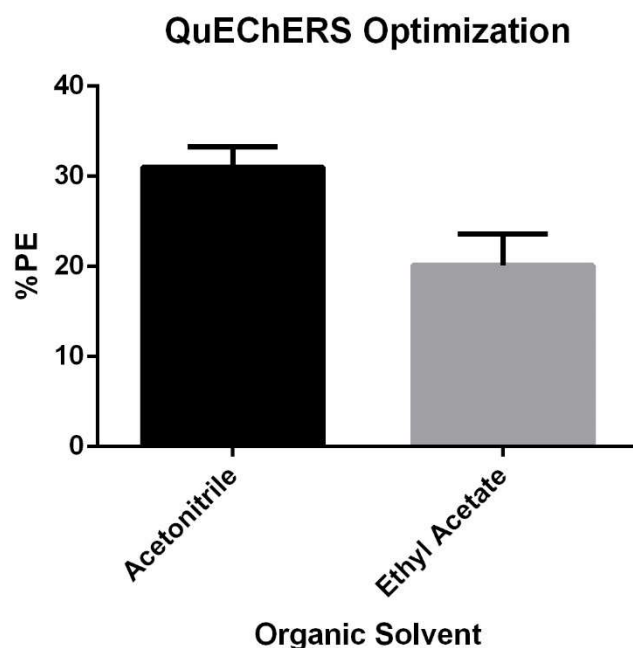
Figure 3.18. LLE Optimization Process. Testing of repeating extractions during the LLE process using duplicate samples with calculated process efficiency.

3.7.4. QuEChERS

From work carried out in-house, QuEChERS has shown significant promise as a reliable extraction process for a wide range of chemical types.[43] This extraction process is compatible with both ACN and ethyl acetate as extraction solvents (enabling a direct comparison to LLE to be made) however, unlike LLE, QuEChERS can provide a faster and safer extraction process by using lower volumes of solvent that are less toxic. Furthermore, with the inclusion of a d-SPE clean-up step, this approach offers significant potential in providing cleaner extracts in the place of the LLE within this protocol. Therefore, to test this hypothesis, an in-house QuEChERS protocol was evaluated in place of the LLE step using ACN or ethyl acetate, PSA and C18 d-SPE.[43]

Unlike the LLE, the QuEChERS process generated variable results using ethyl acetate as organic extraction solvent with a precision of 17.4%. However, this appeared to be solvent related, where the ACN extraction showed much improved precision at 7.5% RSD. Given LLE was performed with ethyl acetate, this suggests the presence of salt within the QuEChERS extraction may be a causative factor in this variability. Further disadvantages in using with QuEChERS method included the %PE; when using acetonitrile, this was slightly better in comparison with ethyl acetate, but the %PE overall remained low in comparison with LLE, see Figure 3.19. Therefore, despite acceptable precision, the choice was made not to continue with acetonitrile for extraction and further work would involve testing the SPE-LLE for liposomal BAY-784 and the gold standard, doxorubicin. Sadly, for the latter drug, inconsistent data was observed and further adjustment to the protocol would be required to adopt this for the drug.

Although the %PE of using acetonitrile was slightly better in comparison with ethyl acetate, the %PE overall was low. Although the precision data was acceptable, <15% RSD, the choice was made not to continue with acetonitrile for extraction. In addition, the results of LLE and QuEChERS were compared to make a judgement which extraction method would be more suitable.

Figure 3.19. QuEChERS Optimization Process. Testing of organic solvents during the QuEChERS process using duplicate samples with calculated process efficiency.

3.7.5. Application for encapsulated drug

After the initial method development, the sample preparation was tested with liposomal drugs in terms of %PE and %REC given the importance of this stage of the work. For this evaluation, the focus was on the recovery of the FD in fraction 2 (eluent) of the SPE process to determine the amount of FD that remains unencapsulated, and the amount of ED in fraction 1. In order to measure the amount of drug within the liposome in this latter fraction, an additional stage to disassemble the particle is required. Interestingly, the first batch of liposomal drugs only showed the FD, see appendix 5, indicating that the liposomes remained intact throughout the LLE, and that trichloroacetic acid was not effective in lysing the liposomes. Therefore, some additional tests exposing the liposomes to an alternative pH (basic) and monitoring the change in nanoparticle size by DLS were undertaken. The data indicated that the liposomes unexpectedly disrupted basic conditions with the addition of 1M sodium hydroxide, rather than acid as per other published protocols. After these adjustments, the SPE and LLE methods were re-evaluated in terms of %REC and %PE by analysing triplicate QCs prepared with the FD spiked

before extraction (SBE) and spiked after extraction (SAE). Given this was the final application of the method, recovery was also established. Pleasingly, when these conditions were checked as independent extractions for the FD very good repeatability was observed for the recovery measurements across both steps, with %RSDs below 5.3%. Furthermore, very good recoveries of the drug were observed with values exceeding 75% for both the SPE and LLE stages regardless of the concentrations tested (see Table 3.16).

Table 3.16. Process Efficiency of SPE and LLE using sodium hydroxide in LLE.

Method	QC level	Average PE (%)	SD	RSD (%)
SPE	Medium	77.1	0.82	1.1
	High	75.4	3.56	4.7
LLE	Medium	82.3	4.37	5.3
	High	92.9	2.25	2.4

After this adjustment the batch of liposome samples were also analysed with the QDa mass spectrometer to confirm the presence of BAY-784 and identify what additional excipients from the process may be detected. BAY-784 has a monoisotopic mass of 671.09, under ESI conditions this would be expected to form a protonated species ($[M+H]^+$ ion), and therefore be observed at m/z 672. Pleasingly at the at anticipated retention time of ~14.2 minutes, a corresponding ion was observed along with evidence of a sodium adduct (see Figure 31).
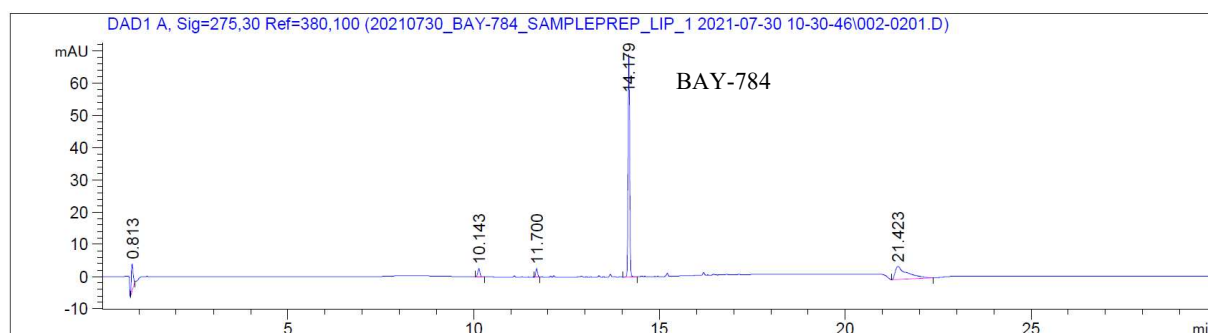
Figure 3.20. Chromatogram of free BAY-784 after SPE clean-up.
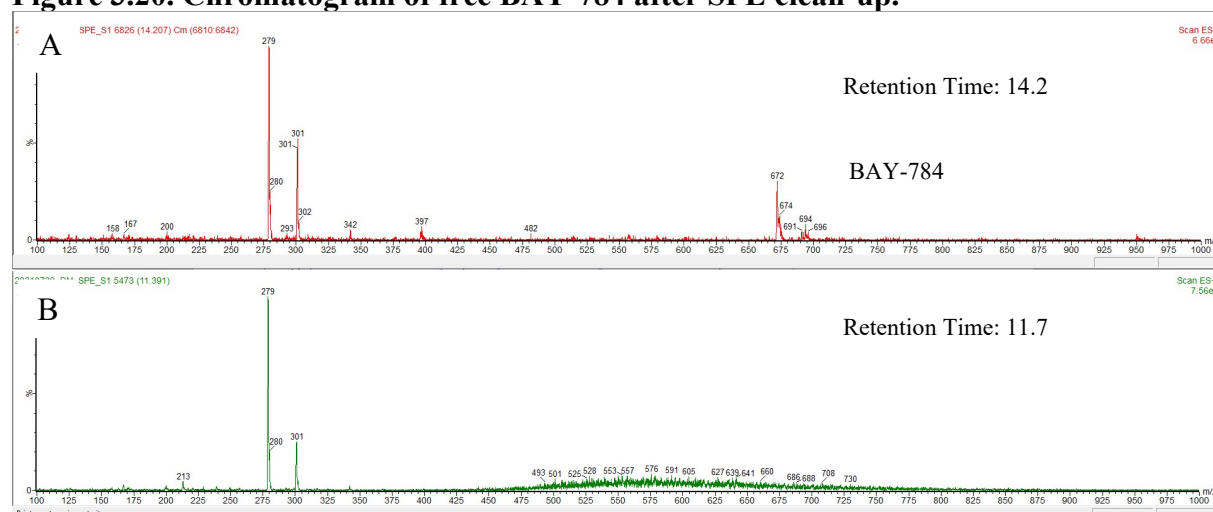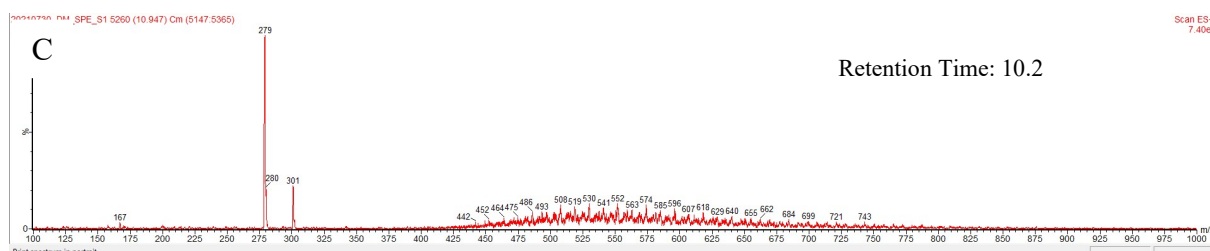
Figure 3.21. Mass Spectrum BAY-784 sample from figure 31. Mass spectrum of peak 14.2 in A) 11.7 B) and 10.2 C).

However, following prolonged analysis of the liposomal drug, further data acquisition was unsuccessful due to a blockage in the LC system. To explore the possibility of nanoparticle aggregation during the extraction each extract was re-analysed using the DLS to measure particle sizes. Interestingly, particles were observed in both the SPE and the LLE extracts, where a larger size distribution was observed for the SPE extract (see Table 3.17). This was unexpected given the SPE process was anticipated to contain the FD only, and very little acknowledgement of particle breakthrough during the extraction was present in past work employing this approach. Given this, the extraction process was further investigated using DLS to understand what may be causative factors for the presence of particles and/or the blockages observed during the LC separation.

Table 3.17. LLE and SPE Extract measured with DLS. Showing the extract of the last step in the sample preparation from both extraction methods measured with DLS.
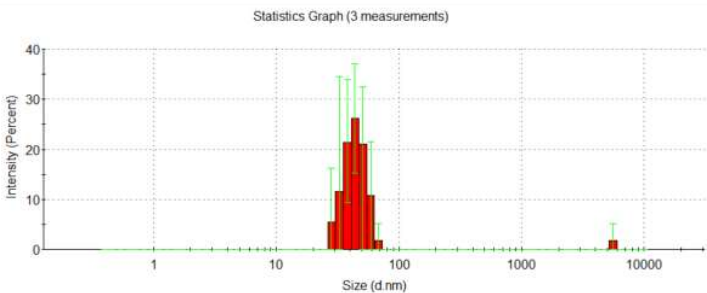
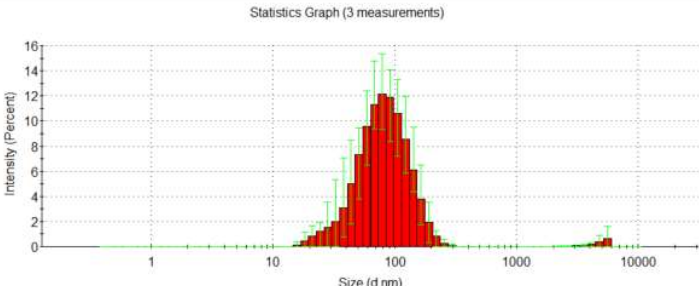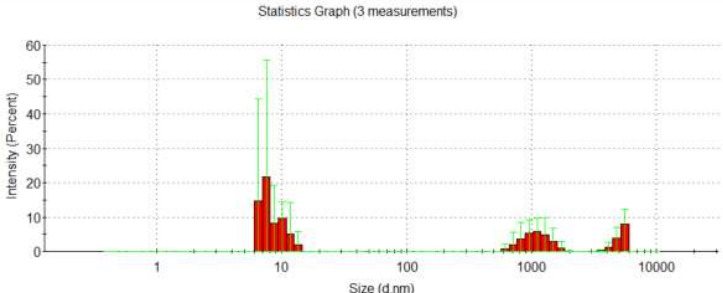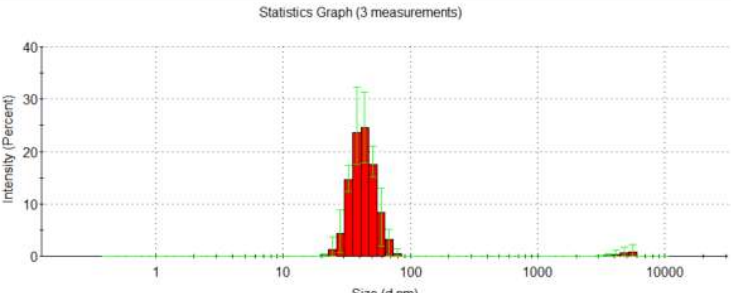| Step	Expecting particles?	DLS data
LLE Extract	Yes	
SPE Extract	No	

To overcome this problem, several adjustments were explored with the sample preparation based on differences in methodologies observed across the papers reporting the use of this tripartite approach. For example, Guillot et al., used trifluoroacetic acid for the conditioning and washing step in SPE [44]; this was applied to examine if a change in pH influenced the interaction between the particles and the stationary phase of the SPE cartridge. However, prior to application with the ED, this change to the SPE protocol was first tested with FD to ensure this was still adsorbing to the cartridge as expected. Interestingly, a lower PE of ~60% was observed for the FD however, given this was not a high reduction in %PE (~10%) and the extraction remained reliable (%6.6 RSD), this was deemed an acceptable change in the process. Furthermore, to reduce the risk of carrying additional particles through the process (due to time limitations of the project), a smaller filter size of 0.2 μm was also used instead of 0.45 μm post fabrication (before SPE).

Unexpectedly, each stage of the SPE sample preparation showed some evidence of nanoparticles with a reasonably discrete band of 50-100 nm present in the initial aqueous wash (see Figure 3.18). However, a much broader distribution (albeit at a lower % abundance) was observed with the secondary aqueous wash, indicating that the sample had not fully exited the sorbent with the initial 0.5 mL wash volume. Furthermore, and more worryingly, a more abundant distribution of particles were observed in the subsequent organic wash and elution steps, indicating the retention of the particles on the sorbent or their potential reformation following the SPE process. Interestingly, this fraction is also showing a change in the distribution of particles following the introduction of TFA within the protocol, with a narrower band of particles of 50-100 nm observed. This suggests that TFA may be encouraging the formation of particles of this size range rather than the breadth of particles observed in the original method. Either way, this data suggests that the tripartite protocol will require additional method development for use with the liposome design of this study.

Table 3.18. DLS data after filtering with 0.2 uM filters per step

Step	Expecting particles?	DLS data
Sample Load + 500 μL 0.5% TFA	Yes	

1000 µL 0.5% TFA	No	
1000 µL H₂O/MeOH; 75/25%	No	
1000 µL 2% Acetic Acid in MeOH	No	

3.8. Concluding Remarks Sample Preparation

The main aim of tripartite sample preparation approach was to test the applicability of this method to the liposomal BAY-784 and establish the absolute amounts of drug within the particle. The initial sample development was evaluated with free drug for each stage of the sample preparation method. This indicated that methanol was the most suitable organic elution solvent for the SPE process along with LLE using 5 mL of ethyl acetate, instead of the proposed QuEChERS method, to extract the drug from a lipid environment (representing the lysed liposome). After the development with free drug, the combined SPE-LLE process was tested with the encapsulated drug however, particles were observed after the clean-up step. Small adaptations were made to resolve this problem, like replacing PBS with trifluoroacetic acid to change the pH however, particles remained, indicating that this may be due to the retention of the liposome on the SPE cartridge or their reformation during the extraction.

Therefore, to properly adopt this protocol, further work is required to better understand the causative factors for this aggregation, and mitigation factors to avoid their production, such as

the use of homogenisers to minimise particle aggregation or an alternative SPE sorbent (Phenomenex)[39] to avoid retention. As was shown in literature [33], [38], this protocol uses small differences than with what is tested in this research, for example, using Waters HLB instead of Phenomenex SPE. However, this does not clarify the results that were found as the particles should not have any interaction with the column.

4. Chapter 4: Drug efficacy testing

## 4.1. Real-Time Glo assay (2D testing)

Real-Time Glo (RT Glo) is an excellent way to monitor the activity of cells over a period of time while investigating drug cytotoxicity. A continuous assay, RT Glo measures the rate of pro-substrate to substrate reduction as a measurement of cell viability, based on the conversion of luciferin into oxyluciferin in the presence of ATP, producing light. In non-viable (or dead) cells, the ruptured membrane means that this cytoplasmic reduction will not occur, providing a decrease of signal, denoting loss of cell viability.

RT Glo was initially used to determine the IC_{50} (inhibitory concentration for 50% of the cells) of BAY-784. High-grade serous ovarian cancer (HGSOC) cells were grown in the presence and absence of increasing concentrations of BAY-784, and cellular activity monitored over a 96-hour exposure period. Results were normalized within each experiment by transforming the results to the relative fold viability of a non-treated control, allowing ease of comparison between treatments and between experiments. IC_{50} curves were plotted against the log concentration, giving the cell specific final IC_{50} values.

4.1.1. IC$_{50}$ determination of BAY-784 in OVCAR-3 and SKOV-3

OVCAR-3 and SKOV-3 cells were treated with increasing concentrations of free drug BAY-784, between 0.5 pM to 100 μM using a factor of 10, and RT Glo measurement reported in Figure 4.1.
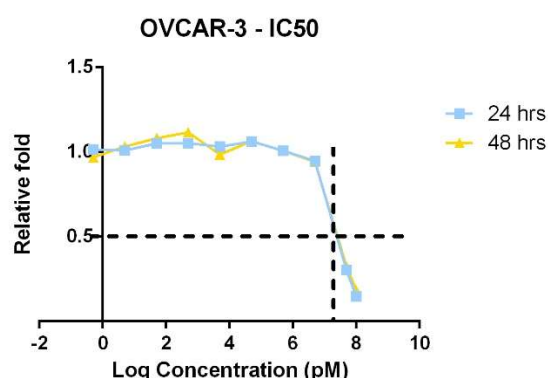
Figure 4.1. BAY-784 Cytotoxicity in OVCAR-3 cells. IC$_{50}$ curves including all tested concentrations for BAY-784, with 0.05 μM to 100 μM reported in. All data shown as average and SD of a minimum of three independent biological repeats with no significant difference in results, $p > 0.05$, up to a concentration ~50 μM. Above this concentration, significant difference was detected in RT Glo analysis ($p < 0.05$).

Dosimetry investigation in OVCAR-3 showed that low concentrations (0.5 pM-5 μM) of BAY-784 had no significant impact on cell viability ($p > 0.05$). At doses higher than 5 μM (figure 4.1b, significantly lower cell viability was observed ($p < 0.05$). Specifically, 50 μM was shown to cause a significant 67.7% reduction in cell viability ($p < 0.05$) after 48h. A further 81.8%. reduction was observed in 100 μM treatments, at the same time point. Log transformed data was used to approximate IC$_{50}$ based on the dosimetry input, determining an IC$_{50}$ for BAY-784 in OVCAR-3 cells of 15.8 μM.
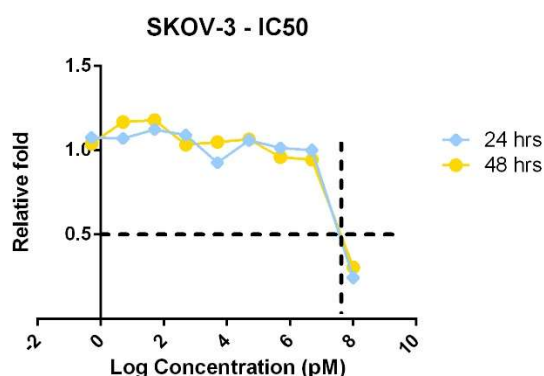
Figure 4.2. BAY-784 Cytotoxicity in SKOV-3 cells. IC_{50} curves including all tested concentrations for BAY-784, with 0.05 µM to 100 µM reported in (B). All data shown as average and SD of a minimum of three independent biological repeats with no significant difference in results, $p>0.05$, up to a concentration ~50 µM. Above this concentration, significant difference is detected in RT Glo analysis ($p<0.05$).

Dosimetry investigation in SKOV-3 showed that low concentrations (0.5 pM-5 µM) of BAY-784 had no significant impact on cell viability (figure 4.2a). At doses higher than 5 µM (figure 4.2b), specifically, 100 µM over 48h, a significant 67.5% reduction in cell viability ($p<0.05$) was observed. Log transformed data calculated an IC_{50} of 31.6 µM for BAY-784 in SKOV-3 cells.

Table 4.1. IC_{50} concentrations of BAY-784 in OVCAR-3 and SKOV-3. IC_{50} is shown with 24 hrs and 48 hrs

Cell Line	IC_{50} 24 hrs	IC_{50} 48 hrs
OVCAR-3	15.8 µM	15.8 µM
SKOV-3	31.6 µM	31.6 µM

Calculated IC_{50} of BAY-784 in SKOV-3 and OVCAR-3 are given in table 4.1 for both 24 hrs and 48 hrs timepoints. The calculated IC_{50}s are consistent irrelevant of timepoint, in SKOV-3 this was 31.6 µM and in OVCAR-3 15.8 µM. However, moving forward, the dose selected was 50 µM for ease of calculations and to ensure a significant effect was seen.

4.1.2. Drug Mechanism of Action (MoA)

The MoA of GnRH in ovarian cancer cells is still under discussion, however, GnRH-R are found in ovarian cancer cells which slow down the proliferation of cells.[8] Therefore, RT Glo assay is a fitting assay as it indicates the cytotoxicity of drugs on cells and not on the cell death. To better understand the mechanism of action of BAY-784, a cell painting assay was used to profile cells and monitor alterations in cellular function in the presence and absence of drug compounds. Whilst there are multiple assays available to monitor downstream effects following drug exposure, such as Western Blots for protein quantification or qPCR to analyse changes in RNA levels, cell painting allows for investigation of drug mechanism of action without complete knowledge of drug-cell interactions. By coupling these outputs to an InCell 6000 for automation, high content analyses (HCA) of large populations can be imaged. In table 4.2, the stains with their target organelles are shown. This experiment was done with only SKOV-3 as

this has shown a more robust response to BAY-784 exposure based on dosimetry experiments and IC$_{50}$ calculations. As such it is expected that a higher proportion of the cell population will survive BAY-784 treatment thus, still be adherent and a suitable model for cell painting.

Table 4.2. Stains with their target organelles. Cell painting stains to show the target organelles in cells.

Stain	Organelle
Hoechst 33342	Nucleus
MitoTracker™	Mitochrondien
Concanavalin A	Endoplasmatic Reticulum
Phalloidin	Cytoskeleton

As is shown in figure 4.3, stains are used to label parts of the cell to be able to follow the working of the drug on cells. These four organelles are stained as these are the main parts of the cell were cell viability or death can be shown.
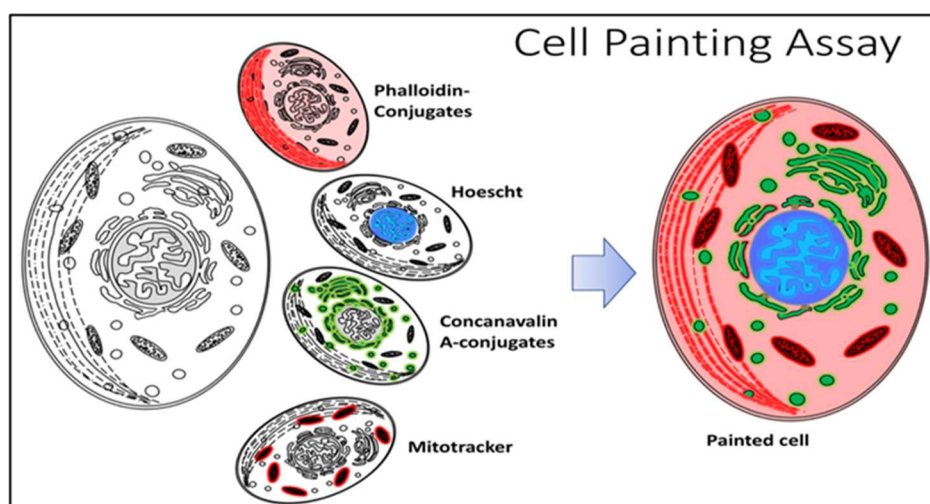
Figure 4.3. A staining assay used in high content imaging to visualise and quantify the phenotypic response of cells to therapeutics.

At the end of the drug exposure time frame (in this case 48 hrs) the cells are fixed and stained with each stain, as outlined in methodology section. The result of the specific staining regimen is a 96-well plate with multiple repeats and high throughput platform analysis for the effect of the BAY-784 on SKOV-3 cells. In addition, images of cell painting assay which were taken during the experiment are shown in figure 4.4 below.
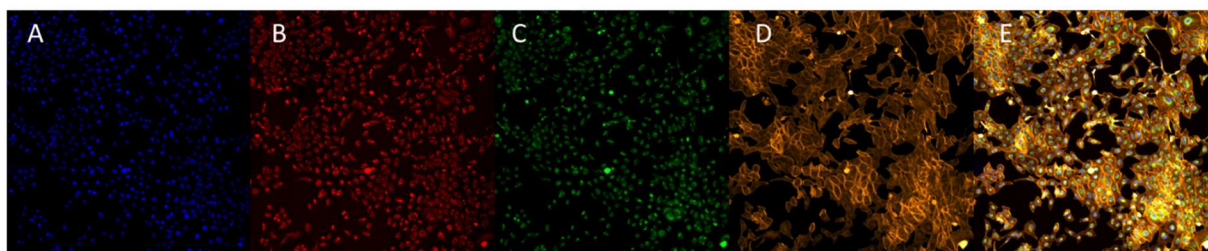
Figure 4.4. The cell painting assay in SKOV-3 cells. The panel shows the four channels imaged in the cell painting assay by the INCell Analyser 6000 at 10X magnification: (A) Hoechst 33342 (nuclei), (B) MitoTracker™ (mitochondria), (C) Concanavalin A (endoplasmic reticulum) and (D) Phalloidin (cytoskeleton). (E) Composite image of all stains.

The aim of cell painting is to compare morphological changes in cells following drug treatments by measuring the fluctuations in the stained components. By monitoring the changes in given cell paints, alongside cell shape and morphology changes, the cell painting assay allows time course experiments to try and ascertain more in-depth knowledge of drug effects on cell phenotype, outside of viability.[45] Every stain has highlighted a specific part of the cell and is therefore, showing the intensity of cells that are still active.

An unsupervised machine learning algorithm is fed the images and determines the principal components (PC, the important variables) that define any observed variation between untreated control and drug treated samples. By allowing this process to be unsupervised, the intention is to provide an unbiased output, where the dataset has not been primed or skewed based on human interpretation. At this stage, three sets of PCs were formed and all three were used to form the three principal component analyses (PCA) plots. In addition to the PCA outputs, we are able to determine cell cycle response following drug exposure as well as cell counts. These are important variables and analysis methods to correlate drug effect, both in terms of cell death, proliferation and cell cycle checkpoint, which are usually inhibited in cancer cells.[45]

4.1.2.1. Cell Counts following BAY-784 treatment in SKOV-3

Prior to the more in-depth pixel analysis of cell paint stain distribution, a more basic analysis was utilised to determine drug effect on the number of cells. Cell counting is a way to determine proliferation rates or suggest the presence of cellular apoptosis in a specific cell line. For cell count outputs, images were analysed and the number of nuclei were quantified for cell counting. Figure 4.5a and b show the cell painting difference between non-treated and treated cells.
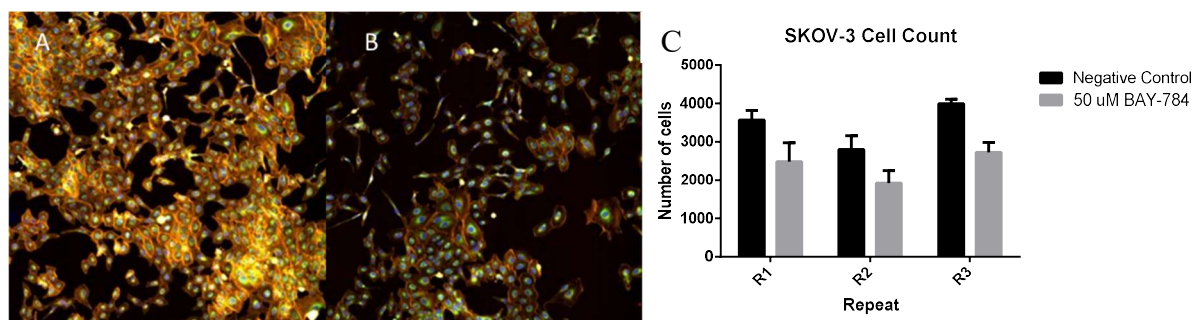
Figure 4.5. Morphology of SKOV-3 of treatment with BAY-784 vs untreated cell. Cell painting photo of untreated SKOV-3 cell in A) and treated with BAY-784 in B) Cell counting graph with untreated and treated cells in C). Each repeat was made from n=3 wells, with 9 image fields taken per well. (21 images per repeat). As described before, cytoskeleton is yellow and a decrease in this colour is shown when treated with BAY-784.

Cells which were treated with 50uM BAY-784 and exposure time of 48 hrs, were shown to have a lower number of cells per well compared to non-treated cotnrols (figure 4.5c). This result was consistent across all repeats. There was 31-32% less cells per well when treated with BAY 784 compared to non-treated controls, with an average reduction of 1079 cells. Whilst this reduction in cell count can't be specifically attributed to either a reduction in proliferation or a greater level of apoptosis, it is clear that BAY-784 has low levels of anti-cancer properties in SKOV-3 cells, consistent with the RTGlo expreriemnts above.

4.1.2.2. Cell cycle

Cell cycle combines a series of events that occurs in a cell to grow and divide. The cell cycle consists of four stages, DNA synthesis (S), Growth (G_1), growth and preparation for mitosis (G_2) and mitosis (M). Cancer is known as an overworking of dividing and growing of cells whereby a tumour is formed. Therefore, cancer often has an influence on the regulation of the cell cycle, and an important part of the cancer drug development process is the accurate determination of cell cycle effect.[45] As the cell nuclei are one for the organelles of interest in the cell paint experiment and are being stained with Hoechst 33342, we can use this output to quantify DNA levels and determine the effect of the drug on the cell cycle. DNA contents fluctuates

throughout the cell cycle with DNA content doubling between G1 and G2/M phases in preparation for mitosis. During cell replication, DNA contents is duplicated. Prior to the parental cell splitting into parental and daughter cells, the total DNA contents will be double that found in a non-proliferating cell.
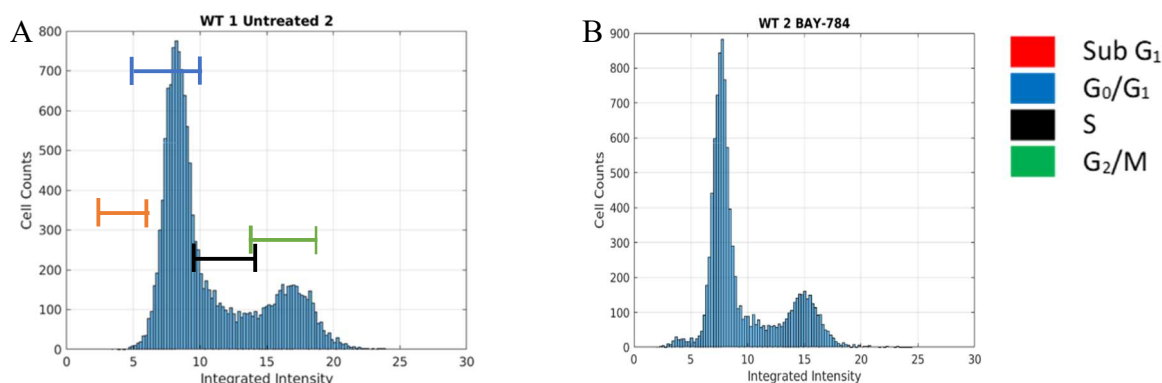
Figure 4.6. Effect of BAY-784 on the SKOV-3. SKOV-3 WT cell line with untreated cells in A) and treatment with BAY-784 in B). Increase of intensity from 2-5 when treated with BAY-784.

The results of the cell cycle assay are shown in figure 4.6. Panel a give both cell cycle regions and the cell cycle analysis in untreated SKOV-3 and panel b shows the shift in profile following BAY-784 treatment. The BAY-784 treatment histogram depicts a larger frequency of cells (proportion of the cell population) at a lower integrated intensity range, ≤ 6. More cells were detected in the subG$_0$ range, the reduction in integrated intensity is caused by DNA fragmentation and indicative of apoptosis.[33] There is no significant change in other cell cycle stages based on this dataset.

4.1.2.3. Principal Component Analysis (PCA)

The cell painting assay, with its high throughput, pixel level information provides the basis for robust statistical analysis of drug affects on cells. The high-quality images were segmented to identify individual cells using Ilastik and Cell Profiler and were utilised to determine relative abundance of each stain/per cell. Using a PCA analysis method, a multivariate way of analysing datasets and uses an algorithm to cluster similar results, we were able to ascertain the differing affects of the compound on SKOV-3 cells. When compared to the inclusion of drugs of known mechanism of action, a visual inspection of the PCA plots can be indicative of BAY-784 effects on the SKOV-3 cells.

For the purpose of this assay, multiple controls or compounds of known mechanism of action were included in the compound array. All compounds utilised are listed along side their mechanism of action and molecular targets within cells in Table 4.3.

Table 4.3. Drugs included in PCA with working mechanism and drug class.

Drug	Broad Drug Class	Drug Class	Approved for OC?
Cisplatin	DNA Intercalator	DNA Intercalator	Yes
Doxorubicin	DNA Intercalator	DNA Intercalator	Yes
SAHA	Epigenetic Modifiers	Pan-HDACi	No
Panobinostat	Epigenetic Modifiers	Pan-HDACi	No
Palbociclib	CDK Inhibitors	CDK4/6i	No
SRA 737	Checkpoint inhibitor	CHK1i	No
ABT-263	Bcl2i	Bcl2i	No
Gefitinib	EGFRi	EGFRi	No

These groups of compounds were selected to cover the a range of mechanisms known to be related to cancer development, including those specifically used to treat OC. For example, CDK inhibitors are used to treat cancers by preventing cell proliferation, while DNA intercalators bind to the cancer DNA causing damage to the DNA, thereby stopping cellular replication. By imaging the cells exposed to these drugs (with known mechanisms of action) and comparing these images to those following BAY-784 treatments, we wanted to explore the MoA of BAY-784 based on cluster presentation in our cell line models (as shown in Figure 4.7A, B and C).

A

B
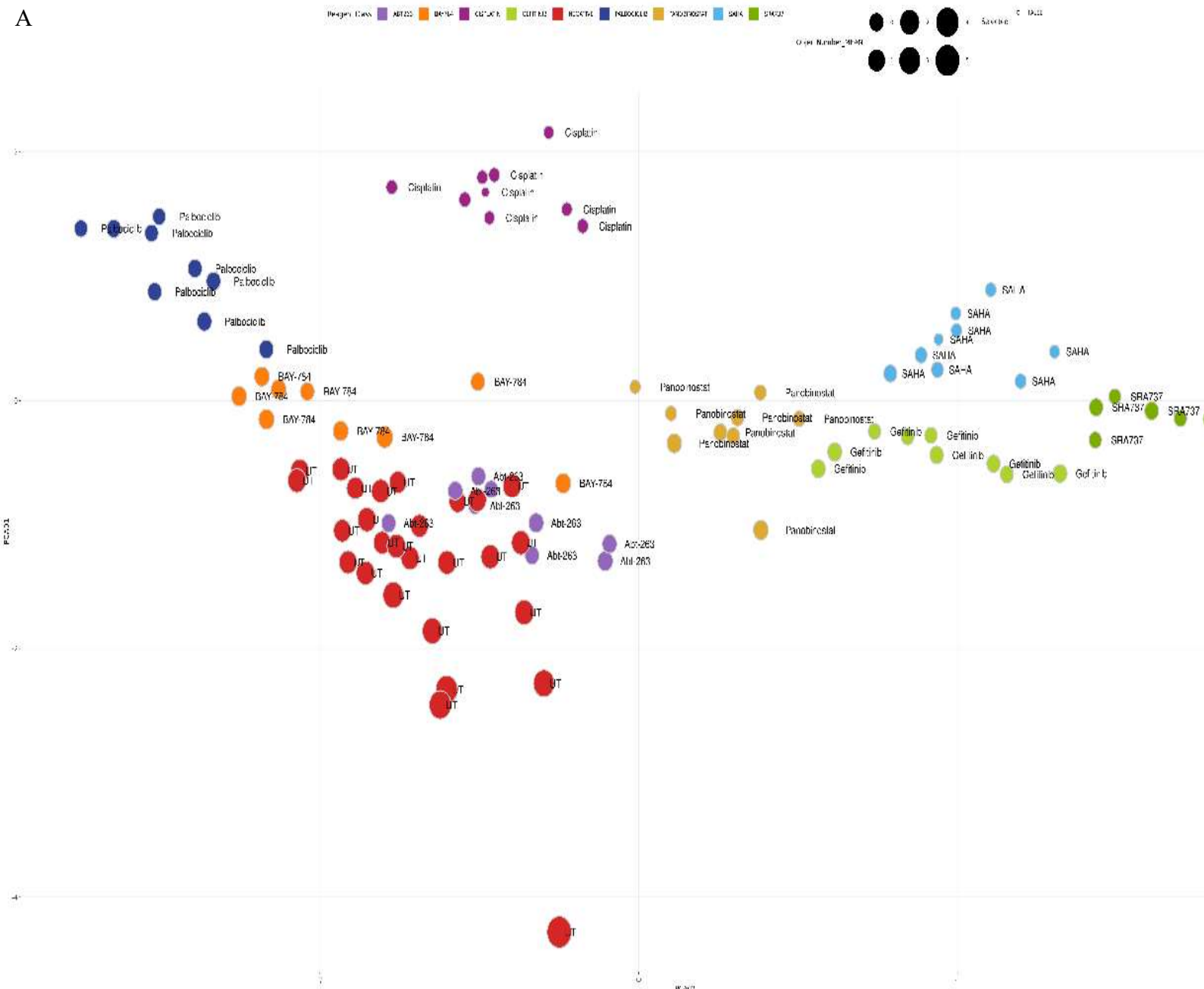
Figure 4.7. Principal component analysis (PCA) of drug compounds in SKOV-3 cells. (A) PC1 compared to PC2. (B) PC2 compared to PC3. (C) PC1 compared to PC3. Each circle represents a sample and each colour represents a drug compound. UT = control.

Clustering of drug compounds by phenotypic similarities in SKOV-3 cells are shown in figure 47. Drugs which are clustered together are thought to have similar working mechanisms in term of their effect on cells. BAY-784 has clustered together in all three figures which suggests that the working of BAY-784 is reproducible. In addition, BAY-784 shows in all three PCs as a close cluster to Palbociclib, indicating that BAY-784 may have a similar effect to Palbociclib. Furthermore, Gefitinib is clustered furthest away in all three PCs indicating that these MoA are most different from each other. In one PC, BAY-784 is also clustered together with ABT-263. Therefore, this drug is less similar to BAY-784 compared with Palbociclib which indicates that BAY-784 and Palbociclib are most similar to each other. For full confidence in MoA elucidation, an additional experiment would need to be carried out to validate this work using more traditional cell and molecular assays such as protocols that measure the presence of DNA damage or apoptosis etc.

Some extra information that is collected from the PC plots are the information that is used for clustering. In table 4.4, an overview of the highest resemblances was showed with the respective description. As can be seen in PC1, the majority of the PC is based on the intensity of the cell stain. Whereby in PC2 and PC3, it is based on the texture and shape of the nuclei.

Table 4.4. Principal components of the drug compounds in SKOV-3 cells. Part of the PCA intensity Information on variables was taken from CellProfiler.

Principal Component	Variables	Variation in the data
Principal Component 1 (PC1)	Mean mitochondrial stain integrated intensity/cell	0.932701055
	Mean ER stain integrated intensity/cell	0.831727104
	Mean ER stain integrated intensity at nuclei site	0.810347085
	Mass displacement per cell using cytoplasm stain	0.788085404
	Mean Cytoplasm texture	-0.828490738
Principal Component 2 (PC2)	Change in cell circularity based cytoplasmic stain?	0.905186350
	Mass displacement at nucleus using cytoplasm stain	0.895602221
	Mean nuclei texture in relation to cytoplasm	0.866996771
	Mean nuclei texture in relation to cytoplasm, alternative measurement	0.829060264

	Change in nuclei shape/area	-0.864210919
Principal Component 3 (PC3)	Change in circularity of nuclei, metric 1	0.896690793
	Mean nuclei texture based on nuclei staining	0.771609082
	Change in circularity of nuclei, metric 4	-0.780523652
	Mean nuclei texture in relation to endoplasmic reticulum	-0.794204129
	Change in cell circularity based mitochondrial stain?	-0.796576255

This data Table 4.4 shows loading scores that suggest BAY-784 is acting in different areas of the cell whereby the nucleus has been named in the majority of the variables. This is consistent with the MoA of Palbociclib, that inhibits CDKs that regulate the cell cycle, and specifically transcription a within the nucleus and mRNA processing. This suggests that BAY-784 is able to operate with anticancer activity using a similar MoA to Palbociclib, by affecting transcription and nuclear function, along with GnRHR antagonism, as reported by the literature. CDK, or protein kinases, are signalling switchboards, frequently deregulated in cancer and signify vulnerable nodes and potential therapeutic targets. Palbociclib, is known to target CDK 4 and 6, and interplay with the MAPK pathway in cancer. Apoptotic cell death induced by antagonists of GnRH-II is permitted *via* the intrinsic cascade through stress- activated mitogen-activated protein kinases (MAPKs) p38- and JNK-induced stimulation of the proapoptotic factor Bax, together with the loss of mitochondrial membrane potential, cytochrome c release, and caspase-3 activation.

4.1.3. Liposomal Drug vs Free Drug on OVCAR-3 and SKOV-3

The final objective of the study was to assess the suitability of Nanoparticle delivery in enhancing the efficacy of BAY-784 in the 2D cell model. The liposome encapsulated BAY-784 fabricated and characterised in section 4.1.1., was tested on OVCAR-3 and SKOV-3 cells. For the treatment with liposomal BAY-784, the concentration is kept at 50 μM to compare the treatments with the IC_{50} of the FD.
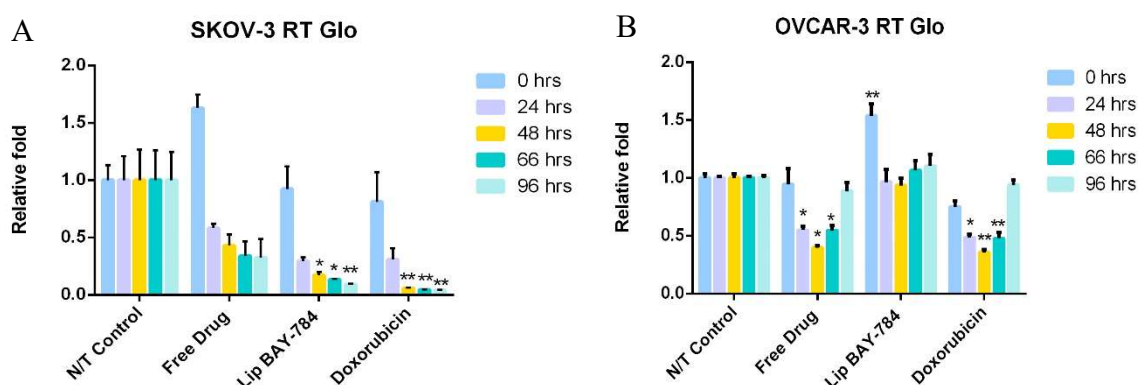
Figure 4.8. Cytotoxicity test of liposomal BAY-784. Cytotoxicity testing of BAY-784, liposomal BAY-784 and doxorubicin over 96 hrs in SKOV-3 A) and OVCAR-3 B). Including asterixis which shows the significant difference of $p < 0.05$.

In figure 48a, a clear decrease in response between liposomal BAY-784 and free drug BAY-784 is detected. The decrease after 96 hrs is 67.6% for FD and 90.9% in liposomal BAY-784 in SKOV-3 while this is 11.3% for FD and an increase of 10.3% with liposomal BAY-784 in OVCAR-3. In addition, no visual change in OVCAR-3 is ascertained for all treatments after 96 hrs. For free drug BAY-784 and doxorubicin, up to 48 hrs a decrease is shown but this can be seen as a decrease in activity in cells while this is just for a certain time. Liposomal drug in OVCAR-3 shows no decrease in OVCAR-3 while SKOV-3 shows a significant difference. In the results of chapter 3.6.2., an uptake of liposomes in SKOV-3 was higher in comparison with OVCAR-3, which can explain the difference of results with liposomal BAY-784 in these two cell lines.

4.2.   Concluding Remarks Biological Efficiency

For the IC_{50} determination in OVCAR-3 and SKOV-3 cell lines, RT Glo bioassay was used to calculate the IC_{50} for BAY-784 and was determined to be a concentration ~50μM. To better understand the MoA cell painting was used to measure the biological impact of BAY-784 on these cell lines. This involved uses different stains to show changes in activity in different parts of the cell following treatment with BAY-784. A PCA was also undertaken to compare these results with other known cancer therapies that function across several MoAs. This experiment showed that BAY-784 worked mainly on the nucleus and has a similar working mechanism as Palbociclib (a CDK inhibitor), affecting transcription and the cell cycle. This was also confirmed with a cell cycle bioassay.

Following these experiments involving free BAY-784, encapsulated BAY-784 was tested which showed a more effective working mechanism in comparison with free BAY-784 in

SKOV-3. This indicates that BAY-784 can operate as an anti-cancer drug, with increased effi-cacy when applied in a liposomal formation for an ovarian cancer cell line (e.g. SKOV-3).

5. Chapter 5: Conclusion

In this research, we have investigated the biological efficacy and stability of a liposome-based nano-encapsulated GnRHR antagonist, BAY-784, as a possible treatment for OC. We have characterised the drug encapsulation and release from the particle and biological efficacy. This required the development and assessment of an analytical method to quantify BAY-784 and doxorubicin using LC-DAD (WP 1). Pleasingly, a good degree of quantitative precision and accuracy was determined across the calibration range tested for both analytes, indicating the suitability of the method in measuring these therapeutics. Within this work we also explored the potential of combining these protocols for a dual measurement method of using similar concentrations. As expected, some decrease in performance was observed when analysing both compounds as a mixture however, acceptable precision and accuracy (within 15%) were observed for all QCs tested. Furthermore, we have also examined the stability of diluted solutions of BAY-784 under different operational and storage conditions (for up to 4 weeks). Good stability was observed, enabling storage and reuse of the drug solutions without having to prepare these fresh on the day of each analysis.

Prior to BAY-784 encapsulation, the uptake of the liposome was tested for each cell line; this was successful for each cell line, with a higher uptake in SKOV-3 in comparison with OVCAR-3. Once assessed the method of encapsulation or incorporation was investigated using Thin-Film hydration (WP3). The results showed that encapsulation provided a greater % uptake of drug into the particle (at 40% encapsulation efficiency) and was comparable with in-house data for doxorubicin (50%). Following fabrication of the liposomal drug, the release process was tested by DLS through adjusting, with the liposomes showing evidence of lysis under basic conditions (pH of 10). This is important given it does not necessarily represent the tumour environment, and so efficacy testing will need to be assured. Furthermore, understanding the lability of the liposomal drug is key in establishing stable storage conditions and informing the drug release during the sample preparation approach.

To measure the absolute amounts of drug within the particle, an extraction protocol to release and concentrate the drug was required. A tripartite approach was tested using a combination of SPE and LLE. The initial sample development was evaluated with free drug for each stage of the and indicated that methanol was the most suitable organic elution solvent for the SPE process, along with ethyl acetate for LLE. The QuEChERS method did not provide sufficient recovery of the drug further work involved a combined SPE-LLE process with the encapsulated drug. Sadly, particles were observed after the clean-up step and despite adaptations to resolve the problem (e.g. changes in pH to limit aggregation) particles remained. This suggested that

the liposomes may exhibit retention on the SPE cartridge or, that they be reforming during the extraction. Therefore, to properly adopt this protocol, further work will be required to better understand the causative factors, along with measure to limit their production.

During this project we have also confirmed the biological efficacy of ´free´ BAY-784 in OVCAR-3 and SKOV-3 cell lines, and this increased following encapsulation within a biodegradable and highly biocompatible liposome (WP 2). A RT Glo bioassay was used to calculate the IC_{50} for BAY-784 and was determined to be a concentration ~50µM. Whilst cell painting was used to measure the biological impact of BAY-784 on these cell lines with the MoA. This involved using different stains to show activity changes in different parts of the cell after exposure to BAY-784. A cell cycle bioassay and PCA plot was also used to compare MoA with other known cancer therapies and showed that BAY-784 worked mainly on the nucleus affecting transcription and the cell cycle, similarly to a CDK inhibitor, Palbociclib. Once established, encapsulated BAY-784 was tested on the OC cells and showed greater efficacy than free BAY-784 in limiting cell growth in SKOV-3. This suggests that the acidic tumour environment may not as important for the drug efficacy and indicates that BAY-784 can operate as an anti-cancer drug, with increased efficacy when applied in a liposomal formation for an ovarian cancer cell line (e.g. SKOV-3).

6. Further work

Sadly, due to the time restrictions, not all of the objectives were completed within the period of study. For the analytical work programme, further work will be required to modify the sample preparation protocol to measure absolute amounts of BAY-784 within the liposome without causing blockages within the SPE/LC-DAD. This will include the use of homogenisers to minimise particle aggregation or an alternative SPE (Phenomenex) sorbent to avoid retention to avoid their production or retention during and following the extraction, respectively. Once completed this will be tested to extract the intact encapsulated drug from the complex matrix (ascites and plasma) conditions.

For the second work program, we will establish the toxicity of the liposomal drug on healthy cells as part of the safety testing. If this provides a desirable outcome, we will combine this therapy with an additional OC drug that operates with a different MoA to assess if liposomal BAY-784 offers benefit as a complementary therapy that can avoid treatment resistance.

Finally, we will assess the kinetics of drug encapsulation and release vs. an established drug (e.g. Doxil) under aqueous and in vitro conditions. This will involve testing the drug in neat aqueous solutions, following prolonged exposure to acidic pH to assess the long-term stability of the liposomal drug within an environment representative of the tumour environment, and in a complex matrix (e.g. plasma and ascites).

7. Chapter 7: Bibliography

[1] T. C. Johnstone, G. Y. Park, and S. J. Lippard, "Understanding and improving platinum anticancer drugs - Phenanthriplatin," in *Anticancer Research*, Jan. 2014, vol. 34, no. 1, pp. 471–476, Accessed: Nov. 01, 2020. [Online]. Available: /pmc/articles/PMC3937549/?report=abstract.

[2] "What Is Cancer? - National Cancer Institute." https://www.cancer.gov/about-cancer/understanding/what-is-cancer (accessed Dec. 10, 2020).

[3] J. Zugazagoitia, C. Guedes, S. Ponce, I. Ferrer, S. Molina-Pinelo, and L. Paz-Ares, "Current Challenges in Cancer Treatment," *Clinical Therapeutics*, vol. 38, no. 7. Excerpta Medica Inc., pp. 1551–1566, Jul. 01, 2016, doi: 10.1016/j.clinthera.2016.03.026.

[4] "The Unique Physiology of Solid Tumors: Opportunities (and Problems) for Cancer Therapy1 | Cancer Research | American Association for Cancer Research." https://aacrjournals.org/cancerres/article/58/7/1408/504980/The-Unique-Physiology-of-Solid-Tumors (accessed Mar. 01, 2022).

[5] W. K. So, J. C. Cheng, S. L. Poon, and P. C. K. Leung, "Gonadotropin-releasing hormone and ovarian cancer: A functional and mechanistic overview," *FEBS Journal*, vol. 275, no. 22. John Wiley & Sons, Ltd, pp. 5496–5511, Nov. 01, 2008, doi: 10.1111/j.1742-4658.2008.06679.x.

[6] "Ovarian Cancer Stages, Survival Rate and Prognosis | OCRA." https://ocrahope.org/patients/about-ovarian-cancer/staging/ (accessed Apr. 14, 2021).

[7] B. Liu, J. Nash, C. Runowicz, H. Swede, R. Stevens, and Z. Li, "Ovarian cancer immunotherapy: Opportunities, progresses and challenges," *Journal of Hematology and Oncology*, vol. 3, no. 1. BioMed Central, p. 7, Dec. 10, 2010, doi: 10.1186/1756-8722-3-7.

[8] C. Gründker and G. Emons, "Role of gonadotropin-releasing hormone (GnRH) in ovarian cancer," *Reprod. Biol. Endocrinol.*, vol. 1, p. 65, Oct. 2003, doi: 10.1186/1477-7827-1-65.

[9] A. Akbarzadeh *et al.*, "Liposome: Classification, preparation, and applications," *Nanoscale Res. Lett.*, vol. 8, no. 1, p. 102, 2013, doi: 10.1186/1556-276X-8-102.

[10] R. BAZAK, M. HOURI, S. EL ACHY, W. HUSSEIN, and T. REFAAT, "Passive targeting of nanoparticles to cancer: A comprehensive review of the literature," *Mol. Clin. Oncol.*, vol. 2, no. 6, pp. 904–908, Nov. 2014, doi: 10.3892/mco.2014.356.

[11] M. F. Attia, N. Anton, J. Wallyn, Z. Omran, and T. F. Vandamme, "An overview of active and passive targeting strategies to improve the nanocarriers efficiency to tumour sites," *J. Pharm. Pharmacol.*, vol. 71, no. 8, pp. 1185–1198, Aug. 2019, doi: 10.1111/jphp.13098.

[12] R. Ghanghoria, P. Kesharwani, R. K. Tekade, and N. K. Jain, "Targeting luteinizing hormone-releasing hormone: A potential therapeutics to treat gynecological and other cancers," *Journal of Controlled Release*, vol. 269. Elsevier B.V., pp. 277–301, Jan. 10, 2018, doi: 10.1016/j.jconrel.2016.11.002.

[13] O. Panknin *et al.*, "Discovery and Characterization of BAY 1214784, an Orally Available Spiroindoline Derivative Acting as a Potent and Selective Antagonist of the Human Gonadotropin-Releasing Hormone Receptor as Proven in a First-In-Human Study in Postmenopausal Women," *J. Med. Chem.*, vol. 63, no. 20, pp. 11854–11881, Oct. 2020, doi: 10.1021/ACS.JMEDCHEM.0C01076/SUPPL_FILE/JM0C01076_SI_002.CSV.

[14] S. Fister, A. R. Günthert, B. Aicher, K. W. Paulini, G. Emons, and C. Gründker, "GnRH-II Antagonists Induce Apoptosis in Human Endometrial, Ovarian, and Breast Cancer Cells via Activation of Stress-Induced MAPKs p38 and JNK and Proapoptotic

Protein Bax," doi: 10.1158/0008-5472.CAN-08-4657.

[15] D. C. Probe, "GnRH-R Antagonist Probe BAY-784 GnRH-R Ant . Probe BAY-784," pp. 1–18, 2018.

[16] L. Panasci *et al.*, "Sensitization to doxorubicin resistance in breast cancer cell lines by tamoxifen and megestrol acetate," *Biochem. Pharmacol.*, vol. 52, no. 7, pp. 1097–1102, Oct. 1996, doi: 10.1016/0006-2952(96)00456-X.

[17] A. Vaghela, A. Patel, A. Patel, A. Vyas, and N. Patel, "Sample Preparation In Bioanalysis: A Review," *Int. J. Sci. Technol. Res.*, vol. 5, p. 5, 2016, Accessed: Mar. 01, 2021. [Online]. Available: www.ijstr.org.

[18] R. Perestrelo *et al.*, "QuEChERS - Fundamentals, relevant improvements, applications and future trends," *Analytica Chimica Acta*, vol. 1070. Elsevier B.V., pp. 1–28, Sep. 06, 2019, doi: 10.1016/j.aca.2019.02.036.

[19] M. I. Aguilar, "Reversed-phase high-performance liquid chromatography.," *Methods Mol. Biol.*, vol. 251, pp. 9–22, 2004, doi: 10.1385/1-59259-742-4:9.

[20] J. Bigelow, "Bioanalytical Tools for Drug Analysis," *Pharmacology*, pp. 279–302, Jan. 2009, doi: 10.1016/B978-0-12-369521-5.00011-7.

[21] L. S. Ettre, "Nomenclature for chromatography (iupac recommendations 1993)," *Pure Appl. Chem.*, vol. 65, no. 4, pp. 819–872, 1993, doi: 10.1351/pac199365040819.

[22] "Factors Affecting Resolution in HPLC." https://www.sigmaaldrich.com/GB/en/technical-documents/technical-article/analytical-chemistry/small-molecule-hplc/factors-affecting-resolution-in-hplc (accessed Mar. 01, 2022).

[23] M. Wilm, "Principles of Electrospray Ionization," *Mol. Cell. Proteomics*, vol. 10, no. 7, Jul. 2011, doi: 10.1074/MCP.M111.009407.

[24] J. J. Pitt, "Principles and applications of liquid chromatography-mass spectrometry in clinical biochemistry.," *Clin. Biochem. Rev.*, vol. 30, no. 1, pp. 19–34, Feb. 2009, Accessed: Dec. 28, 2020. [Online]. Available: http://www.ncbi.nlm.nih.gov/pubmed/19224008.

[25] A. AM, C.-B. MM, and F. AC, "Linear regression for calibration lines revisited: weighting schemes for bioanalytical methods," *J. Chromatogr. B. Analyt. Technol. Biomed. Life Sci.*, vol. 774, no. 2, pp. 215–222, Jul. 2002, doi: 10.1016/S1570-0232(02)00244-1.

[26] S. H. Hansen and S. Pedersen-Bjergaard, *Bioanalysis of Pharmaceuticals - Sample Preparation, Seperation Techniques and Mass Spectrometry*, 2015th ed. Copenhagen: Wiley, 2005.

[27] S. Imre, L. Vlase, and D. L. Muntean, "Bioanalytical method validation," *Rev. Rom. Med. Lab.*, vol. 10, no. 1, pp. 13–21, 2008, doi: 10.5958/2231-5675.2015.00035.6.

[28] T. L. Riss *et al.*, "Cell Viability Assays," *Assay Guid. Man.*, Jul. 2016, Accessed: Feb. 25, 2022. [Online]. Available: https://www.ncbi.nlm.nih.gov/books/NBK144065/.

[29] A. L. Niles, R. A. Moravec, and T. L. Riss, "In Vitro Viability and Cytotoxicity Testing and Same-Well Multi-Parametric Combinations for High Throughput Screening," *Curr. Chem. Genomics*, vol. 3, no. 1, p. 33, 2009, doi: 10.2174/1875397300903010033.

[30] "Cell Proliferation Kit II (XTT) | Sigma-Aldrich." https://www.sigmaaldrich.com/catalog/product/roche/11465015001?lang=en&region=GB (accessed Jan. 06, 2021).

[31] P. Corporation, "RealTime-Glo™ MT Cell Viability Assay Instructions for Use of Products G9711, G9712 and G9713," Accessed: Sep. 21, 2021. [Online]. Available: www.promega.com.

[32] M. G. Papich, "Doxorubicin Hydrochloride," *Papich Handb. Vet. Drugs*, no. 1907, pp.

309–312, 2021, doi: 10.1016/b978-0-323-70957-6.00183-7.

[33] J. Zhong *et al.*, "Pharmacokinetics of liposomal-encapsulated and un-encapsulated vincristine after injection of liposomal vincristine sulfate in beagle dogs," *Cancer Chemother. Pharmacol.*, vol. 73, no. 3, pp. 459–466, 2014, doi: 10.1007/s00280-013-2369-5.

[34] B. K. Matuszewski, M. L. Constanzer, and C. M. Chavez-Eng, "Strategies for the Assessment of Matrix Effect in Quantitative Bioanalytical Methods Based on HPLC-MS/MS," *Anal. Chem.*, vol. 18, no. 2, pp. 3019–3030, 1998, doi: 10.1021/ac020361s.

[35] C. L. Chen *et al.*, "Differential role of gonadotropin-releasing hormone on human ovarian epithelial cancer cell invasion," *Endocrine*, vol. 31, no. 3, pp. 311–320, 2007, doi: 10.1007/s12020-007-0041-8.

[36] J. N. Miller and J. C. Miller, *Statistics and Chemometrics for Analytical Chemistry*, vol. 14, no. 6. 2014.

[37] V. Makwana, J. Karanjia, T. Haselhorst, S. Anoopkumar-Dukie, and S. Rudrawar, "Liposomal doxorubicin as targeted delivery platform: Current trends in surface functionalization," *International Journal of Pharmaceutics*, vol. 593. Elsevier B.V., p. 120117, Jan. 25, 2021, doi: 10.1016/j.ijpharm.2020.120117.

[38] F. Yang, H. Wang, M. Liu, P. Hu, and J. Jiang, "Determination of free and total vincristine in human plasma after intravenous administration of vincristine sulfate liposome injection using ultra-high performance liquid chromatography tandem mass spectrometry," *J. Chromatogr. A*, vol. 1275, pp. 61–69, 2013, doi: 10.1016/j.chroma.2012.12.026.

[39] Z. Liu *et al.*, "Pharmacokinetics of a liposomal formulation of doxorubicin in rats," *Saudi Pharm. J. SPJ*, vol. 25, no. 4, p. 531, May 2017, doi: 10.1016/J.JSPS.2017.04.019.

[40] A. Gonzalez Gomez, S. Syed, K. Marshall, and Z. Hosseinidoust, "Liposomal Nanovesicles for Efficient Encapsulation of Staphylococcal Antibiotics," *ACS Omega*, vol. 4, no. 6, pp. 10866–10876, Jun. 2019, doi: 10.1021/acsomega.9b00825.

[41] J. O. Eloy, M. Claro de Souza, R. Petrilli, J. P. A. Barcellos, R. J. Lee, and J. M. Marchetti, "Liposomes as carriers of hydrophilic small molecule drugs: Strategies to enhance encapsulation and delivery," *Colloids and Surfaces B: Biointerfaces*, vol. 123. Elsevier, pp. 345–363, Nov. 01, 2014, doi: 10.1016/j.colsurfb.2014.09.029.

[42] * B. K. Matuszewski, and M. L. Constanzer, and C. M. Chavez-Eng, "Strategies for the Assessment of Matrix Effect in Quantitative Bioanalytical Methods Based on HPLC−MS/MS," *Anal. Chem.*, vol. 75, no. 13, pp. 3019–3030, Jul. 2003, doi: 10.1021/AC020361S.

[43] R. Townsend, G. Keulen, C. Desbrow, and A. R. Godfrey, "An investigation of the utility of QuEChERS for extracting acid, base, neutral and amphiphilic species from example environmental and clinical matrices," *Anal. Sci. Adv.*, vol. 1, no. 3, pp. 152–160, Oct. 2020, doi: 10.1002/ansa.202000018.

[44] A. Guillot, A.-C. Couffin, X. Sejean, F. Navarro, M. Limberger, and C.-M. Lehr, "Solid Phase Extraction as an Innovative Separation Method for Measuring Free and Entrapped Drug in Lipid Nanoparticles," *Pharm. Res. 2015 3212*, vol. 32, no. 12, pp. 3999–4009, Jul. 2015, doi: 10.1007/S11095-015-1761-8.

[45] M.-A. Bray *et al.*, "Cell Painting, a high-content image-based assay for morphological profiling using multiplexed fluorescent dyes," *Nat. Protoc.*, vol. 11, no. 9, p. 1757, Sep. 2016, doi: 10.1038/NPROT.2016.105.
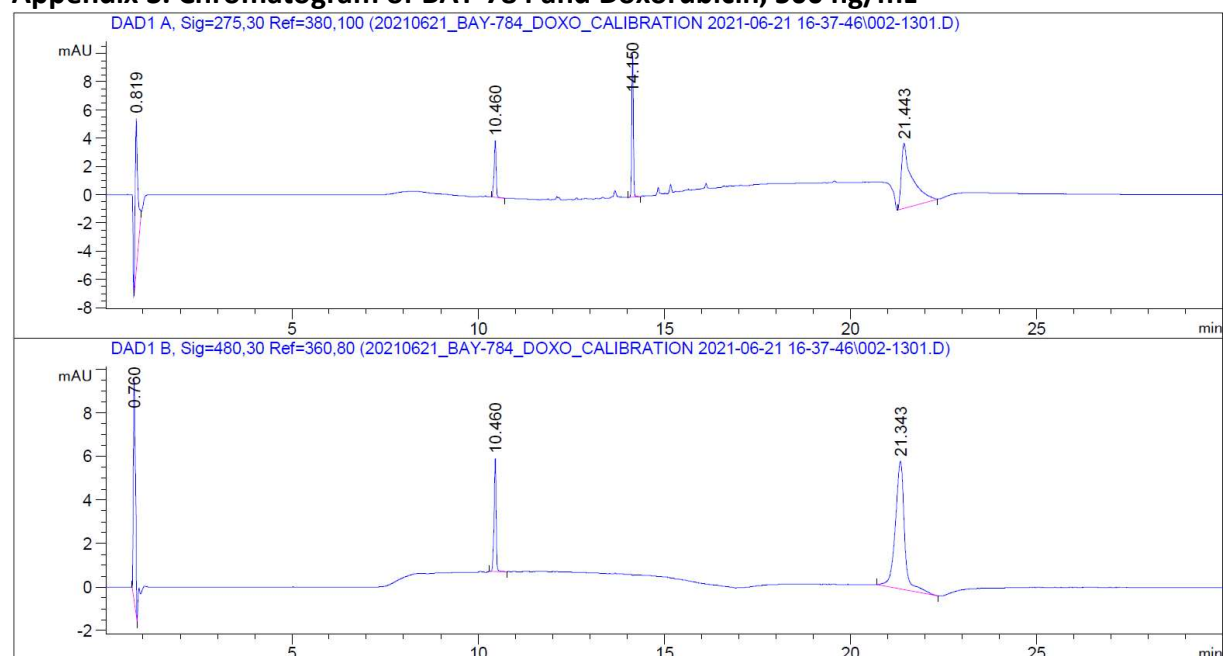
Appendix

## Appendix 1 Stability Testing Freeze-Thaw cycle sub-stock 1

QC Level	Area (mAu)	y	Theo Conc	20%	15%	P/F FDA	Accuracy	Mean Conc	St Dev	%Acc Mean	% Prec
Low 1	53.57	843.21	1000	200		P	-15.68				
Low 2	62.23	1008.42	1000	200		P	0.84	935.30	84.22	-6.47	9.00
Low 3	59.39	954.25	1000	200		P	-4.57				
Medium 1	107.72	1876.61	2000		300	P	-6.17				
Medium 2	120.57	2121.87	2000		300	P	6.09	2081.86	188.46	4.09	9.05
Medium 3	127.13	2247.11	2000		300	P	12.36				
High 1	238.19	4366.94	4500		675	P	-2.96				
High 2	248.84	4570.18	4500		675	P	1.56	4625.92	290.89	2.80	6.29
High 3	268.25	4940.64	4500		675	P	9.79				

Appendix 2. Stability Testing Freeze-Thaw cycle sub-stock 2

QC Level	Area (mAu)	y	Theo Conc	20%	15%	P/F FDA	Accuracy	Mean Conc	St Dev	%Acc Mean	% Prec
Low 1	50.07	776.29	1000	200		F	-22.37				
Low 2	52.14	815.85	1000	200		P	-18.42	813.28	35.77	-18.67	4.40
Low 3	53.81	847.70	1000	200		P	-15.23				
Medium 1	105.05	1825.65	2000		300	P	-8.72				
Medium 2	110.07	1921.50	2000		300	P	-3.93	1880.82	49.54	-5.96	2.63
Medium 3	108.70	1895.31	2000		300	P	-5.23				
High 1	261.42	4810.22	4500		675	P	6.89				
High 2	244.56	4488.40	4500		675	P	-0.26	4587.86	192.93	1.95	4.21
High 3	243.33	4464.95	4500		675	P	-0.78				

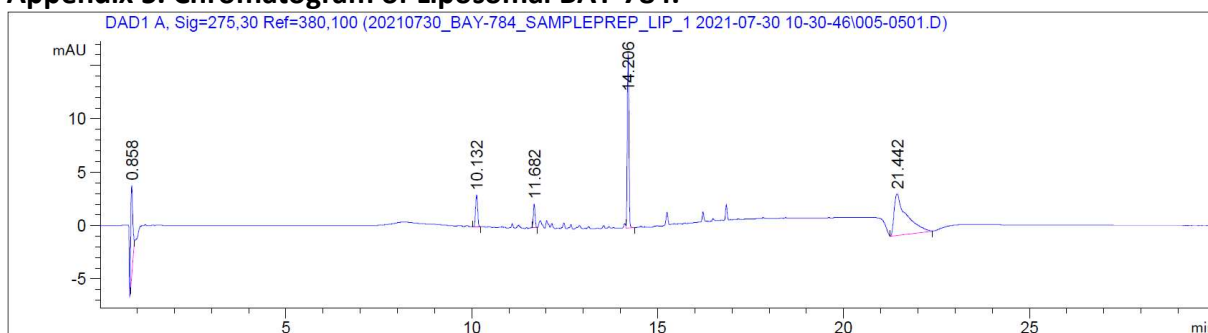## Appendix 3. Chromatogram of BAY-784 and Doxorubicin, 500 ng/mL
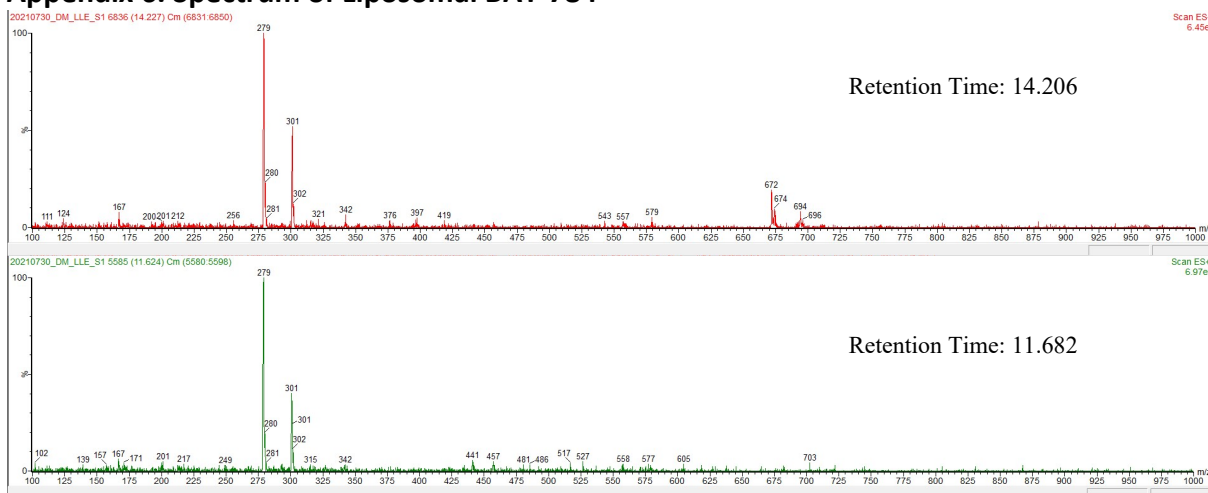
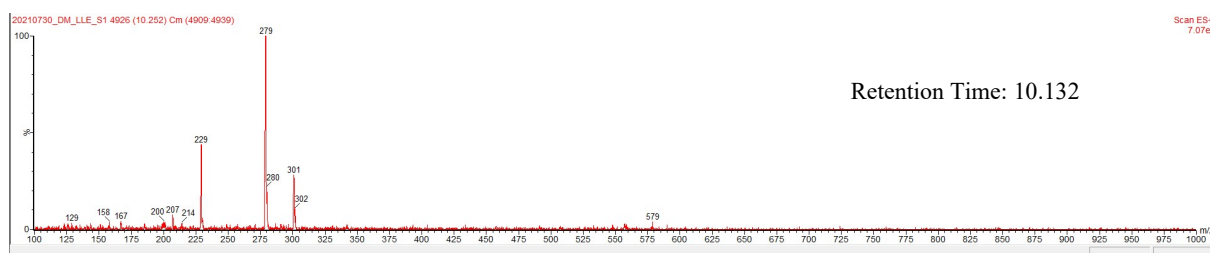## Appendix 4. Chromatogram of BAY-784 and Doxorubicin, 5000 ng/mL
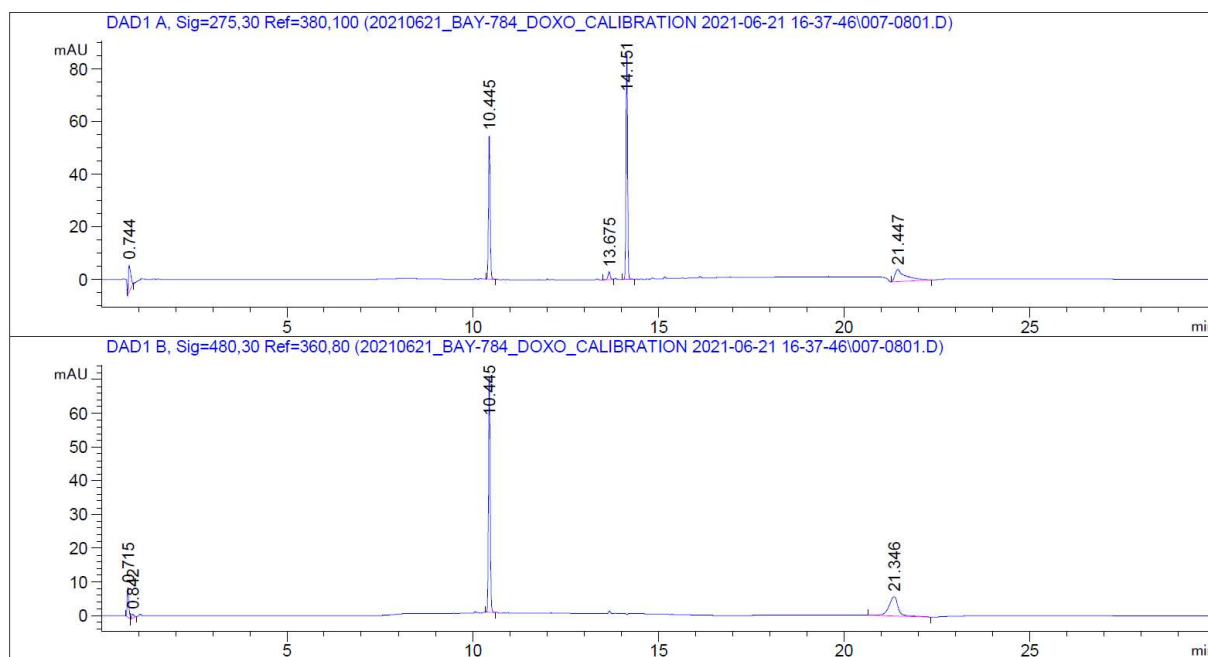
Appendix 5. Chromatogram of Liposomal BAY-784.

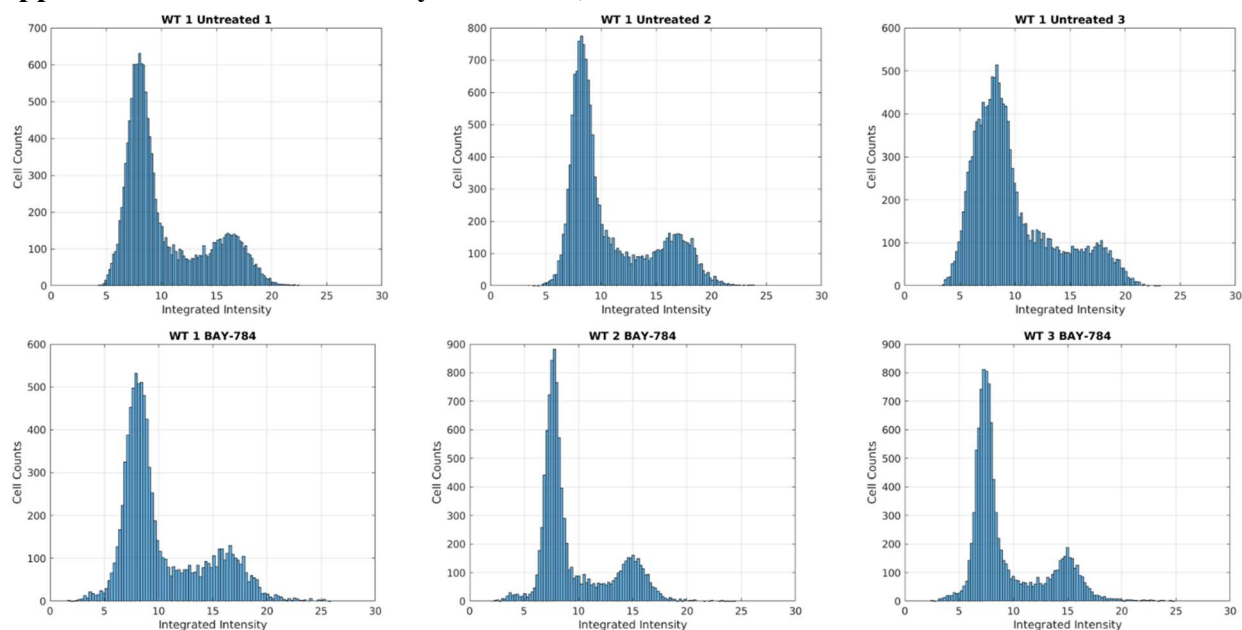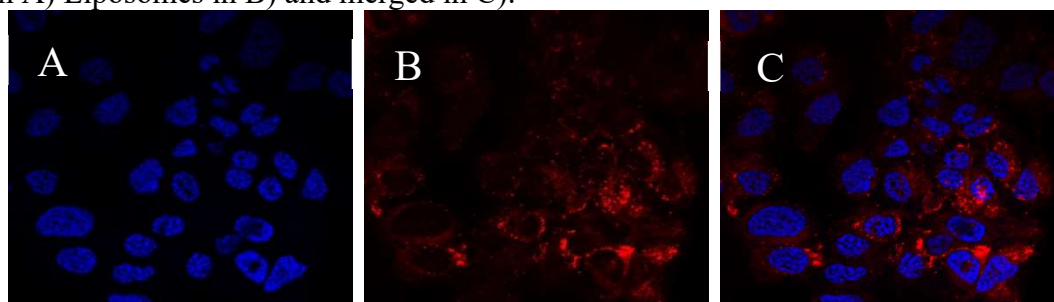## Appendix 6. Spectrum of Liposomal BAY-784

Retention Time: 14.206

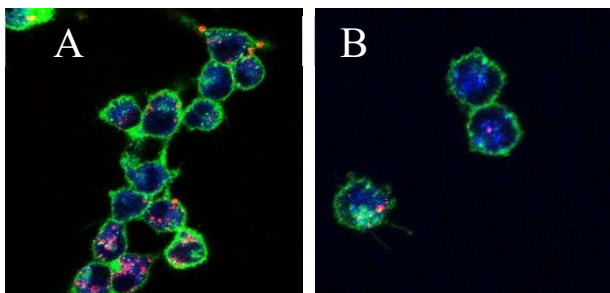Retention Time: 11.682

Retention Time: 10.132

**Appendix 7. Additional Cell Cycle Results, untreated and treated.**

Appendix 8. Morphology of liposomal uptake in SKOV-3. Staining with Hoechst (Nuclei) in A) Liposomes in B) and merged in C).

Appendix 9. Morphology of liposomal uptake in SKOV-3 and OVCAR-3. Confocal images of liposomes in SKOV-3 A) and OVCAR-3 B).

Appendix 10. Cytotoxicity of BAY-784, liposomal BAY-784 and Doxorubicin.
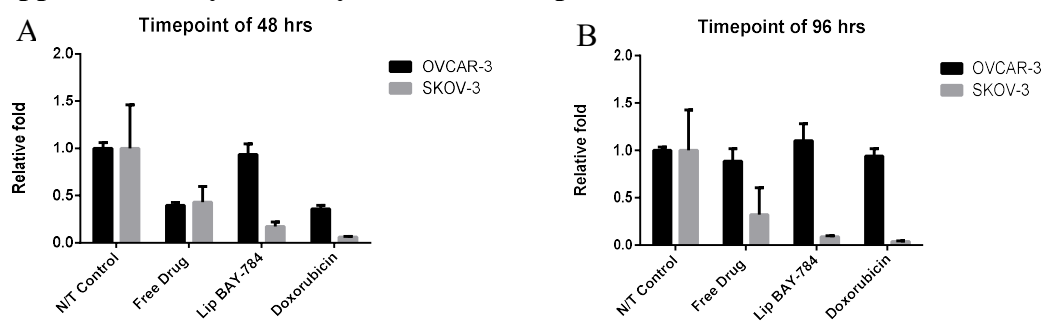
Appendix 11. ¹H-NMR Spectrum of FD BAY-784 and bursted liposome BAY-784.